

University of St Andrews



Full metadata for this thesis is available in
St Andrews Research Repository
at:

<http://research-repository.st-andrews.ac.uk/>

This thesis is protected by original copyright

NMR Studies of Molecular Motions in Solids

being a thesis by

Roger Alexander Spark

Submitted for the degree of
Doctor of Philosophy
in the Faculty of Science of the
University of St. Andrews

October 1999



Declaration

I, Roger Alexander Spark, hereby certify that this thesis, which is approximately 28,000 words in length, has been written by me, that it is a record of work carried out by me and that it has not been submitted in any previous application for a higher degree.

I was admitted as a research student in October, 1995 and as a candidate for the degree of Doctor of Philosophy in October, 1996; the higher study for which this is a record was carried out in the University of St. Andrews between 1995 and 1998.

Signed October 1999

Certification

I hereby certify that the candidate has fulfilled the conditions of the Resolution and Regulations appropriate for the degree of Doctor of Philosophy in the University of St. Andrews and that the candidate is qualified to submit this thesis in application for that degree.

Signed October 1999

Copyright (Unrestricted)

In submitting this thesis to the University of St. Andrews I understand that I am giving permission for it to be made available for use in accordance with the regulations of the University Library for the time being in force, subject to any copyright vested in the work not being affected thereby. I also understand that the title and abstract will be published, and that a copy of the work may be made and supplied to any bona fide library or research worker.

© Signed October 1999

Abstract

A convenient method was detailed for calibration of MAS NMR probes over the temperature range 173-373 K, using known solid phase changes. The subsequent calibration plot gives an equation to calculate sample temperatures, accurate to ± 3 K. It was confirmed that there is a variation of sample temperature with spinning speed which appears to obey a squared relationship.

A series of diols, including 2,2-disubstituted-propane-1,3-diols where the substituted group is methyl, ethyl, hydroxymethyl, cyclohexyl and cycloheptyl, were studied by solid-state CP/MAS NMR. Other diols studied were 1,4-butanediol, *cis*-1,2-cyclopentanediol, *trans*-1,3-cyclopentanediol, 1,2-dihydroxybenzene (catechol) and 1,2-di(hydroxymethyl)benzene. Of these compounds 2,2-dimethylpropane-1,3-diol, 2,2-diethylpropane-1,3-diol and 1,1-di(hydroxymethyl)cycloheptane yielded dynamic data, 1,1,1-tris(hydroxymethyl)ethane could not be measured due to a phase change in the $T_{1\rho}$ range and the remaining compounds displayed no detectable dynamic phenomena.

The making and breaking of hydrogen bonds is being observed, and due to appreciable $T_{1\rho}$ relaxation for the CH_2OH carbons there is rotation around the C- CH_2OH bond. Because of the symmetrical nature of the molecules and small $T_{1\rho}$ relaxation for the quaternary carbon there is also a degree of rotation around the C_2 axis. In addition 1,1-di(hydroxymethyl)cycloheptane undergoes pseudorotation of the ring where C-4 shows maximum motion (C-3 has E_a of 12.3 kJ mol^{-1} increasing through the ring to 24.7 and 44.7 kJ mol^{-1} for C-2 and $\underline{\text{C}}\text{H}_2\text{OH}$ respectively). 2,2-Dimethylpropane-1,3-diol has E_a of $46 \pm 3 \text{ kJ mol}^{-1}$, in good agreement with $\Delta G^\ddagger_{262 \text{ K}}$ of 49.7 kJ mol^{-1} (derived from CH_3 coalescence). 2,2-Diethylpropane-1,3-diol showed E_a of 86.4 kJ mol^{-1} for methyl carbons and an average of $72 \pm 1 \text{ kJ mol}^{-1}$ for CH_2OH and $\underline{\text{C}}\text{H}_2\text{CH}_3$ carbons. $\Delta G^\ddagger_{334 \text{ K}}$ of 61.7 kJ mol^{-1} for 1,1,1-tris(hydroxymethyl)ethane was derived from CH_2OH coalescence.

Acknowledgements

Thanks are due, firstly, to Frank Riddell. His guidance and enthusiasm have been a great inspiration throughout this project and this, coupled with his knowledge, has enabled me to become almost “at one with Boris”. I think each item of hardware and each diode required unwelcome attention at some point.

Thanks, too, to my colleagues in the lab. Martin and Ken took me under their wing right at the start and introduced me to the idiosyncrasies of chemistry research. Martin provided me with the memory of a Christmas party on the 1st of July, complete with carols and paper hats. Ken had the pleasure of sharing a cottage with me in darkest, coldest Kingask, and the dubious honour of being my best man too! As well as many rounds over the ancient links.

Diane (or Daine) accompanied me on our great adventure in Orlando, Florida (yes, Disney too) for the conference / paid holiday. Thanks for that by the way, and more besides, to the EPSRC. Jukka was a constant source of amusement, moreso before he mastered the English language, and his coq au vin and fine Finnish vodka have gone down in St Andrews’ folklore.

Who else? Josep, for painting the lab red. Mariano, for painting the lab blue. Wojtek, for his funny hat. Sina, and his vesicles. Jenny, for her roses and gloopy solutions. Craig, for his mutterings and his humour. Mark, for his vesicles, again, and for introducing me to fine Turkish food. Zoe, Bruce and Volkmar for welcome distractions. I have many fond memories of our Hungarian colleagues. I have spent many fine evenings with Zsolt, Agnes, Gabor (come on Boris, light my fire!), Tamas and Feri.

Since leaving St Andrews I have relied on both Andy and Avril for regular support and conversation, I think Avril probably understands the offside rule now too. It’s just a shame they are so far away. Similar thanks go to Robert and Heather, for always being so welcoming and such good company, sometimes at short notice! Sorry.

Finally, on a professional level, it would be improper not to mention the following people; Marjorie, Bobby and Melanja. Maryjane and Russell for their work on the crystal structure in Appendix A. And Doug, Martin and Scott for marking my card.

Contents

Declaration, Certification & Copyright	ii
Abstract	iii
Acknowledgements	iv
Table of Contents	v
Index of Tables, Figures and Spectra	viii

Project aims and objectives	1
------------------------------------	----------

Chapter 1 - Introduction	6
---------------------------------	----------

Literature	6
Nuclear Magnetic Resonance (NMR) spectroscopy	12
¹³ C NMR	13
Solid-state ¹³ C NMR	14
Problems experienced in solid-state ¹³ C NMR	14
Dipolar couplings between ¹³ C and ¹ H	14
Chemical Shielding Anisotropy (CSA)	15
Long spin-lattice relaxation times (T ₁) for ¹³ C	15
Techniques used to overcome these problems	15
Cross-Polarisation (CP)	15
Magic Angle Spinning (MAS)	16
The phenomenon of relaxation	17
Spin-lattice (longitudinal) relaxation, T ₁	18
Spin-spin (transverse) relaxation, T ₂	19
T _{1ρ} relaxation	19
The rotating frame of reference	21
Quantification of T _{1ρ} relaxation	22
Calculation of rate constants and activation parameters	23
Line shape analysis	26

Chapter 2 - Calibration of the Variable Temperature Unit (VTU)	27
---	-----------

Survey of existing calibration routines	27
Experimental	29
Descriptions of phase changes used for study	30
Calibration plot and corrective equation	31
Heating effects at various Magic Angle Spinning speeds	33

Use of lineshapes of <i>N</i> -benzyl- <i>tert</i> -butyl- <i>N</i> -methylammonium bromide	35
Relationship of spinning speed to temperature	38
Conclusion	39

Chapter 3 - Synthesis	40
------------------------------	-----------

1,2-Benzenedimethanol	40
<i>cis</i> - and <i>trans</i> -2-(Hydroxymethyl)cyclopentanol	40
preparation of <i>cis</i> -2-(hydroxymethyl)cyclopentanol	42
preparation of <i>trans</i> -2-(hydroxymethyl)cyclopentanol	43
1,1-Di(hydroxymethyl)cyclobutane	44
preparation of diethyl 1,1-cyclobutanedicarboxylate	44
preparation of 1,1-di(hydroxymethyl)cyclobutane	45
1,1-Di(hydroxymethyl)cyclohexane and 1,1-di(hydroxymethyl)cycloheptane	45
<i>N</i> -Benzyl-2-methylcyclobutylamine	46
preparation of pentaerythritol bromide	46
preparation of methylenecyclobutane	48
preparation of <i>N</i> -(1-methylcyclobutyl)-acetamide	49
preparation of 1-methylcyclobutylamine	50
<i>N,N</i> -Dibenzylhexamethyleneiminium bromide	51
<i>N,N</i> -Dibenzylpyrrolidinium bromide	51
Deuteration of relevant diol type compounds	52

Chapter 4 - Preparation of <i>cis</i>- and <i>trans</i>-Cyclopentane-1,3-diol	54
--	-----------

Literature survey	54
Formation of <i>cis</i> -cyclopentane-1,3-diol	59
irradiation reaction of cyclopentadiene with singlet oxygen	60
Formation of <i>trans</i> -cyclopentane-1,3-diol	62
disiamylboronation of cyclopentadiene	63
Formation of <i>cis</i> - and <i>trans</i> -cyclopentane-1,3-diol	64
<i>via</i> deacetylated 3,5-dibromocyclopentene	65
acetylation with 15-crown-5 ether	66
Separation of <i>cis</i> - and <i>trans</i> -cyclopentane-1,3-diol	67
separation using benzaldehyde dimethylacetal	67
separation using <i>n</i> -butylboronic acid	69

Chapter 5 - Diol compounds studied by solid-state CP/MAS NMR	70
Butane-1,4-diol 1	72
2,2-Dimethylpropane-1,3-diol 2	72
investigation of deuteriated 2,2-dimethylpropane-1,3-diol	77
2-Ethyl-2-methyl-propane-1,3-diol 3	79
2,2-Diethylpropane-1,3-diol 4	80
1,1-Di(hydroxymethyl)cyclohexane 5	84
1,1-Di(hydroxymethyl)cycloheptane 6	84
<i>cis</i> -1,2-Cyclopentanediol 7	88
<i>trans</i> -1,3-Cyclopentanediol 8	90
1,2-Dihydroxybenzene (Catechol) 9	90
1,2-Di(hydroxymethyl)benzene 10	92
1,1,1-Tris(hydroxymethyl)ethane 11	94
Pentaerythritol 12	96
Summary	97
Crystallographic data	98
Investigation of deuteriated diols	99
Conclusion	100
Chapter 6 - Tetraalkylammonium halides	101
Drying of samples for the study	102
Tetraethylammonium chloride (TEACl)	104
Tetraethylammonium bromide (TEABr) and iodide (TEAI)	108
Tetrapropylammonium chloride (TPACl)	110
Tetrapropylammonium bromide (TPABr)	112
Tetrapropylammonium iodide (TPAI)	113
Conclusion	114
Chapter 7 - Other compounds studied	115
<i>N,N</i> -Dibenzylhexamethyleneiminium bromide	115
Compounds supplied by Ferenc Fülöp	115
FF/675 Chloride	116
FF/675 Bromide	120
Dihydrooxazine	121
Heterocyclic aldehyde	122
Meldrum's Acid derivatives	122
Experimental	124
Appendix A: Crystal structure of 1,1,1-tris(hydroxymethyl)ethane	134
Appendix B: Computer program to calculate relaxation times	139

Index of Tables, Figures and Spectra

Chapter 2

Table 1	Purity and melting point of temperature standards	29
Table 2	Phase transitions studied as temperature calibration controls	30
Figure 1	Calibration plot of data presented in Table 1	31
Spectra 1	Methyl resonance of pivalic acid around phase change	32
Spectra 2	Lineshapes of methyl coalescence of <i>N</i> -benzyl- <i>tert</i> -butyl- <i>N</i> -methyl-ammonium bromide at 6 kHz	36
Spectra 3	Lineshapes of methyl coalescence of <i>N</i> -benzyl- <i>tert</i> -butyl- <i>N</i> -methyl-ammonium bromide at 286 K	37
Table 3	Temperature as a function of spinning speed	38
Figure 2	Plot of temperature against spinning speed	38

Chapter 3

Table 1	Melting points of protonated and deuteriated diol compounds	53
---------	---	----

Chapter 4

Table 1	Melting points and boiling points of <i>cis</i> - and <i>trans</i> -cyclopentane-1,3-diol	58
Table 2	Melting points of ester derivatives of <i>cis</i> - and <i>trans</i> -cyclopentane-1,3-diol	59
Table 3	Distribution of diol isomers in hydroboration of cyclopentadiene	62

Chapter 5

Table 1	$T_{1\rho}$ data for 2,2-dimethylpropane-1,3-diol	73
Spectra 1	Spectra of 2,2-dimethylpropane-1,3-diol from 240 K to 314 K	74
Spectra 2	Spectra of methyl resonance of 2,2-dimethylpropane-1,3-diol around coalescence at 262 K	75
Figure 1	Plot of $\ln(T_{1\rho})$ against $1/T$ for 2,2-dimethylpropane-1,3-diol	76
Table 2	Energies of activation derived for 2,2-dimethylpropane-1,3-diol	76

Table 3	$T_{1\rho}$ data for deuteriated 2,2-dimethylpropane-1,3-diol	78
Figure 2	Plot of $\ln(T_{1\rho})$ against $1/T$ for O^1H and O^2H 2,2-diethylpropane-1,3-diol	78
Table 4	Energies of activation derived for deuteriated 2,2-dimethylpropane-1,3-diol	79
Table 5	$T_{1\rho}$ data for 2,2-diethylpropane-1,3-diol	80
Spectra 3	Spectra of 2,2-diethylpropane-1,3-diol from 200 K to RT	81
Spectra 4	Spectra of CH_3 resonance of 2,2-dimethylpropane-1,3-diol from 200 K to RT	82
Figure 3	Plot of $\ln(T_{1\rho})$ against $1/T$ for 2,2-diethylpropane-1,3-diol	83
Table 6	Energies of activation derived for 2,2-diethylpropane-1,3-diol	83
Table 7	$T_{1\rho}$ data for 1,1-di(hydroxymethyl)cycloheptane	85
Spectra 5	Spectra of di(hydroxymethyl)cycloheptane from 284 K to 323 K	86
Figure 4	Plot of $\ln(T_{1\rho})$ against $1/T$ for 1,1-di(hydroxymethyl)cycloheptane	87
Table 8	Energies of activation derived for 1,1-di(hydroxymethyl)-cycloheptane	87
Spectra 6	Spectra of <i>cis</i> -cyclopentane-1,2-diol from 200 K to 268 K	89
Spectra 7	Spectra of <i>trans</i> -cyclopentane-1,3-diol from 192 K to 240 K	91
Spectra 8	Spectra of catechol from 200 K to 320 K	93
Spectra 9	Spectra of 1,1,1-tris(hydroxymethyl)ethane from RT to 354 K	95
Table 9	Activation energy (E_a) data for diol compounds	97
Table 10	Free energy of activation (ΔG^\ddagger_C) data for diol compounds	98
Table 11	Coalescence data for deuteriated diol compounds	99

Chapter 6

Table 1	Differential Scanning Calorimetry data for tetraalkylammonium halides	101
Table 2	Purity and melting point of tetraalkylammonium halides	102
Spectra 1	Spectra of TEACl from RT to 354 K	105
Table 3	$T_{1\rho}$ data for TEACl	106
Figure 1	Plot of $T_{1\rho}$ against temperature for methyl carbons of TEACl	106
Figure 2	Plot of $\ln(T_{1\rho})$ against $1/T$ for TEACl	107
Table 4	Energies of activation derived for TEACl	107
Spectra 2	Spectra of TEABr from 318 K to 366 K	109
Table 5	$T_{1\rho}$ data for TPACl	111
Table 6	$T_{1\rho}$ data for TPABr	112

Chapter 7

Table 1	Melting points of FF/675 salts	116
Table 2	$T_{1\rho}$ data for FF/675 chloride	117
Figure 1	Plot of $T_{1\rho}$ against temperature for FF/675 chloride	117
Table 3	Correlation times and rate constants derived for methyl carbons of FF/675 chloride	118
Figure 2	Plot of $\ln(k)$ against $1/T$ for FF/675 chloride	119
Table 4	Energy of activation derived for methyl of FF/675 chloride	119
Table 5	$T_{1\rho}$ data for FF/675 bromide	120
Figure 3	Plot of $T_{1\rho}$ against temperature for FF/675 bromide	121

Dedication

I dedicate this thesis to the people who mean the most to me.

Firstly, to my family.

My mum and dad and my sister Brenda, who have sometimes found it hard to understand why I have been in St Andrews for the last eight years. And David and the boys, Marc and Ryan, I will always look out for you.

Most importantly, to my wife, Claire.

For everything.

Project aims and objectives

Conformational or intramolecular motions in organic molecules in the solution or gas phases are most readily followed by dynamic NMR techniques.^{1,2} The most widely used technique is dynamic line broadening which arises when the rate of the intramolecular process (e.g. ring inversion or bond rotation) is about the same as the chemical shift difference (in Hz) between the exchanging sites. It should be noted that this technique is applicable to a narrow band of motional frequencies, typically in the range 10 to 10^4 s^{-1} . This limited range automatically limits the precision of any activation parameter determination. The range can be extended to somewhat slower rate regimes (down to *ca.* 10^{-1} s^{-1}) by magnetisation transfer or 2D EXSY methods, which rely on the exchange taking place on a timescale comparable with the nuclear relaxation time. A large body of literature exists in this area and the conformational analysis of organic molecules in solution is well understood.^{1,3} Much less is known about conformational motions of molecules in solids.

Many of the interactions present in solids that give rise to effects in their NMR spectra are averaged out in solution by rapid isotropic molecular tumbling. Because of these interactions, intramolecular motions in crystalline organic solids can be followed by a wider variety of NMR techniques extending over a much greater range of rates than in solution. Until recently this field has been dominated by NMR physicists. We now seek to join experienced organic chemists, chemical crystallographers and NMR physicists in a serious attempt to examine chemically interesting cases, relate activation parameters to solid-state structure as well as developing new computational methods to assist in extracting rate information from solid-state NMR measurements.

For static crystalline samples quadrupolar splitting samples in the ^2H spectra of deuteriated molecules arise from an interaction of the nuclear quadrupole with local electric field gradients. The latter are associated with chemical bonds. Motions that

¹ Sandstrom J., *Dynamic NMR Spectroscopy*, Academic Press, London, (1982)

² Ross B. D., True N. S., *J. Amer. Chem. Soc.*, **105**, (1983) 4871

produce a directional averaging give rise to a spectral frequency change similar to that mentioned above for liquids, but in a higher rate range (*ca.* 10^3 to 10^5 s^{-1}). Fluctuating electric field gradients also produce spin lattice relaxation of the 2H nucleus and the correlation time for the motion can be inferred if details of the quadrupole interaction are known. Modulation of the electric field gradient in molecular solids is usually produced by rotational molecular or segmental motion. This technique has proved of particular value in chain-like structures, e.g. polymers or lipids where selective deuteration along the chain can characterise the motion of different segments. This approach is most sensitive to motions near to the 2H resonance frequency (10^7 to 10^8 s^{-1}).

Here, however, we are concerned with ^{13}C CP/MAS NMR which gives high resolution solid-state spectra. In CP/MAS NMR, magnetisation transfer and 2D EXSY methods give access to slower rates than in NMR because of the much longer ^{13}C spin lattice (T_1) relaxation times (down to 10^{-3} s^{-1}). Dynamic line broadening in solids gives rates in the same range as for solutions. At faster rates the method of maximum dynamic line broadening has been fairly widely employed.⁴ This arises when the rate of the incoherent molecular motion is similar to the rate of the coherent precessional frequency of the decoupling radio frequency field. This reduces the decoupling efficiency, broadens the lines and gives a single rate constant in the region $5-10 \times 10^4$ s^{-1} .

At the University of Kent, Canterbury, it was proposed to develop a series of computer programs to allow the calculation of B^2 values for a given molecular geometry and a given mode of molecular motion. The programs would be of a general nature and allow data to be input either from known molecular motions such as those contained in the Cambridge Crystallographic Data Base, or from a crude molecular structure which is then refined using, for example, MM2 calculations to give a better molecular geometry. The molecular geometry would then be used to calculate values for the ^{13}C - 1H dipolar

³ Riddell F. G., *The Conformational Analysis of Heterocyclic Compounds*, Academic Press, London, (1980)

⁴ Rothwell W. P., Waugh J. S., *J. Chem. Phys.*, **74**, (1981) 2721

interaction. The interaction dependence on the orientation of the crystallite and all internuclear vectors, both inter- and intramolecular, must be taken into account and lattice sums constructed. It is common as in, for example, the *tert*-butyl systems⁵ for some interactions to be averaged out by the very rapid motions (CH_3 in this case) and these become ineffective in the relaxation process of interest. It is necessary, therefore, to take account of this rapid motion, calculate the residual interaction and thus the fraction of this that is actually modulated by the motion in order to calculate B^2 . The theoretically calculated values of B^2 for the mode(s) of motion will then be used for comparison with the experimentally derived values, or as an input to calculate rates of intramolecular motions from relaxation data where B^2 was not available experimentally. A second program linked to the first would then be able to take $T_{1\rho}$ data derived experimentally as a function of temperature and calculate best fit rate data.

In St Andrews work would concentrate on synthesis of appropriate compounds, solid-state NMR measurements and the X-ray crystallography. The types of molecular motion to search for in the solid state have been guided by the “principle of least distress”, the basic idea of which is that the conformational motions most likely to be observed in the solid are those that cause least distress to the lattice structure of the solid.^{5,6,7,8,9,10,11} Accordingly, conformational changes that have low volume changes during the molecular motion have been looked at first. It was intended to extend the work into functional groups that have progressively larger volume changes.

The initial experimental work within the group has been on *tert*-butyl group rotations,^{5,10,11} and has recently been extended to rotations of trimethylammonium,⁸ ethyl,⁹ *iso*-propyl⁸ *tert*-amyl⁸ and phenyl groups.^{6,7} The work has also extended into

⁵ Riddell F. G., Arumugam S., Harris K. D. M., Rogerson M., Strange J. H., *J. Am. Chem. Soc.*, **115**, (1993) 1881

⁶ Riddell F. G., Bruce P. G., Lightfoot P., Rogerson M., *J. Chem. Soc., Chem. Commun.*, (1994) 209

⁷ Riddell F. G., Bremner M., Strange J. H., *Magn. Reson. Chem.*, **32**, (1994) 118

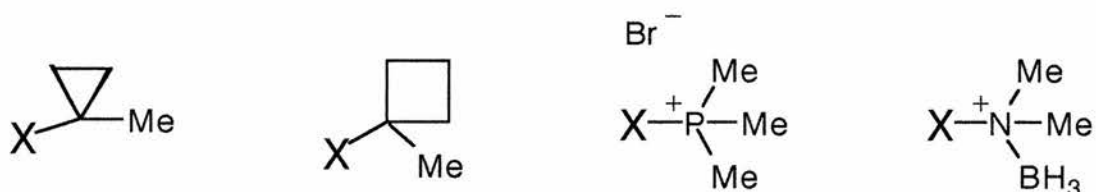
⁸ Riddell F. G., Rogerson M., *J. Chem. Soc., Perkin Trans. 2*, (1996) 493

⁹ Riddell F. G., Cameron K. S., Alder R., unpublished results

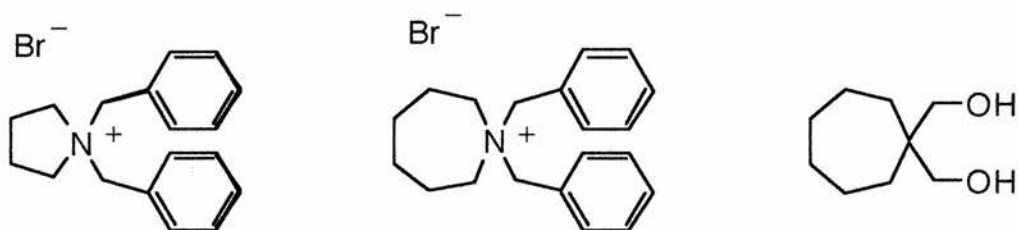
¹⁰ Riddell F. G., Fülöp F., unpublished results

other motions such as pseudorotations of five- and seven-membered rings. The idea behind the design of molecules to study has been to have the conformationally interesting motion in one segment of the molecule and to connect that to a larger portion of the molecule likely to have sufficiently strong intermolecular interactions that would form a rigid reference frame. These molecules should be amenable to standard syntheses with as few steps as possible.

It is now proposed to extend the range of groups for study while keeping the same general approach to the chemistry. Typically interesting types of structure for the study of bond rotations and for comparison with *tert*-butyl and similar groups include, for example the following, where X is the section of the molecule that will act to form a rigid reference frame in the crystal structure:



Typically interesting ring pseudorotations should be found in compounds such as:



In addition the work of Dobson *et al.* has shown that 180° rotations of phenyl groups in solids are observable by CP/MAS NMR.¹² In particular they have used dynamic lineshape changes and maximum dynamic broadening, but not $T_{1\rho}$ relaxation measurements, to measure the rates of these rotations. There are several examples where phenyl rotations in organic solids can be studied by a combination of $T_{1\rho}$, lineshape analysis and 2D EXSY methods.^{6,7,8}

¹¹ Riddell F. G., Arumugam S., Anderson J. E., *J. Chem. Soc., Chem. Commun.*, (1991) 1525

¹² Twyman J. M., Dobson C. M., *J. Chem. Soc., Chem. Commun.*, (1988) 786

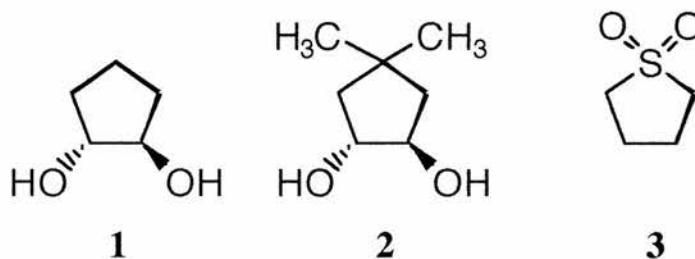
As indicated earlier, ^2H NMR can also give information about some of these types of molecular motions. However, the approach described here is preferable; (1) there is no need to prepare specifically deuteriated compounds to study, (2) the ^{13}C resonances in CP/MAS spectra are much sharper and are immediately assigned, and (3) in many cases the rates can be measured by magnetisation transfer or 2D EXSY, lineshape analysis, $T_{1\rho}$ and maximum dipolar broadening,⁷ covering a far greater rate range than is possible with ^2H NMR. The ^2H and ^{13}C methods are complementary, but in the systems described here the ^{13}C CP/MAS method is superior because of the different but complementary techniques that can be used to check for internal consistency and give a much greater temperature (and therefore rate) range with consequently better activation parameters.

The School of Chemistry in St Andrews is ideally equipped to carry out the experimental part of this work, with a suitably high field solid-state NMR spectrometer (Bruker MSL500) and additional expertise in X-ray crystallography. The Physics Department in Canterbury has substantial expertise in the application of solid-state NMR measurements, particularly of relaxation times, to problems of molecular motions in solids, in the preparation of computer programs for the evaluation of NMR data and in the computer simulation of molecular motions. The combination of the two departments offers the skills in organic chemistry, experimental and theoretical solid-state NMR, computer programming and X-ray crystallography which are required.

Introduction

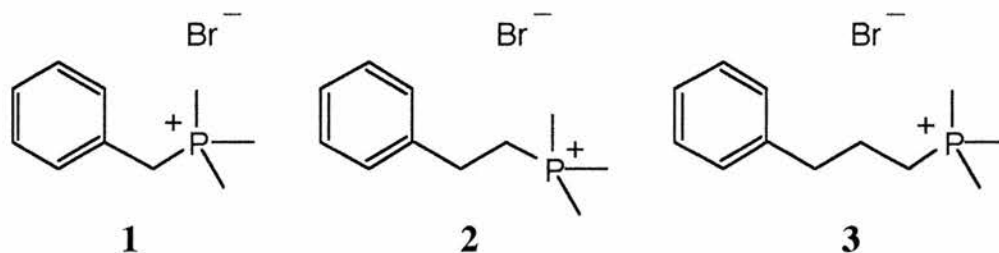
Literature

Five-Membered Ring Rotations, Pseudorotations and Hydrogen Bond Exchange Dynamics in the Solid State Studied by NMR Spectroscopy¹



¹³C CP/MAS NMR studies were carried out on *trans*-cyclopentane-1,2-diol **1**, 4,4-dimethyl-*trans*-cyclopentane-1,2-diol **2** and sulfolane **3** at various temperatures. The results strongly indicate that pseudorotation processes are occurring and that there are dynamic hydrogen bond exchange processes occurring also. The nature of the process in sulfolane is a molecular reorientation about an internal C₂ axis, although pseudorotation cannot be ruled out. The activation energy for ring pseudorotation in **2** is *ca.* 30 kJ mol.⁻¹, and assuming the activation energy for dynamic hydrogen bond exchange is 50-60 kJ mol.⁻¹, then the observed activation energy of 77 kJ mol.⁻¹ for **1** is the sum of the ring pseudorotation and hydrogen bond exchange processes.

Intramolecular Motions in Crystalline Phosphonium Salts Studied by ³¹P and ¹³C CP/MAS NMR Spectroscopy²



¹ Riddell F. G., Cameron K. S., Holmes S. A., Strange J. H., *J. Am. Chem. Soc.*, **119**, (1997) 7555

² Riddell F. G., Rogerson M., Turnbull W. B., Fülöp F., *J. Chem. Soc., Perkin Trans. 2*, (1997) 95

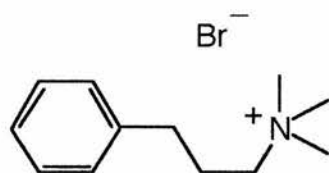
Three homologous trimethylphosphonium bromides with benzyl **1**, 2-phenylethyl **2** and 3-phenylpropyl **3** groups were synthesised and studied by solid-state NMR. For **2** and **3** a combination of dynamic lineshape changes and $T_{1\rho}$ measurements of ^{13}C and ^{31}P nuclei allowed the activation parameters to be derived. There was excellent agreement between the three independent NMR methods for the rates of rotation and activation parameters of the rotation processes. Variability in the activation parameters was apparent with free energy of activation varying from less than 30 to 43 kJ mol^{-1} . Crystallographic data provided for **2**.

Intramolecular Motions in a series of Crystalline Benzylammonium Bromides and Dibenzylamines Studied by CP/MAS NMR³

A series of 15 compounds including ammonium bromides containing one or two benzyl groups with H, methyl, *iso*-propyl, *tert*-butyl and *tert*-amyl substituents and dibenzylamine with *N-iso*-propyl, *N-tert*-butyl and *N-tert*-amyl substituents were synthesised and studied by CP/MAS NMR. The results suggest there is a dramatically wide range of molecular motions occurring in this simple series of compounds. A combination of 2D EXSY, dynamic lineshape analyses and $T_{1\rho}$ measurements revealed the extent of intramolecular group motions, including rotations of methyl, *tert*-butyl, *tert*-amyl and phenyl groups. Rates of rotation and activation parameters are derived where appropriate. In the case of benzyl-*tert*-butylammonium bromide, which has two independent molecules in the asymmetric unit, the independent processes of *tert*-butyl rotation in the two molecules have vastly different activation energies that differ by *ca.* 16 kJ mol^{-1} .

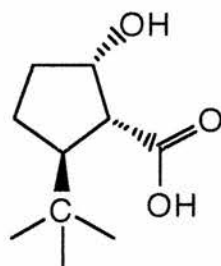
³ Riddell F. G., Rogerson M., *J. Chem. Soc., Perkin Trans. 2*, (1996) 493

Dynamic Processes in Solids: Three Large-Amplitude Processes Revealed in a Simple Quaternary Ammonium Salt⁴



¹³C CP/MAS NMR spectra of trimethyl(3-phenylpropyl)ammonium bromide showed evidence of three independent rotational processes; in order of increasing activation energy they are methyl rotation ($\Delta G^\ddagger_{200\text{ K}} = \text{ca. } 30 \text{ kJ mol.}^{-1}$), trimethylammonium rotation ($E_a = 41.6 \text{ kJ mol.}^{-1}$, $\Delta G^\ddagger_{246\text{ K}} = \text{ca. } 43.4 \text{ kJ mol.}^{-1}$) and phenyl rotation ($\Delta G^\ddagger_{305\text{ K}} = \text{ca. } 55 \text{ kJ mol.}^{-1}$). The rotation of the other two *N*-methyl groups is not measurable by CP/MAS NMR and so must be rotating faster than the one that is observed to broaden.

Phase Dependence of Conformational Motions in Solids. The *tert*-Butyl Rotation in (1*R**, 2*S**, 5*R**)-5-*tert*-Butyl-2-hydroxycyclopentanecarboxylic acid⁵



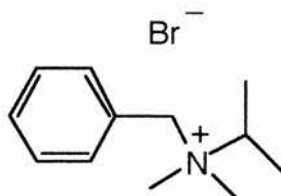
(1*R**, 2*S**, 5*R**)-5-*tert*-butyl-2-hydroxycyclopentane carboxylic acid exists in several solid phases, two of which were investigated in this paper: phase I obtained by crystallisation and phase II obtained by heating above 70 °C. Phase II appears to be the stable phase at ambient temperature. Phase III, which reverts to phase II on standing at room temperature, is obtained by cooling the melt to room temperature.

The rates of rotation of the *tert*-butyl groups in phases I and II were measured by ¹³C CP/MAS NMR techniques. The activation parameters for the *tert*-butyl group rotation differ markedly between the two phases: phase I, $\Delta H^\ddagger = 59.0 \pm 2.1 \text{ kJ mol.}^{-1}$

⁴ Riddell F. G., Cameron K. S., Turnbull W. B., *Magn. Reson. Chem.*, **33**, (1995) 841

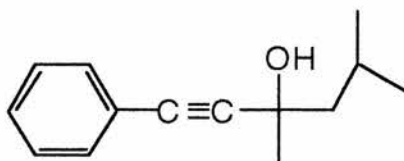
and $\Delta S^\ddagger = 51.6 \pm 8.1 \text{ J K}^{-1} \text{ mol}^{-1}$; and phase II, $\Delta H^\ddagger = 43.9 \pm 2.5 \text{ kJ mol}^{-1}$ and $\Delta S^\ddagger = 28.3 \pm 9.3 \text{ J K}^{-1} \text{ mol}^{-1}$. The structure of phase I has been solved by X-ray diffraction.

Probing Molecular Motion by Solid-State NMR Spectroscopy and High Resolution Powder X-Ray Diffraction⁶



Benzyltrimethylammonium bromide showed evidence of a high activation energy for rotation of one of the *N*-methyl groups ($E_a = 28 \text{ kJ mol}^{-1}$) whilst a powder X-ray diffraction study showed that one of the *N*-methyl groups was exceptionally hindered in the solid.

¹³C CP/MAS NMR Study of a Phenyl Group Rotation in the Solid-State Using $T_{1\rho}$, Lineshape and 2D EXSY Measurements⁷

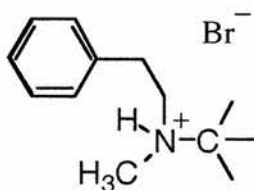


3,5-Dimethyl-1-phenylhex-1-yn-3-ol was studied using $T_{1\rho}$ measurements, lineshape analysis and 2D EXSY over the temperature range 219-284 K. Lineshape and 2D EXSY methods gave energy of activation for the phenyl rotation of $58.6 \pm 3.0 \text{ kJ mol}^{-1}$. In good agreement with this $T_{1\rho}$ measurements gave an activation energy for the rotation of $58.7 \pm 3.6 \text{ kJ mol}^{-1}$.

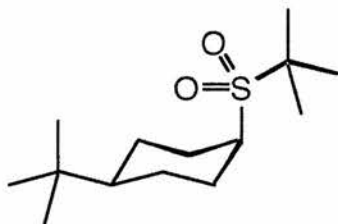
⁵ Riddell F. G., Bernáth G., Fülöp F., *J. Am. Chem. Soc.*, **117** (1995) 2327

⁶ Riddell F. G., Bruce P. G., Lightfoot P., Rogerson M., *J. Chem. Soc., Chem. Commun.*, (1994) 209

⁷ Riddell F. G., Bremner M., Strange J. H., *Magn. Reson. Chem.*, **32**, (1994) 118

Activation parameters of *N*-(2-phenylethyl)-*N*-methyl-*tert*-butylammonium bromide⁸

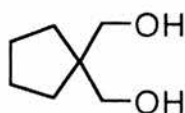
Activation parameters were derived for *N*-(2-phenylethyl)-*N*-methyl-*tert*-butylammonium bromide; $\Delta H^\ddagger = + 51.8 \text{ kJ mol.}^{-1}$, $\Delta S^\ddagger = + 19.6 \text{ J K}^{-1} \text{ mol.}^{-1}$ and $\Delta G^\ddagger_{298 \text{ K}} = + 45.6 \text{ kJ mol.}^{-1}$.

A ¹³C CP/MAS NMR Study of a Double *tert*-Butyl Group Rotation in the Solid State Using $T_{1\rho}$ and Lineshape Measurements⁹

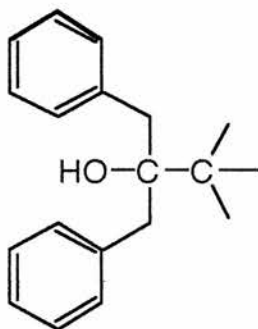
cis-4-*tert*-Butyl-1-(*tert*-butylsulfonyl)cyclohexane was studied using lineshape analysis and $T_{1\rho}$ measurements over the temperature range 202-320 K. The 1-*tert*-butylsulfonyl group shows $\Delta H^\ddagger = 38.2 \pm 1.5 \text{ kJ mol.}^{-1}$ and $\Delta S^\ddagger = + 9.4 \pm 5.9 \text{ J K}^{-1} \text{ mol.}^{-1}$. The 4-*tert*-butyl group shows $\Delta H^\ddagger = 33.5 \pm 3.2 \text{ kJ mol.}^{-1}$ and $\Delta S^\ddagger = + 10.3 \pm 13.5 \text{ J K}^{-1} \text{ mol.}^{-1}$.

⁸ Spark R. A., Senior Honours Project report, University of St. Andrews, (1994)

⁹ Riddell F. G., Arumugam S., Harris K. D. M., Rogerson M., Strange J. H., *J. Am. Chem. Soc.*, **115**, (1993) 1881

Free energy of activation data for 1,1-di(hydroxymethyl)cyclopentane¹⁰

Data were derived for free activation of energy for 1,1-di(hydroxymethyl)cyclopentane; $\Delta G_{313 \pm 2 \text{ K}}^{\ddagger} = + 60.8 \text{ kJ mol.}^{-1}$ derived from coalescence of $\underline{\text{C}}\text{H}_2\text{OHs}$ and $\Delta G_{315 \pm 2 \text{ K}}^{\ddagger} = 60.2 \text{ kJ mol.}^{-1}$ derived from coalescence of ring CH_2s .

Restricted C-C Bond Rotation in a Solid Measured by Solid State NMR Spectroscopy¹¹

1,1-Dibenzyl-2,2-dimethylpropan-1-ol showed a coalescence phenomenon in its ¹³C solid state CP/MAS NMR spectrum consistent with slowing of rotation of the *tert*-butyl group about the C(1)-C(2) bond with an activation energy of $54.8 \text{ kJ mol.}^{-1}$, 16 kJ mol.^{-1} higher than in solution.

¹⁰ Ross S. R., Senior Honours Project report, University of St. Andrews, (1992)

¹¹ Riddell F. G., Arumugam S., Anderson J. E., *J. Chem. Soc., Chem. Commun.*, (1991) 1525

Nuclear Magnetic Resonance (NMR) spectroscopy

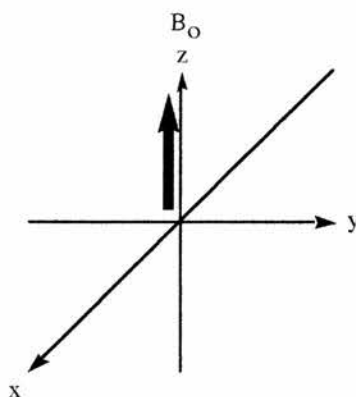
Atomic nuclei observable by NMR have a nuclear spin quantum number, I , which makes them behave in a similar way to tiny bar magnets when subjected to a magnetic field, B_0 . The magnetic moments of each nucleus can align themselves in $(2I + 1)$ ways. ^1H and ^{13}C both have $I = 1/2$, so they can align themselves in one of two ways; in the direction of the magnetic field (low energy state), or against the direction of the field (high energy state). The precessional frequency of the nuclei in the external field is ω_0 (the Larmor frequency) and is directly proportional to the strength of the external field, B_0 :

$$\omega_0 = \gamma B_0$$

where, B_0 = strength of external field

γ = magnetogyric ratio (constant for a given nucleus)

The vector sums of the millions of nuclear magnets give rise to a net nuclear magnetisation parallel to the magnetic field, B_0 .



A powerful radiofrequency (RF) pulse is then applied close to the Larmor frequency, the effect being to excite some of the nuclei. The RF pulse serves to generate an electromagnetic field along the x -axis and to tip the magnetisation towards the xy plane. The magnetisation now precesses in the xy plane at the Larmor frequency.

However, the excited nuclei lose their extra energy and relax back along the z -axis. A receiver coil picks up the resultant oscillation of magnetisation in the xy plane during what is called the acquisition period, and gives a complicated wave pattern called

the free induction decay (FID). The FID contains frequency information about all of the nuclear spins. The FID is converted into a frequency spectrum by Fourier transform, which is a mathematical conversion of the interference pattern.

This project involves gathering information on the compounds by ^{13}C NMR spectroscopy in the solid state. Historically, huge problems have had to be overcome to make these techniques more common in the modern laboratory.

^{13}C NMR

Carbon-13 NMR has several advantages over proton NMR in terms of its power to elucidate organic structures.¹² First, ^{13}C NMR provides information about the backbone of the molecule rather than the periphery. In addition, the chemical shift range for ^{13}C in a number of compounds is about 200 ppm, compared with only up to about 15 ppm for ^1H ; less overlap of peaks is the consequence. Because the natural abundance of ^{13}C is only about 1.1 %, spin-spin coupling between carbon nuclei is a rare occurrence since chances of having two ^{13}C adjacent in the same molecule are negligible, and ^{13}C - ^{12}C coupling does not occur because $I = 0$ for ^{12}C . Finally, good methods exist for decoupling the interaction between ^{13}C and ^1H , giving carbon spectra consisting of only single lines.

Analysis of the ^1H nucleus is relatively easy because of its high abundance (99.98 %) and high sensitivity. Carbon-13 accounts for only 1.1 % of carbon nuclei, and the small magnetogyric ratio, which is about 0.25 that of the proton, combine to make ^{13}C NMR about 5700 times less sensitive than ^1H NMR.

The most important developments in ^{13}C signal enhancement include high field strength magnets, Fourier transform instruments, and ^1H decoupling by double resonance techniques. Without these developments, the method would be restricted to the study of highly soluble low-molecular weight solids, neat liquids and isotopically enriched compounds.

¹² Skoog D. A., Leary J. J., Principles of Instrumental Analysis, 4th Ed., Saunders College Publishing, Fort Worth, (1992) 344

Solid-state ^{13}C NMR^{13,14}

NMR of solid materials is still a less popular spectroscopic technique than high resolution solution NMR. It is interesting to note that the very first NMR experiments were carried out on both liquids and solids, in fact the first ^1H observation was on paraffin wax. However, it soon became evident that conventional high resolution techniques were not possible for solids.

Problems experienced in solid-state ^{13}C NMR

The main difference between the measurement of molecular dynamics in the liquid and solid states is the timescale involved and the geometry of the molecular motions. These affect the signal by modulating interactions between the spins and their environment. There are three principal reasons why high resolution spectra are difficult to achieve for solids:

Dipolar couplings between ^{13}C and ^1H

Heteronuclear dipolar couplings between ^{13}C and ^1H , which are of the order of tens of kHz, produce severe line broadening because they are dependent on the angle between the ^1H - ^{13}C vector and the magnetic field. Whilst isotropic tumbling averages out these interactions in solution, this cannot happen in a normal solid. Strong homonuclear dipolar couplings between ^{13}C spins can be neglected due to the low natural abundance of ^{13}C (*ca.* 1.1 %). In such diluted spin systems the heteronuclear dipolar interactions between ^1H and ^{13}C are dominant.

¹³ Blümli P., Blümich B., *Spectroscopy Europe*, **7**, (1995) 8

¹⁴ Kalinowski H.-O., Berger S., Braun S., *Carbon-13 NMR Spectroscopy*, Wiley, Chichester, (1988) 79

Chemical Shielding Anisotropy (CSA)

The orientation dependent magnetic shielding of the nuclear spins, which gives rise to the CSA, typically lead to a broadening of the ^{13}C resonance of about 10 kHz at a magnetic field of 4 Tesla. Different molecular orientations give rise to many lines for each resonance on the NMR spectrum, which is observed as severe line broadening. Rapid molecular motion for solutions again averages out the effect to zero.

Long spin-lattice relaxation times (T_1) for ^{13}C

Molecular motions in solids are reduced when compared to liquids and so the dipolar relaxation produced as a result of molecular tumbling in liquids is virtually absent.

The dependence of ^{13}C NMR spectra on the distribution of orientations, as well as on the slow motions of the molecules, provides the main applications of NMR spectroscopy. It is useful to investigate samples in the solid state since their physical properties are of more interest than their chemical structure. In addition, the chemical structure can be analysed using "liquid-like" solid-state NMR spectra which can be generated by special experimental techniques.

Techniques used to overcome these problems

Difficulties posed by reduced molecular motions in solids can be overcome by ^1H high power decoupling, and the techniques collectively known as CP/MAS (cross-polarisation / magic angle spinning) NMR.

Cross-Polarisation (CP)

The strong magnetic moment and high abundance of the ^1H nucleus can be utilised to enhance the signal intensity of the ^{13}C spins. Utilisation of this technique to observe ^{13}C resonances is called cross-polarisation.

A 90° ^1H pulse is first applied along the x' -axis. The phase of the ^1H transmitter is then shifted 90° along the y' -axis to spin lock the ^1H magnetisation, and the ^{13}C transmitter is turned on so that both RF fields meet the Hartmann-Hahn condition:

$$\gamma_{\text{C}}B_{\text{IC}} = \gamma_{\text{H}}B_{\text{IH}}$$

Under these conditions, the magnetisation from the large ^1H reservoir is transferred into the ^{13}C spin system.

After use of the dipolar couplings between ^1H and ^{13}C for cross-polarisation, the couplings become a nuisance as they give rise to line broadening. The broadening can be removed by applying a particularly intense dipolar decoupling (DD) field (typically 50-100 kHz, *ca.* 100 Watts power) on the ^1H channel during acquisition of the ^{13}C signal, for which a specially designed probe is essential. However, the signals are still broadened by chemical shielding anisotropy (CSA).

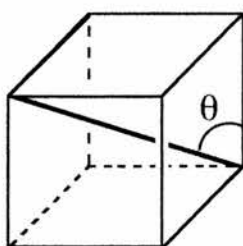
Magic Angle Spinning (MAS)

The chemical shielding anisotropy broadening, and also the dipolar coupling, are proportional to $(3\cos^2\theta - 1)$ where θ is the angle between the magnetic field and the internuclear vector. This term vanishes at 54.7° , the "magic angle", where the sample is observed to imitate the motions of the molecules in a liquid.

$$\text{i.e. when } (3\cos^2\theta - 1) = 0$$

$$\theta = 54^\circ 44' \text{ (} 54.7^\circ \text{)}$$

The magic angle, 54.7° , is the angle created when a diagonal vector adjoins the opposite vertices of a cube.



If the entire sample is mechanically rotated at this angle with a frequency higher than the chemical shift anisotropy, then the CSA vanishes from the spectrum. At lower spinning speeds a series of spinning sidebands, whose intensity is similar to the CSA pattern, is observed.

For MAS, the solid sample is placed inside a small turbine called a rotor which is air-borne and driven by a stream of gas. This limits the speed of rotation to typically 10 kHz, although nowadays supersonic turbines and probes are available. The spectrum consists of centre bands and sidebands which occur at multiples of the spinning frequency. These sidebands can be removed either by higher spinning speeds or by a total suppression of spinning sidebands (TOSS) pulse sequence.

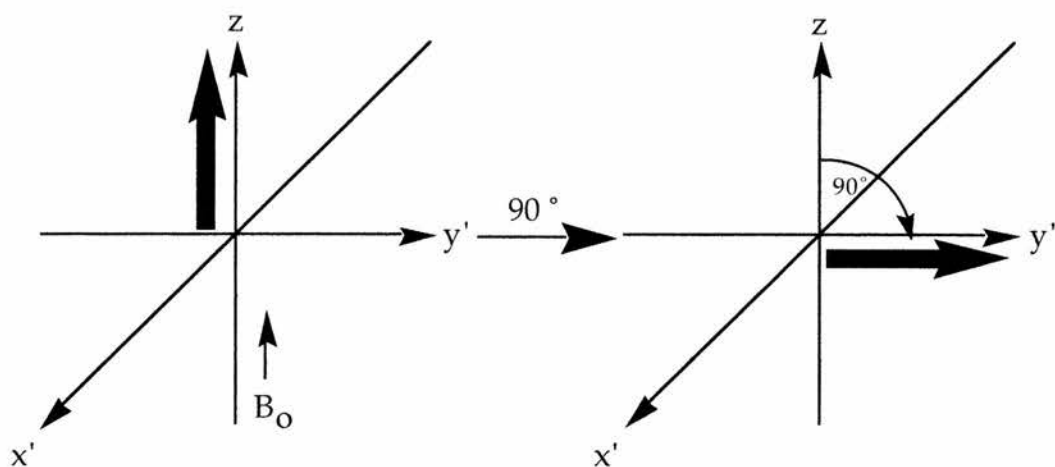
When combining these techniques, the acquisition of high resolution ^{13}C spectra for solids is now made possible.

The phenomenon of nuclear relaxation

Initially, the nuclei are precessing around the z-axis. An RF pulse can then be applied which rotates the nuclei away from the z-axis. The extent of rotation depends on the length of the pulse t_p as given by the equation:

$$\alpha = \gamma B_1 t_p$$

where α is the angle of rotation in radians. For many pulse NMR experiments, a pulse length is chosen so that α is 90° or $\pi/2$ radians.



Typically the time required to achieve this angle is 1 to 10 μs , depending upon the magnitude of B_1 . Once the pulse is terminated, nuclei begin to relax and return to their equilibrium position around the z -axis. Relaxation takes place by one of two independent mechanisms,¹⁵ one involving spin-lattice interactions and the other spin-spin interactions. After several seconds, these interactions cause the nuclei to return to their original state.

Spin-lattice (longitudinal) relaxation, T_1

Spin-lattice relaxation (also known as longitudinal relaxation) is characterised by a relaxation time T_1 , which is a measure of the average lifetime of the nuclei in the higher energy state. T_1 is dependent upon the magnetogyric ratio of the absorbing nuclei and the mobility of the lattice. It can be seen that spin-lattice relaxation takes place along the z -axis and the magnetisation along the z -axis increases until it returns to its original value. Spin-lattice relaxation is most effective when molecular motions are close to the Larmor frequency.

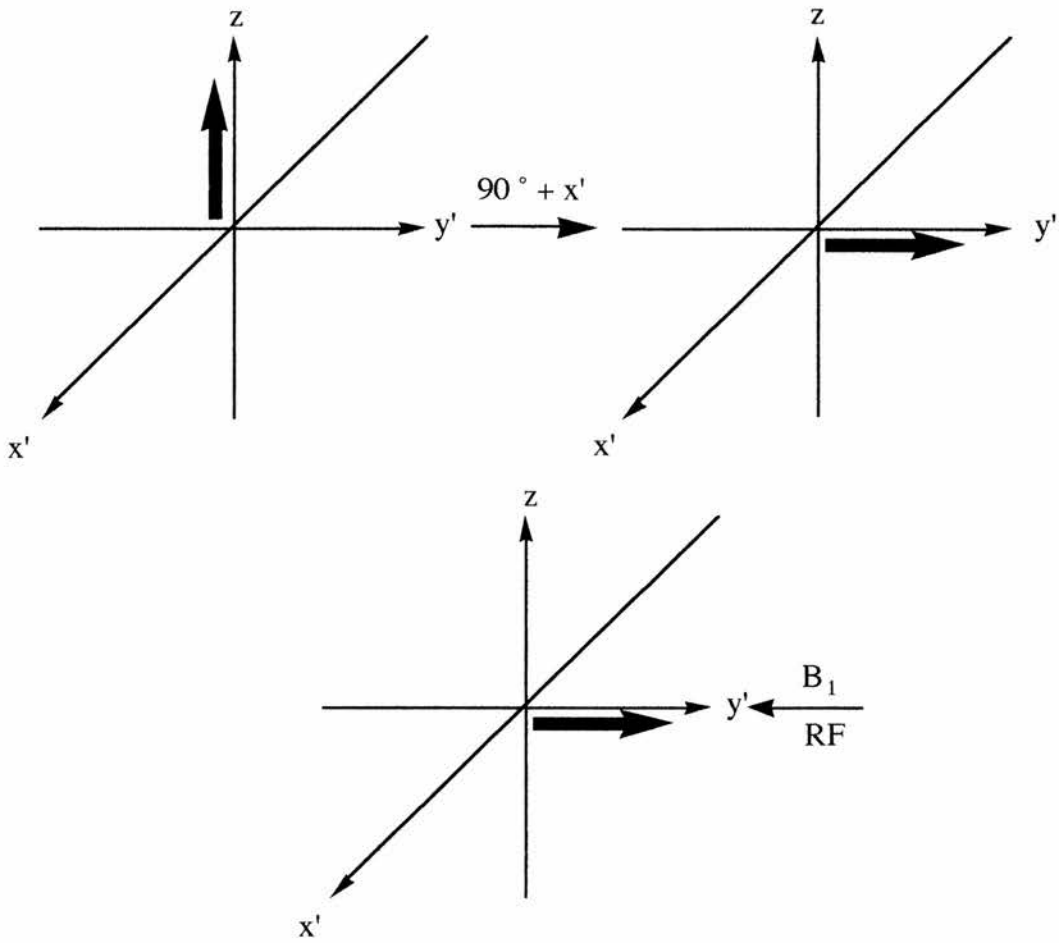
¹⁵ Abraham R. J., Fisher J., Loftus P., Introduction to NMR Spectroscopy, Wiley, Chichester, (1988) 82 Introduction.

Spin-spin (transverse) relaxation, T_2

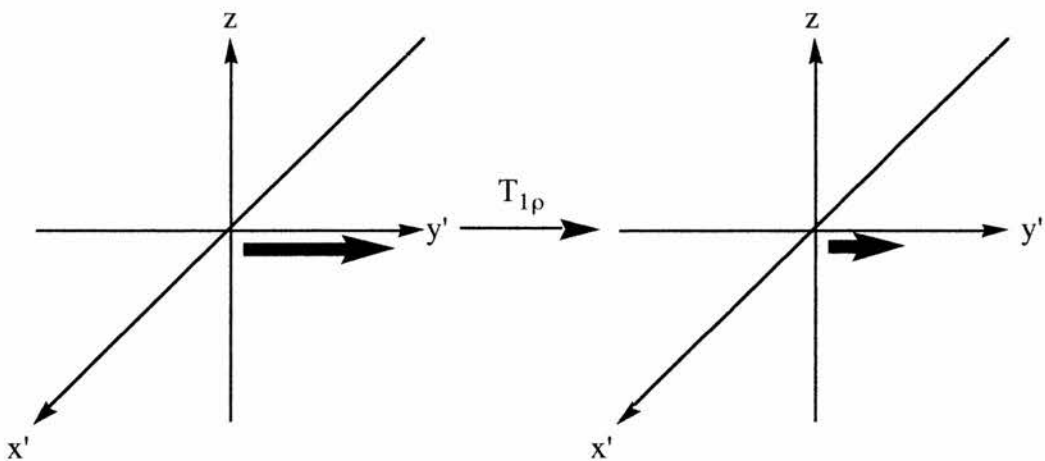
Spin-spin relaxation (also known as transverse relaxation) is characterised by a relaxation time T_2 , which is due to a combination of effects. For many liquids, T_2 and T_1 are about the same, but for most crystalline solids T_2 is so small (as low as 10^{-4} s) as to preclude the use of samples of these kinds for high-resolution spectra unless special techniques are employed. In spin-spin relaxation, nuclei exchange spin energy with one another so that some now precess faster than the Larmor frequency, whereas others travel more slowly. The result is that the spins begin to fan out in the xy plane. Ultimately, this leads to a decrease to zero of the magnetic moment along the y-axis. It is clear that no residual magnetic component can exist in the xy plane by the time relaxation is complete along the z-axis, which means that $T_2 \leq T_1$.

 $T_{1\rho}$ relaxation

The spins of the nuclei are aligned in the magnetic field along the z-axis, and are precessing at frequencies in the MHz range (the Larmor frequency). If a 90° pulse is applied along the x'-axis the spins are flipped over onto the y'-axis. A radiofrequency field B_1 (typically 20-100 kHz), which is very much smaller than B_0 (125.758 MHz), can then be used to spin lock the magnetisation along the y'-axis.



The nuclei then precess around the y' -axis at the frequency of the spin locking field. The magnetisation of spins, immediately on cessation of the RF pulse, begins to decay with time from the y' -axis back to the z -axis. The mechanism of this relaxation can best be described as spin-lattice relaxation in the rotating frame.

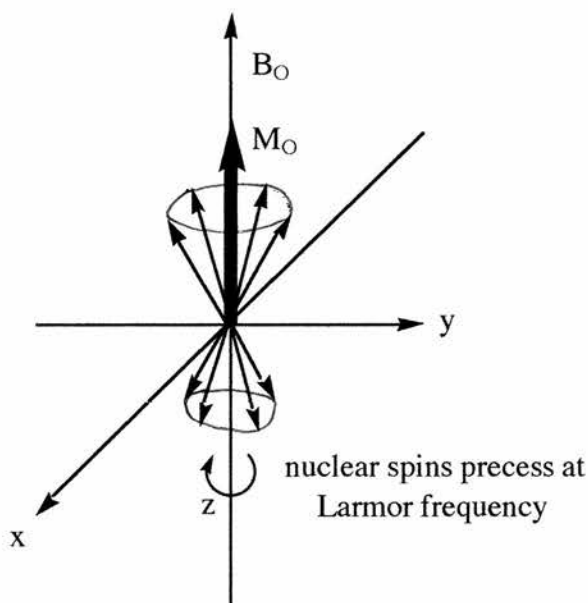


The rate at which the magnetisation decays from the y' -axis back to the z -axis is characterised by the $T_{1\rho}$ relaxation time.

It should be noted that the $T_{1\rho}$ process works in opposition to cross-polarisation, which involves a build up of polarisation with time. The more efficient the $T_{1\rho}$ relaxation is, the less the magnetisation is allowed to build up due to cross-polarisation. The $T_{1\rho}$ relaxation is most efficient when the rate of rotation of the rotating group is equal to the precessional frequency of the spin locked signal, which is in the 20-100 kHz region.

The rotating frame of reference¹⁶

As described earlier, if a sample containing nuclei of $I = 1/2$ is placed in a magnetic field B_0 , then the nuclei will precess around the direction of the field at the Larmor frequency. Since the nuclei have a spin of $1/2$, they have an orientation which is either aligned with or opposed to the direction of B_0 .

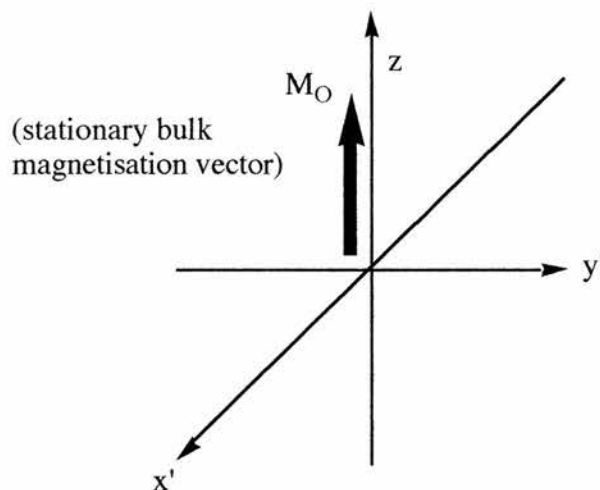


Since there is a slight excess of nuclei aligned with the magnetic field, this will give rise to a resultant magnetic vector, M_0 , which lies in the same direction as B_0 . This

¹⁶ Skoog D. A., Leary J. J., Principles of Instrumental Analysis, 4th Ed., Saunders College Publishing, Fort Worth, (1992) 318

description of the nuclear motions is referred to as the stationary or laboratory frame of reference.

If, however, we were able to rotate the laboratory frame at the Larmor frequency around the z-axis, then the nuclei would no longer appear to precess, but would become stationary. The vector sum, M_O , in the z direction is now of interest.



The magnetic behaviour is now completely described by the magnetisation vector M_O acting along B_O . This system is referred to as a 'rotating frame' and its effect is to simplify the description of the effects produced by the application of a radiofrequency pulse. The x and y axes rotating at the Larmor frequency are then denoted x' and y' .

Quantification of $T_{1\rho}$ relaxation

By measuring the intensities of spectral lines after a variable spin lock period at each temperature, then the rate of decrease in signal intensity ($T_{1\rho}$) can be calculated. A graph of $\ln(\text{intensity})$ versus time delay, for each temperature, will give a straight line with slope equal to $-1 / T_{1\rho}$. Typical time delays employed on our spectrometer range from 1 μs to a limit of around 15 ms due to the duty cycles of the transmitters.

Thus, $T_{1\rho}$ values can be calculated for a range of temperatures. Where a molecular motion modulates $T_{1\rho}$, a plot of $T_{1\rho}$ versus temperature gives ideally an inverted bell shaped curve with a minimum when the rate of rotation approximates to the precessional frequency of the nuclei in the spin lock field.

Calculation of rate constants and activation parameters

The rate of rotation of the precessing group around a given bond at a given temperature can be worked out using:⁸

$$\frac{1}{T_{1\rho}} = \frac{B^2\tau}{1+\omega_1^2\tau^2} \quad \cdot \quad \cdot \quad \cdot \quad (1)$$

where, $B^2 = {}^{13}\text{C}-{}^1\text{H}$ dipolar interaction strength

τ = correlation time for group rotation

ω_1 = precessional frequency of ${}^{13}\text{C}$ in spin lock

At minimum of $T_{1\rho}$:

$$\omega_1^2\tau^2 = 1$$

$$\begin{aligned} \therefore \frac{1}{T_{1\rho(\min)}} &= \frac{B^2\tau}{1+(1)} \\ &= \frac{B^2\tau}{2} \end{aligned}$$

$$T_{1\rho(\min)} = \frac{2}{B^2\tau}$$

$$B^2 = \frac{2}{T_{1\rho(\min)}\tau} \quad \cdot \quad \cdot \quad \cdot \quad (2)$$

ω_1 can be derived from the 90° pulse width for ${}^{13}\text{C}$, and since $(\omega_1^2\tau^2) = 1$ at the minimum for $T_{1\rho}$, equation (2) allows B^2 to be determined experimentally.

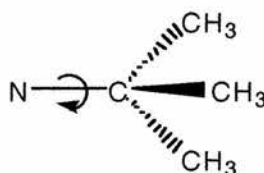
Now that $T_{1\rho}$, B^2 and ω_1 are known, τ can be calculated for any given temperature, using equation (1).

The rate constant, k , can then be deduced from:

$$k = 1 / \tau$$

or, for *tert*-butyl for example: $k = 3 / \tau$

The factor 3 in the equation relates specifically to *tert*-butyl rotation; the correlation time τ is for a complete rotation, but chemistry conventions refer to the rate for 1/3 of a rotation because there is a local C_3 axis of symmetry along the N-C bond for a *tert*-butyl group.



$T_{1\rho}$ values give rates, k , which are typically between 10^4 and 10^7 sec^{-1} .

When the accumulated $T_{1\rho}$ data do not pass through a minimum (usually due to $T_{1\rho}$ minimum being outwith the measurable temperature range), and as a result an experimentally derived B^2 value cannot be obtained, it is possible to derive the activation energy for the rotation.

At higher temperatures than temperature when $T_{1\rho(\text{min})}$ occurs:

$$\omega_1^2 \tau^2 \ll 1 \quad \implies \quad T_{1\rho} = \frac{k}{3B^2}$$

$$T_{1\rho} \propto k$$

At lower temperatures than temperature when $T_{1\rho(\text{min})}$ occurs:

$$\omega_1^2 \tau^2 \gg 1 \quad \implies \quad \frac{1}{T_{1\rho}} = \frac{B^2}{\omega_1^2} \times \frac{k}{3}$$

$$T_{1\rho} \propto k^{-1}$$

As $T_{1\rho}$ is proportional to the rate, k , a plot of $\ln(T_{1\rho})$ versus $1/T$ gives the energy of activation (E_a) at high temperature for the rotation process from the asymptotic slope, which is $-E_a/R$. Therefore $E_a = -\text{slope} \times R$.

The Eyring equation,¹⁷ utilised in transition state theory, states that:

$$\frac{3}{\tau} = \frac{kT}{h} e^{\Delta S^\ddagger/R} e^{-\Delta H^\ddagger/RT}$$

where, k = Boltzmann constant

h = Planck constant

If a graph is then plotted of $\ln(k/T)$ against $1/T$, the gradient gives us the enthalpy of activation, ΔH^\ddagger , as:

$$\text{gradient} = -\Delta H^\ddagger/R$$

And the entropy of activation, ΔS^\ddagger , can be found from the y-intercept, as:

$$\text{y-intercept} = \ln(k/h) + \Delta S^\ddagger/R$$

Since ΔH^\ddagger and ΔS^\ddagger are known, then ΔG^\ddagger can be calculated at a given temperature:

$$\Delta G^\ddagger = \Delta H^\ddagger - T\Delta S^\ddagger$$

¹⁷ Laidler K. J., Meiser J. H., Physical Chemistry, Benjamin/Cummings Publishing Co., Menlo Park California, (1982) 380

Line Shape Analysis

Line shape analysis is an alternative means of assessing the rate constant, k . It is a computer tool which analyses the coalescence patterns of the NMR spectra. The coalescence pattern occurs in the region where the rate of rotation is similar to the chemical shift difference, in Hz i.e. 10^3 - 10^4 sec^{-1} .

Normally, the temperatures of spectra which are analysed for line shape changes are lower than those from which $T_{1\rho}$ data is calculated. The data obtained by this method can therefore be used to complement $T_{1\rho}$ data, because line shape changes occur at lower rotation rates. Data from both methods are used to construct Arrhenius and Eyring plots and hence calculate activation parameters for the molecular motion.

Calibration of the MAS Temperature Controller

The establishment of accurate sample temperatures in MAS NMR is an important but difficult problem. It is important because MAS NMR measurements are being used increasingly for the study of molecular dynamics, such as molecular motions and exchange processes, kinetics of chemical reactions and phase changes in the solid state. Obviously, the correct extraction of activation parameters from experimental data depends upon the accurate measurement of sample temperatures.

Survey of existing calibration procedures

A number of samples have been suggested for the measurement of temperature, including samarium acetate (^{13}C nucleus),^{1,2} isotopically labelled ammonium nitrate³ and tetraazaannulene (^{15}N),^{4,5} P_4S_3 (^{31}P),⁶ lanthanide stannates (^{119}Sn),⁷ lithium manganese oxides (^6Li and ^7Li)⁸ and, most recently, lead (II) nitrate (^{207}Pb).⁹ All of these samples are inorganic and most of them rely heavily upon paramagnetically induced temperature dependences of chemical shifts. However, all of these methods rely upon some external method or unspun sample to establish sample temperatures, e.g. the 'methanol thermometer', in which the chemical shift difference between CH_3 and OH is measured. Such 'thermometer samples' are dependent on an even earlier calibration in high-resolution, low-power NMR.

In our experience the samarium acetate sample, which relies upon ^{13}C measurements, is a poor means of calibration with small frequency changes with

¹ Campbell G. C., Crosby R. C., Haw J. F., *Anal. Chem.*, **58**, (1986) 3127

² Campbell G. C., Crosby R. C., Haw J. F., *J. Magn. Reson.*, **69**, (1986) 191

³ Anderson-Altmann K. L., Grant D. M., *J. Phys. Chem.*, **97**, (1993) 11096

⁴ Wehrle B., Aguilar-Parilla F., Limbach H.-H., *J. Magn. Reson.*, **87**, (1990) 584

⁵ Aguilar-Parilla F., Wehrle B., Limbach H.-H., *J. Magn. Reson.*, **87**, (1990) 592

⁶ Bjorholm T., Jakobson H. J., *J. Magn. Reson.*, **84**, (1989) 204

⁷ Grey C. P., Cheetham A. K., Dobson C. M., *J. Magn. Reson.*, Ser. A **101**, (1993) 204

⁸ Morgan K. R., Collier S., Burns G., Ooi K., *J. Chem. Soc., Chem. Commun.*, (1994) 1719

⁹ van Gorkom L. C. M., Hook J. M., Logan M. R., Hanna J. V., Wasylishen R. E., *Magn. Reson. Chem.*, **33**, (1995) 791

temperature relative to the linewidth. The rest of the samples rely upon nuclei other than ^{13}C , necessitating probe retuning to run standard organic samples. It was apparent, therefore, that a better ^{13}C -based method for calibration of MAS sample temperatures was needed, which involves no 'thermometer samples' and gives the temperature reading directly, enabling the temperature controller-MAS probe combination to be recalibrated regularly. It is always recommended to recalibrate the MAS probe when an important electronic or pneumatic component has been replaced, such as the stator block.

The obvious method to employ to calibrate the temperature of solid samples is the use of established solid-solid phase changes. The temperatures at which phase changes occur in many organic samples have been accurately determined, and provided that the spectral changes are clear at the point of phase transition, are reproducible, rapid and do not display hysteresis (versus temperature), they are likely to be suitable for probe temperature calibration. The probe has been calibrated in the past¹⁰ by obtaining spectra from compounds with such known solid-solid phase changes; *d*-camphor (374 K), *d,l*-camphor (350 K), pivalic acid (280.1 K), *d*-camphor (244.5 K) and adamantane (208.6 K).

A similar approach was reported previously with two of the four compounds reported in this chapter, although the phase change temperature of one sample appears to have been incorrectly stated.¹¹ (Reference 11 gives an apparently incorrect value for the phase change in *d*-camphor of 238 K. Parsonage and Stavely¹² give a value of 244.5 K which appears to be from Table 2 in Ref. 13. The value of 244.5 K gives us a linear calibration plot from four samples which 238 K would clearly not, giving support to this value. In addition, in Ref. 11 only two phase changes were examined, insufficient to detect this error in a calibration plot. The incorrect value of 238 K appears to derive from a misinterpretation of less reliable data given in Ref. 14).

¹⁰ Riddell F. G., Arumugam S., Harris K. D. M., Rogerson M., Strange J. H., *J. Amer. Chem. Soc.*, **115**, (1993) 1881

¹¹ Haw J. F., Crook R. A., Crosby R. C., *J. Magn. Reson.*, **66**, (1986) 551

¹² Parsonage N. G., Stavely L. A. K., *Disorder in Crystals*, Clarendon Press, Oxford, (1978) 641

¹³ Schäfer K., Wagner U., *Z. Electrochem.*, **62**, (1958) 328

¹⁴ Yager W. A., Morgan S. O., *J. Am. Chem. Soc.*, **57**, (1935) 2071

Experimental

In order to attain consistency in the heating effects due to spinning, all phase changes were obtained at a spinning speed of $6.0 \text{ kHz} \pm 0.2 \text{ kHz}$ and constant bearing gas pressure. Since heating occurs at the bearing points⁹, and since the temperature of the spinning sample is generally controlled by the temperature of the bearing gas, it seemed important to stabilise this potential source of variability. Spinning speed was only varied from 6.0 kHz to avoid interference from spinning side-bands. In all cases where phase changes were being observed, the samples were left at the pre-set temperature until no further change was visible in the spectrum, generally *ca.* 10 minutes. A useful guide to this is the exact spinning speed as indicated by the fibre optic sensor, as this increases with increasing temperature and stabilises as temperature equilibrium is achieved. In addition, all samples were cycled several times in both directions through the phase transition to ensure that the changes were rapid, reversible and reproducible.

A wide variety of suitable temperature standards for phase changes are given in Ref. 15. From the numerous compounds listed we tried a variety and eventually selected four that are readily available in most chemical laboratories, and that cover the temperature range *ca.* 200 K to 350 K at regular intervals. They are, in order of phase transition temperature (Table 2), adamantane (208.6 K), *d*-camphor (244.5 K), pivalic acid (280.1 K) and 1,4-diazabicyclo[2.2.2]octane (DABCO) (351.1 K). These samples were used as received from Aldrich Chemical Company (Table 1) with no further purification.

Purity and melting point of temperature standards

Compound	Purity*	M.p.*
Adamantane	99+ %	209-12 °C (sublimes)
<i>d</i> -Camphor	99 %	178-80 °C
Pivalic acid	99 %	33-5 °C
DABCO	98 %	158-60 °C

* purity and m.p., as detailed in Aldrich Chemical Co. catalogue

Table 1

¹⁵ Parsonage N. G., Stavely L. A. K., Disorder in Crystals, Clarendon Press, Oxford, (1978) 608, 641
Calibration of the MAS Temperature Controller.

Descriptions of phase changes used for study

The phase change for adamantane was clearly seen as a reduction in the intensity of the peak due to the CH₂ groups at 38.56 ppm and its replacement below the phase transition by a broader peak at 38.17 ppm. The phase change for *d*-camphor involved a change in all resonances. The phase change for pivalic acid involved the *tert*-butyl CH₃ signal at 27.55 ppm being replaced by a doublet in the lower temperature phase at 27.25 ppm and 27.75 ppm, as seen in Spectra 1. The phase change for DABCO involved the replacement of the signal at 48.94 ppm below the phase transition, by a broader signal at 48.23 ppm above the phase transition. It should be noted that at our higher field, the residual dipolar coupling for DABCO in Ref. 11 is no longer present. In all cases the phase changes took place over a range of *ca.* 4 K on the temperature controller unit, which would be consistent with a temperature gradient of *ca.* 4 K over the sample. The temperature controller setting observed for each compound is shown in Table 2.

Phase transitions studied as temperature calibration controls

Compound	Transition (low → high)	Literature phase change temperature (K)	Temperature controller setting (K)
Adamantane	Tetragonal → F.c.c.	208.6 ¹²	183
<i>d</i> -Camphor	Tetragonal (?) → Hexagonal	244.5 ¹²	231
Pivalic acid	Tetragonal → F.c.c.	280.1 ¹⁶	269
DABCO	Hexagonal → F.c.c.	351.1 ¹²	362.5

F.c.c. = face centred cubic

Table 2

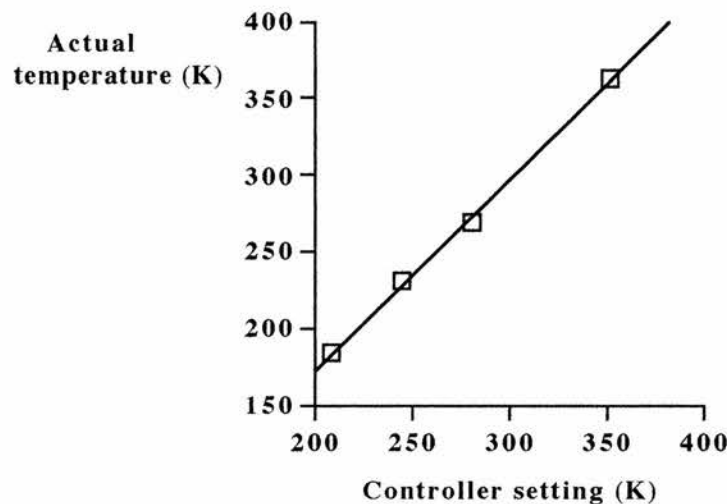
¹⁶ Parsonage N. G., Stavely L. A. K., Disorder in Crystals, Clarendon Press, Oxford, (1978) 608

Calibration of the MAS Temperature Controller.

Calibration plot and corrective equation

These phase changes are clear, rapid and readily reproducible and do not suffer from any temperature hysteresis. They provide a linear relationship between temperature controller setting and actual sample temperature (Figure 1) that is of use over the temperature range 173-373 K. They form a very convenient and direct method for the calibration of temperature controllers for MAS probes. Also, provided samples are of similar characteristics to those employed here and are spun under similar conditions to the calibration samples, then the relationship obtained forms a reliable method for converting from temperature control settings to actual sample temperatures.

Calibration plot of data presented in Table 1

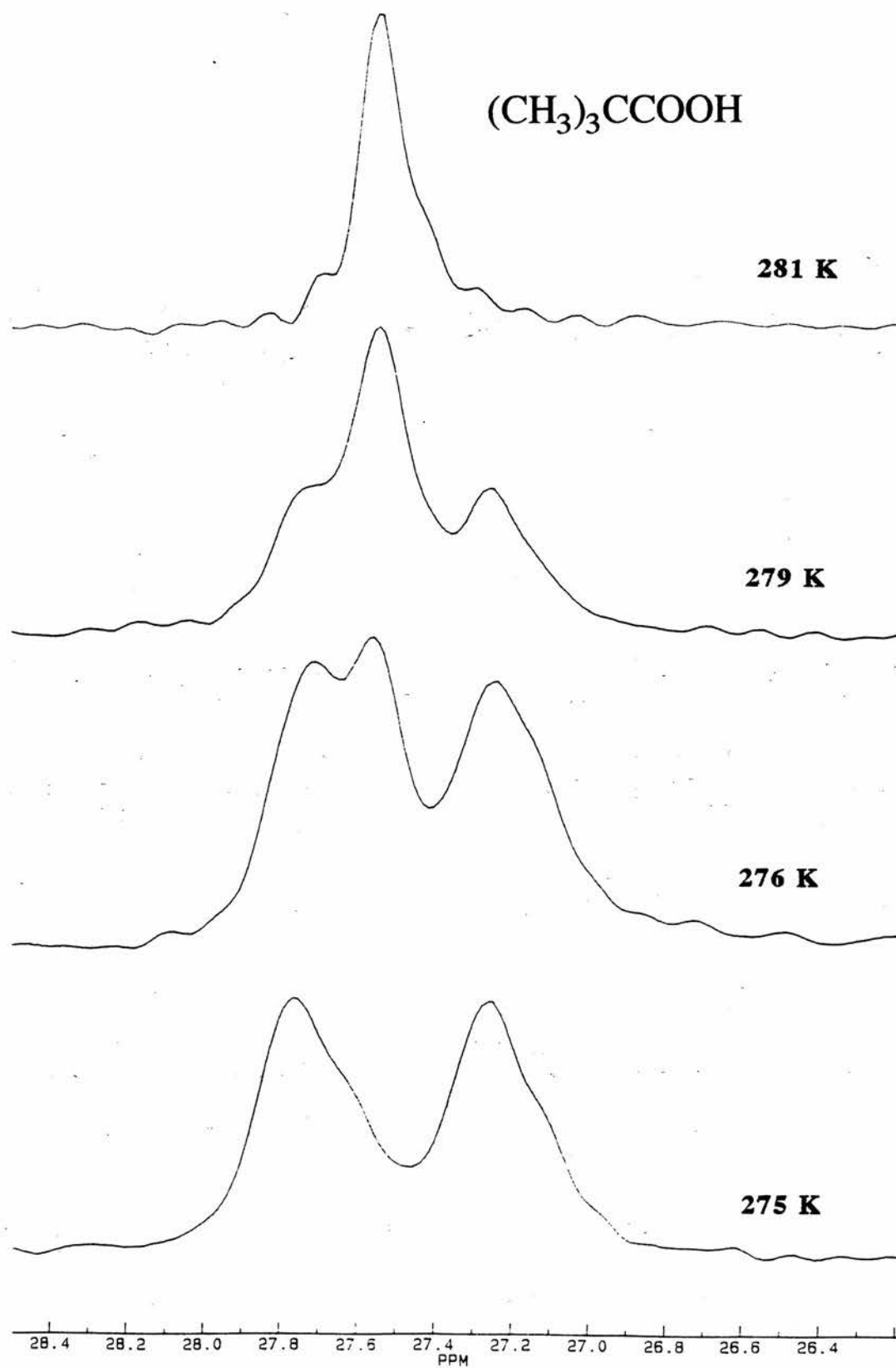


Actual temperature = $0.799 \times (\text{controller setting}) + 62.2$; ($r^2 = 0.999$)

Figure 1

Spectra 1

Methyl resonance of pivalic acid around phase change



Calibration of the MAS Temperature Controller.

It is worth noting that with our equipment the actual temperatures are always closer to ambient than the controller setting. The temperature controller employed is designed to work with a variety of NMR and EPR probes, through a sensing thermocouple. Since the thermocouple controls the temperature of the bearing gas, it seems that the variations observed may arise from mixing of the drive gas, at ambient temperature, with the hot or cold bearing gas or from the heating or cooling effect of the drive gas on the sample taking the sample temperature closer to ambient.

Haw *et al.*¹¹ criticised the use of phase changes for MAS probe temperature calibration for several reasons; the length of time taken for the phase changes to occur, spinning problems accompanying the phase change and the number of samples required. In practice, no spinning problems were experienced and the time taken for the phase change in all cases is comparable to the length of time one would leave a sample to temperature equilibrate in any case (*ca.* 10 minutes). The sole disadvantage is the requirement to use four separate samples, but this is overcome by the direct nature of the experiment.

Heating Effects At Various Magic Angle Spinning Speeds

It was proposed to investigate the heating effects of spinning partially stabilised zirconia rotors at high frequencies, up to 12 kHz, in the MAS probe. It has been suggested that there may be such an effect, to the extent of a few degrees or more.

van Gorkom *et al.* reported⁹ the heating effects at high Magic Angle Spinning speeds of a sample of lead (II) nitrate by solid-state Pb-207 NMR. A number of significant observations were reported;

- i) Pb-207 spectra of lead (II) nitrate are highly sensitive to variations in temperature. The ²⁰⁷Pb chemical shift has a linear dependence on temperature; increases in temperature cause a change in chemical shift to higher frequency (downfield shift). The linewidth and the number of spectral components are also affected.
- ii) There is a heating effect, due to friction, when the sample is subjected to MAS at high speeds. Initial increase in the drive gas pressure serves to cool the sample,

evidenced by the slight upfield shift of the ^{207}Pb signals. At higher MAS speeds, further increases in the drive and bearing pressures induce a downfield shift, indicating the sample is being heated. Frictional heating is greatly increased and overwhelms the cooling effect.

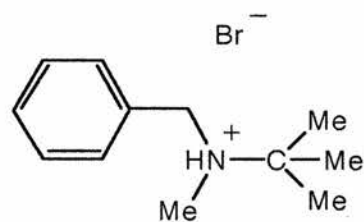
- iii) Localised thermal regions were identified within the lead (II) nitrate sample. The rotor was packed with lead (II) nitrate in the bottom, middle and top of the rotor, along with potassium bromide, to assess the heating effect within the rotor. Lineshapes obtained were a good indication of temperature. The bottom and top of the rotor were found to be the hottest, where the friction with the bearing gas and stator block is the greatest. The temperature differences in the sample were found to differ by as much as 5 K at 12 kHz.
- iv) Dissipation of heat was found to be less effective for rotors made from zirconia, attributed to their poor thermoconductive properties. The heating effects were less pronounced for silicon nitride rotors, which allow rapid and efficient heat transfer throughout the rotor.
- v) Parallel experiments with a 7 mm zirconia rotor showed only the effect of overall sample heating with increased spinning speed, which seemed greater in the larger rotor, and no localised heating effects.

It was pointed out, finally, that lead (II) nitrate possesses characteristics which could be exploited to calibrate the temperature of MAS probes, since it;

- is readily available, stable, non-hygroscopic,
- has an intermediate resonance frequency,
- is sensitive and gives narrow linewidths at high MAS speeds; rapid acquisition,
- shows uniform behaviour throughout temperature range.

Use of lineshapes of *N*-benzyl-*tert*-butyl-*N*-methylammonium bromide

To quantify the variation in sample temperature with spinning speed, the well marked coalescence of *N*-benzyl-*tert*-butyl-*N*-methylammonium bromide (right),¹⁷ arising from the slow rotation of the *tert*-butyl group, was



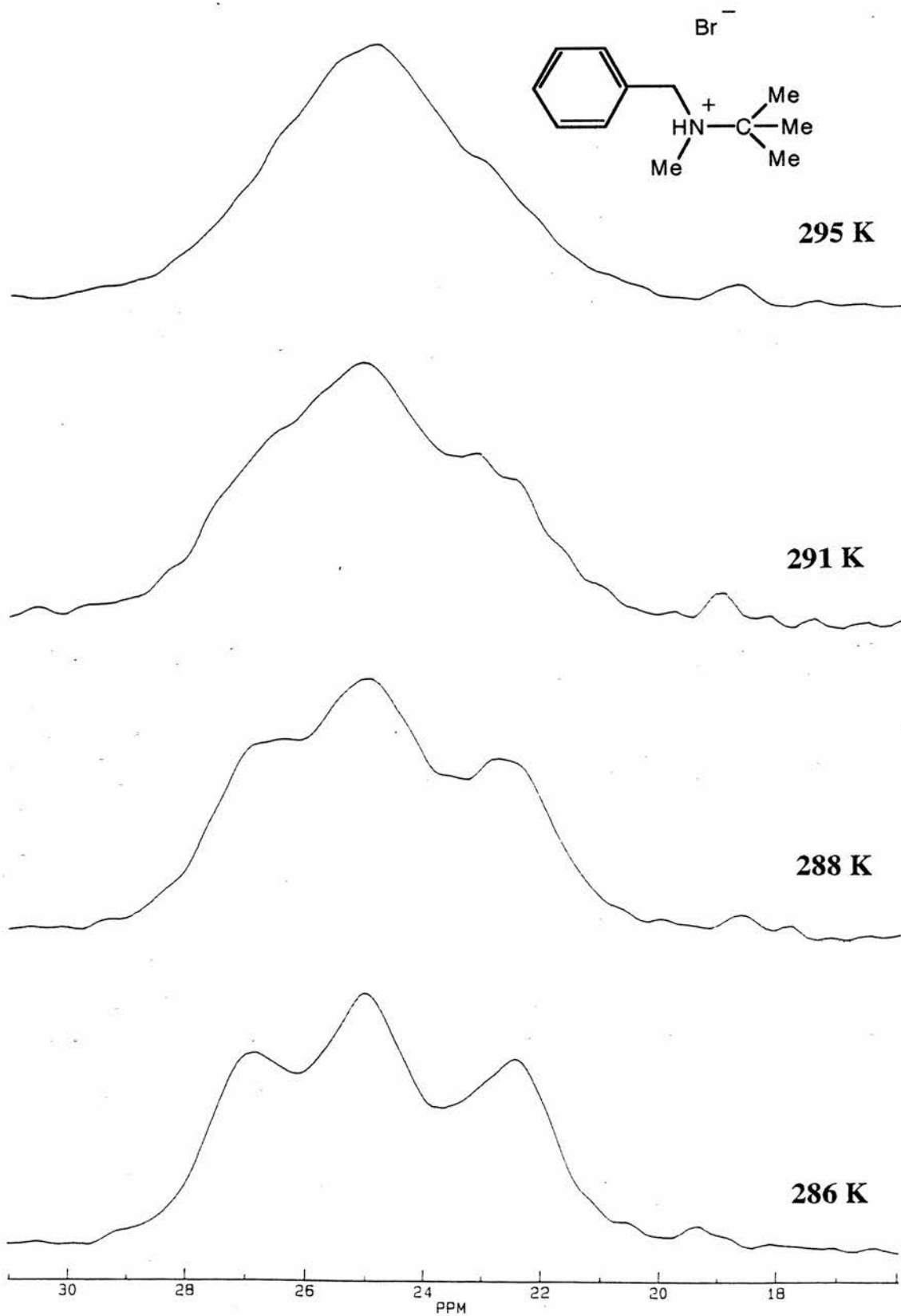
investigated. The three methyls of the *tert*-butyl group in this compound undergo a very clear singlet to triplet coalescence as the temperature is lowered in the range 290-270 K. By then running the sample at different spinning speeds at the same temperature controller setting, and matching their lineshapes against spectra obtained under temperature calibrated conditions, the heating effect can be assessed.

Initially, *N*-benzyl-*tert*-butyl-*N*-methylammonium bromide was run at 286 K and 6 kHz to obtain the approximate central point of the coalescence. Then, to establish the variation in lineshape with temperature, the sample was maintained at a spinning speed of 6 kHz (Spectra 2) and the temperature varied and the lineshape changes with varying temperature recorded. The temperature was then returned to 286 K, and the sample was run at various spinning speeds (Spectra 3) in an attempt to match the lineshapes of the different spinning speeds with the corresponding temperatures. The results are reported in Table 3.

¹⁷ Riddell F. G., Rogerson M., *J. Chem. Soc., Perkin Trans. 2*, (1996) 493

Spectra 2

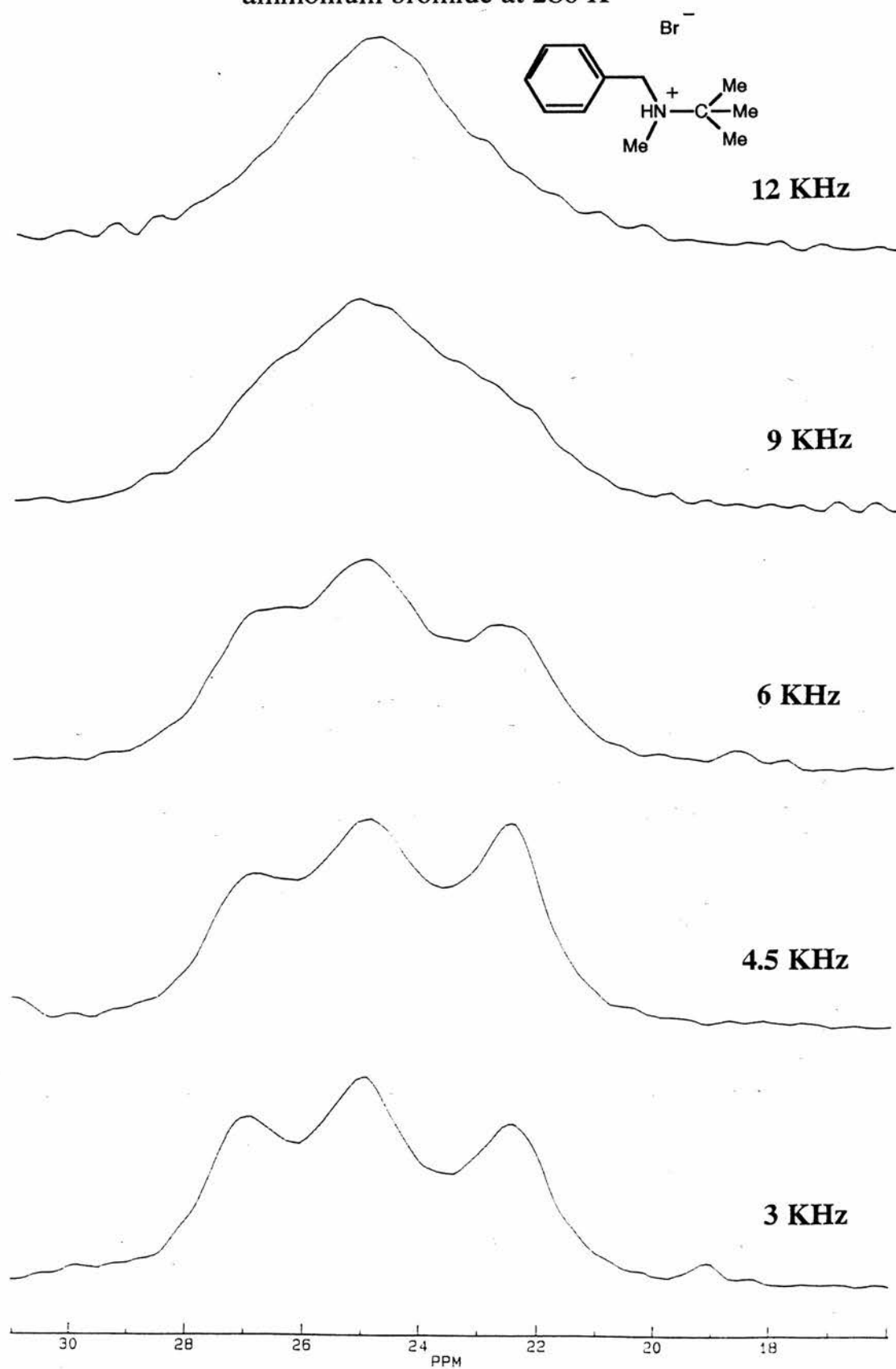
Lineshapes of methyl coalescence of *N*-benzyl-*tert*-butyl-*N*-methylammonium bromide at 6 kHz



Calibration of the MAS Temperature Controller.

Spectra 3

Lineshapes of methyl coalescence of *N*-benzyl-*tert*-butyl-*N*-methylammonium bromide at 286 K



Calibration of the MAS Temperature Controller.

Temperature as a function of spinning speed

Spinning speed (kHz) ^a	Temperature from lineshape (K) ^a
3.0	286
4.5	287
6.0	288
9.0	291
12.0	295

^a these data give the relationship; $T \text{ (K)} = 0.066 [v_{\text{rot}} \text{ (kHz)}]^2 + 285.5$ ($r^2 = 0.999$)

Table 3

Relationship of spinning speed to temperature

When spinning speed is plotted against temperature a second order polynomial relationship is apparent (Figure 2).

Plot of spinning speed against temperature

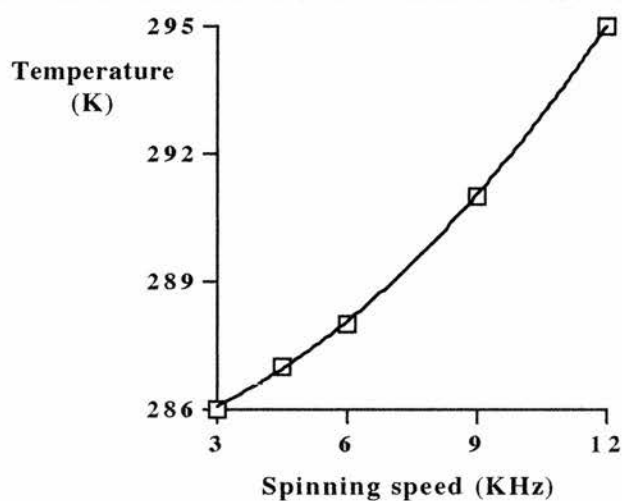


Figure 2

Comparison of the two sets of spectra shows an approximate temperature increase of the samples in the MAS probe of *ca.* 1 K per kHz increase in spinning speed. This allows a correction to be made to the previously obtained calibration to correct for variations of spinning speed away from 6 kHz.

Doty and Ellis showed in principle that the variation of sample temperature should be proportional to the square of the spinning speed.¹⁸ On close inspection the observed variation in temperature with speed is seen to vary in a non-linear manner consistent with a second power relationship. This is confirmed by plotting the square of the spinning speed against temperature, where a linear relationship with a regression coefficient of 0.999 is obtained.

Conclusion

The phase changes in the samples examined form a very convenient set of standards for the calibration of the temperature controllers for MAS probes in the range 173-373 K. The calibration should be performed, as far as possible, under identical conditions of bearing gas pressure and spinning speed. When experimental observations are subsequently made on other samples at variable temperature, the spinning speed and bearing gas pressure should be as similar as possible to the conditions employed for the calibration.

Samples for the calibration were used as received from the Aldrich Chemical Co. and were not checked for purity or moisture content. This would be worthwhile doing when carrying out future calibrations bearing in mind the findings in Chapter 6, where the presence of moisture was seen to affect greatly the $T_{1\rho}$ relaxation times of those compounds studied. However, the elegant straight calibration curve obtained here would seem to vindicate these methods to some extent.

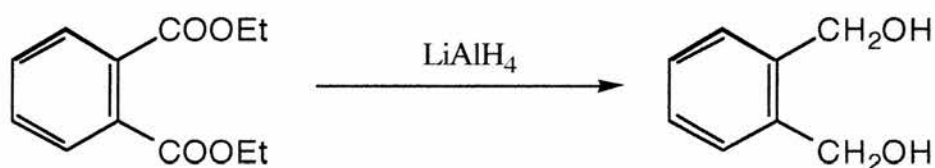
It is confirmed that there is a variation of sample temperature with spinning speed which appears to obey a squared relationship. Laboratories carrying out variable temperature MAS NMR should regularly recalibrate the temperature controller of the probe, especially when critical electronic or pneumatic components such as stator blocks have been changed.

¹⁸ Doty F. D., Ellis P. D., *Rev. Sci. Instrum.*, **52**, (1981) 1868

Synthesis

The main objective of this project was to investigate the molecular dynamics of simple organic compounds in the solid state, namely group rotations, ring pseudorotations and hydrogen bond exchanges. To this end, compounds of interest which are commercially available may be studied or may be synthesised using, in the main, well established organic chemistry methodology and techniques. This chapter describes the synthesis of these simple organic compounds to be studied subsequently by solid-state CP/MAS NMR. Details of the methods and analyses can be found in the Experimental section.

1,2-Benzenedimethanol



Before reduction diethylphthalate was purified¹ by washing with aqueous sodium carbonate and water and drying over calcium chloride. The liquid product was filtered, distilled under reduced pressure and stored under vacuum (over P₂O₅).

The reduction reaction with lithium aluminium hydride yielded 1,2-benzenedimethanol in 29 % yield, which was recrystallised from ether to give colourless plates which were ground to an off-white powder. The solid was clean by ¹H NMR.

cis- and *trans*-2-(Hydroxymethyl)cyclopentanol

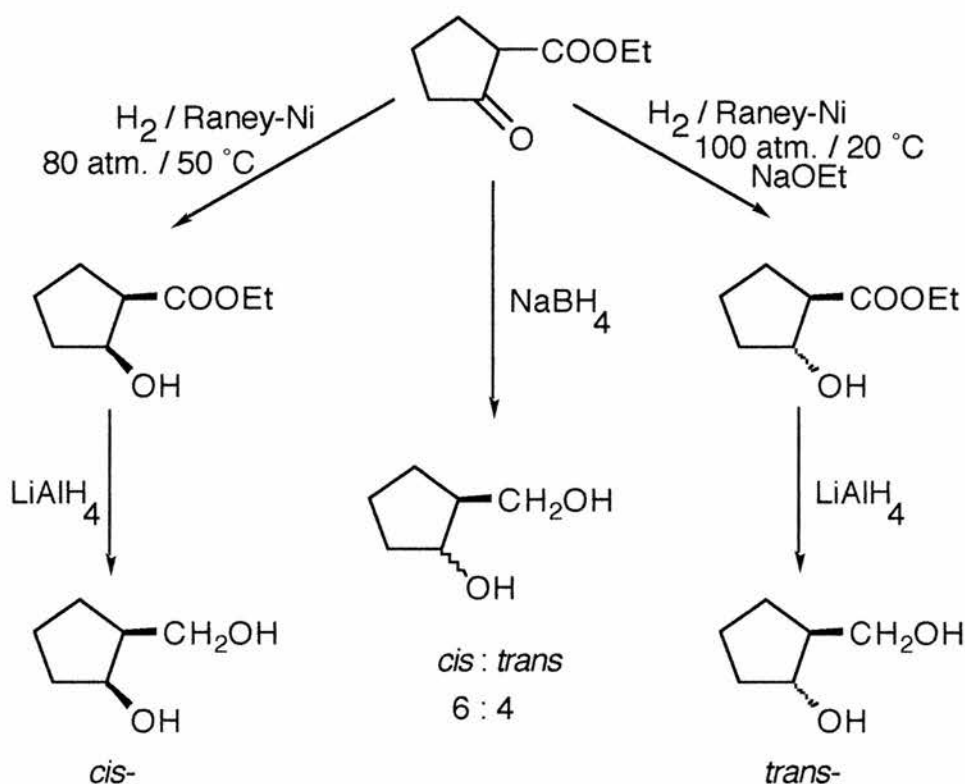
Prof. Fülöp of Szeged, Hungary, suggested these compounds may be suitable diols for study. The preparation of *cis*-methanolcyclopentanol from ethyl cyclopentanone-2-carboxylate is reported,² via *cis*-ethyl cyclopentanol-2-carboxylate. It is

¹ Perrin D. D., Armarego W. L. F., Purification of Laboratory Chemicals, Pergamon Press, Oxford, 3rd Ed., (1988) 149

² Kovács Ö., Szilágyi J., Schneider G., *Magyar Kémiai Folyóirat*, **71**, (1965) 93

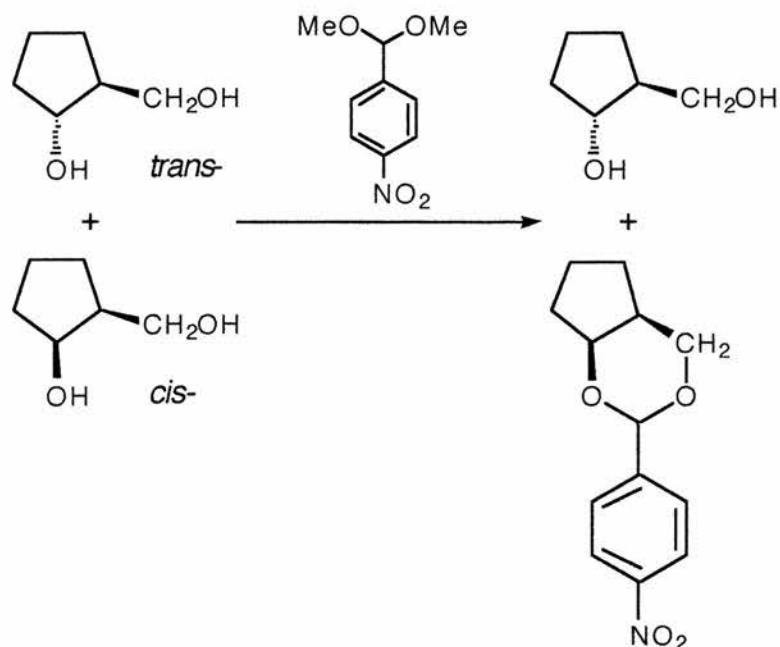
carried out under specific reaction conditions of temperature and pressure i.e. 50 °C and 80 atmospheres hydrogen pressure in the presence of Raney-Nickel catalyst to yield the intermediate *cis*-cyclopentanol. Lithium aluminium hydride reduction then affords the *cis*-diol.

The *trans*-isomer may be prepared under similarly harsh conditions of pressure in the presence of sodium ethoxide i.e. 100 atmospheres hydrogen pressure (at 20 °C) in the presence of Raney-Nickel catalyst. The prepared *trans*-cyclopentanol is then reduced to the corresponding diol with lithium aluminium hydride. Shown below is a scheme of the reactions to both *cis*- and *trans*-2-methanolicyclopentane.



Treatment of the starting cyclopentanone with sodium borohydride yields the desired cyclopentanolcarboxylate, but as a mixture of isomers i.e. *cis* 6:4 *trans*. However, this route is useful in itself since the two isomers can be separated by treatment with *p*-nitrobenzaldehyde dimethyl acetal.³

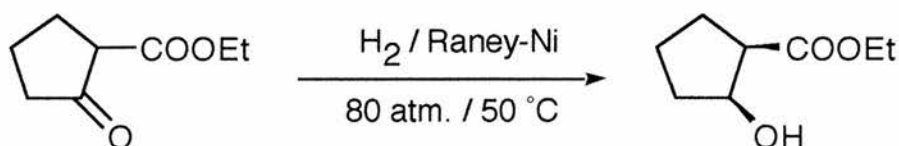
³ Finch N., Fitt J. J., Hsu I. H. S., *J. Org. Chem.*, **40**, (1975) 206



The *cis*-isomer forms a *p*-nitrobenzylidene derivative with the dimethyl acetal, whereas the *trans*-isomer does not give rise to such a derivative with *p*-nitrobenzaldehyde. The products are then easily separated by column chromatography.

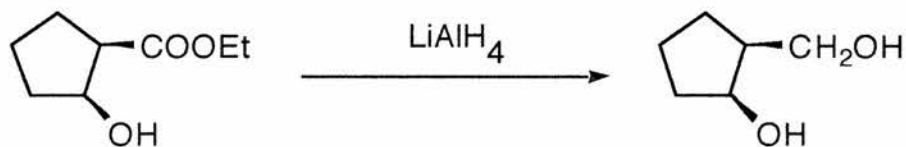
Prof. Fülöp provided a sample of *cis*-ethyl cyclopentanol-2-carboxylate for reduction. However, lithium aluminium hydride reduction was incomplete, evidenced by presence of the ethyl signal in the ^1H NMR spectrum; CH_2 quartet at δ 3.8 and CH_3 triplet at δ 0.9. It was then necessary to synthesise the cyclopentanolcarboxylate from ethyl cyclopentanone-2-carboxylate.

preparation of *cis*-2-(hydroxymethyl)cyclopentanol



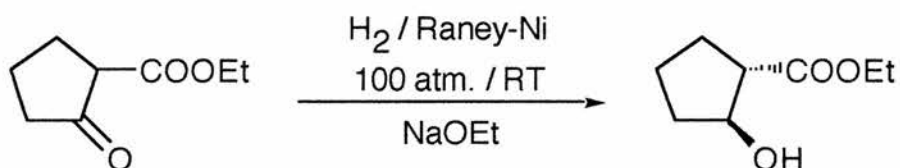
An autoclave reaction was carried out, initially for 5 hours, at 50 °C and 80 atmospheres hydrogen pressure, but the reaction was incomplete by ^1H NMR; the alkanone starting material contains a triplet centred at δ 3.1 ($J = 9$ Hz) whereas the alcohol

gives rise to a broad singlet at δ 3.1. The reaction was repeated under the same conditions of temperature and pressure, but left overnight. This time there was no evidence of the starting material by NMR.



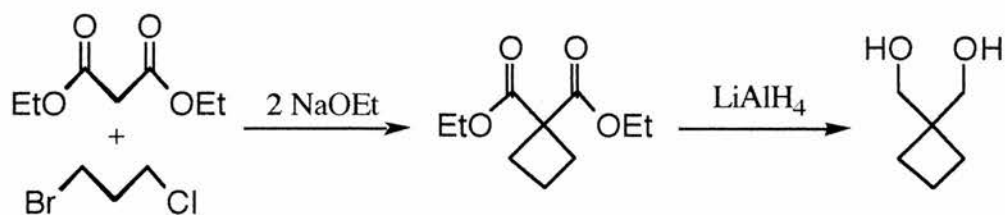
However, attempts to carry out the reduction with lithium aluminium hydride failed to yield efficiently the desired *cis*-2-(hydroxymethyl)cyclopentanol. Two reductions, using 1.23 and 2.1 equivalents of lithium aluminium hydride, gave ratios of starting material to product of approximately 1:2 and 2:5 respectively.

preparation of *trans*-2-(hydroxymethyl)cyclopentanol



One experiment was attempted to try and make the *trans*-2-(hydroxymethyl)-cyclopentanol directly. Slightly different reduction conditions were employed when compared to the preparation of the *cis*; 100 atmospheres hydrogen pressure, ambient temperature and, importantly, in the presence of ethoxide. On opening the autoclave the reaction solution was a pink colour, which progressed to a deep scarlet colour after the extractions with ether. Distillation yielded a clear liquid product, leaving a dark residue. However, ¹H NMR indicated that the product was unreacted starting material, evidenced by a triplet at 3.15 ppm.

1,1-Di(hydroxymethyl)cyclobutane



preparation of diethyl 1,1-cyclobutanedicarboxylate

Diethyl 1,1-cyclobutanedicarboxylate was formed from diethylmalonate and 1-bromo-3-chloropropane, following the method of Mariella and Raube.⁴ Alternative methods used 1,3-dibromopropane as the dihaloalkane,^{5,6,7,8} and Walborsky reported peroxide-catalysed addition of hydrogen bromide to diethyl allylmalonate followed by intramolecular alkylation.⁹

All reactants were freshly prepared or distilled to ensure they were as dry as possible.¹⁰ Sodium ethoxide, prepared from sodium and anhydrous ethanol, was added to a mixture of diethyl malonate and 1-bromo-1-chloropropane at 80 °C. After addition was complete reflux was continued and ethanol was then removed by distillation at atmospheric pressure. Diethyl 1,1-cyclobutanedicarboxylate was confirmed by ¹H NMR, although small impurities were observed at 1.72 and 3.35 ppm which was consistent with a sample of diethyl 1,1-cyclobutanedicarboxylate ex. Lancaster.

⁴ Mariella R. P., Raube R., *Org. Synth.*, **33**, (1953) 23

⁵ *Org. Synth.*, **23**, (1943) 16

⁶ Cason, Allen, *J. Org. Chem.*, **14**, (1949) 1036

⁷ Perkin, *J. Chem. Soc.*, **51**, (1887) 1

⁸ Kishner, *J. Russ. Phys. Chem. Soc.*, **37**, (1905) 507; also uses 1-bromo-3-chloropropane as dihaloalkane

⁹ Walborsky, *J. Am. Chem. Soc.*, **71**, (1949) 2941

¹⁰ Absolute ethanol reacted with sodium, freshly distilled diethyl phthalate added and mixture refluxed for 2 hours, and ethanol distilled under atmospheric pressure and stored over molecular sieves; Old sample of 1-bromo-3-chloropropane distilled under reduced pressure and stored over molecular sieves; Diethylmalonate, 99 %, stored over molecular sieves.

preparation of 1,1-di(hydroxymethyl)cyclobutane

Initial reduction of the diester with 1.27 equivalents of LiAlH_4 , gave a product with considerable amounts of starting material; ^1H NMR indicated a ratio of starting material to diol of *ca.* 9:10. Subsequent reactions, with up to 2 equivalents of LiAlH_4 , gave ratios of up to approximately 3.8:100 by ^1H NMR. This product was twice distilled and gave a final ratio of 2.1:100. A sample of >99 % purity would be desirable for solid-state NMR study.

**1,1-Di(hydroxymethyl)cyclohexane
and 1,1-Di(hydroxymethyl)cycloheptane**

Volkmar Weiß, a project student from The University of Berlin in Germany, synthesised both of these cyclic diol compounds.¹¹

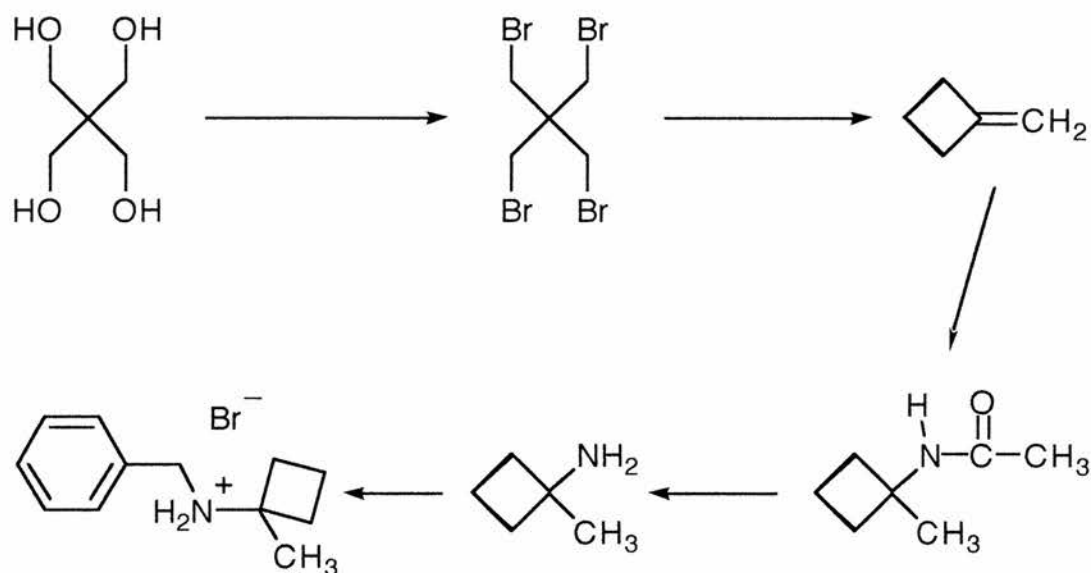


The cyclohexanediol was obtained from diethylmalonate and 1,5-dibromopentane, using alkoxide to remove both active protons sequentially. After nucleophilic attack on the dibromopentane each time, the second of which formed the 6-membered ring, lithium aluminium hydride of the cyclic diester yielded the diol.

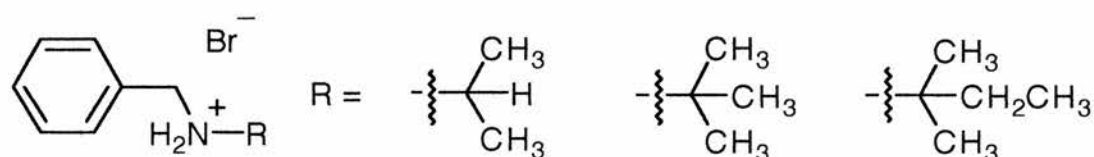
To improve the efficiency of the cycloheptanediol reaction, an intermediate step was introduced since the 7-membered ring is thermodynamically more unstable. The active protons were removed in separate steps, and the intermediate product, diethyl-6-bromohexylmalonate, was isolated.

¹¹ Weiß V., Organic Research Project report, University of St. Andrews, (1996) 1-2

***N*-Benzyl-2-methylcyclobutylamine**

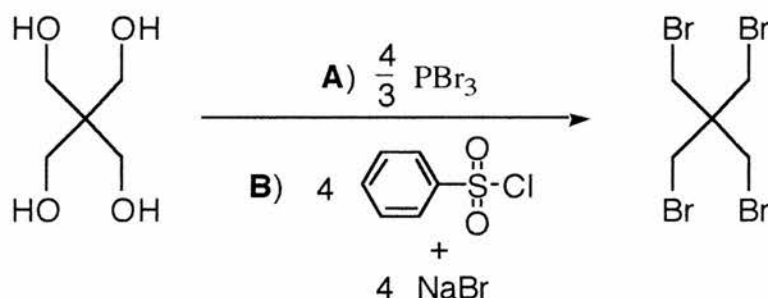


N-Benzyl-2-methylcyclobutylamine was intended to be synthesised as an analogous compound to those studied by solid-state CP/MAS NMR by Martin Rogerson.¹² The rotation of groups of the type *iso*-propyl, *tert*-butyl and *tert*-amyl were measured in benzylated tertiary ammonium salts of the type shown above.



By replacing these groups with 1-methylcyclobutylamine, the 'principle of least distress' will be maintained and results will serve as a comparison with Ref. 13.

preparation of pentaerythrityl bromide



¹² Rogerson M., Ph.D. thesis, University of St. Andrews, (1995) 36

The first attempt to prepare pentaerythrityl bromide used phosphorus tribromide which reacts with alcohols to form intermediate organic esters, which are good leaving groups and can be displaced by halide ions. The method of Schurink was followed¹³ which involved reacting pentaerythritol with PBr_3 at 170-80 °C for 20 hours. The reaction mixture, which was a deep orange-red colour, ignited spontaneously when exposed to air; the flaming flask was therefore extinguished. It was without doubt caused by the formation of hydrides of phosphorus, which are capable of igniting spontaneously as warned in Ref. 13.

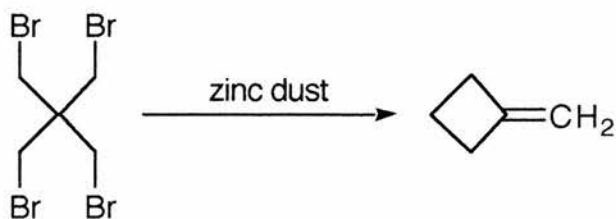
The method of Herzog was then used,¹⁴ which reacts benzenesulfonyl chloride with pentaerythritol, the benzenesulfonate leaving group then being replaced by bromide from sodium bromide. Benzenesulfonyl chloride was added dropwise to pentaerythritol in pyridine, a yellow colour being produced immediately which developed to red. Reaction temperature was maintained below 35 °C and addition took a total of 80 minutes. The slurry was added to a methanolic solution of aqueous hydrochloric acid and stirred vigorously, where a bright blue colour developed; the blue colour of electrons in liquid ammonia. After cooling the benzenesulfonate ester was filtered, the granular product retaining the characteristic blue colour. Washing with water and methanol only slightly reduced the colour. The damp benzenesulfonate was stirred in a solution of sodium bromide in diethylene glycol at 140-50 °C for 14 hours, after which the colour was orange-brown. After cooling to 10 °C the tan product was filtered and recrystallised from acetone, yielding a solid of off-white glistening plates. A substantial amount of product was recovered from the mother liquors (26 % of a total yield of 61 %), which was more tan in colour than the main batch. The products were collected separately and were noticeably very dense.¹⁵

¹³ Schurink H. B., *Org. Synth.*, **17**, (1937) 73 (*Org. Synth.*, Coll. Vol. **2**, (1943) 476)

¹⁴ Herzog H. L., *Org. Synth.*, **31**, (1951) 82

¹⁵ density 2.596 from Aldrich Chemical Co. catalogue

preparation of methylene cyclobutane



Initial attempts to carry out this reaction used the methods of Roberts *et al.*,¹⁶ Shand Jnr *et al.*¹⁷ and Conia *et al.*¹⁸ In accordance with Ref. 16, pentaerythrityl bromide (10 g) was added portionwise (to avoid vigorous frothing) to a solution of zinc bromide and zinc dust in aqueous ethanol. Distillation at 100 °C failed to yield any product; the small scale of the reaction was later seen as a limiting factor. A similar procedure from Ref. 17 gave a distillate which contained sufficient moisture to form a separate layer. After washing the distillate with water, which gave one layer, and (MgSO₄) the product did not resemble methylene cyclobutane by ¹H NMR.

The method of Conia *et al.* was then followed,¹⁸ on a significantly larger scale (120 g pentaerythrityl bromide). Pentaerythrityl bromide, zinc dust and water were stirred mechanically at 85 °C before adding a solution of conc. hydrochloric acid in ethanol. This reaction is so vigorous that the first attempt resulted in the reaction mixture being forced through the rest of the distillation apparatus; they used a 12 litre flask for reasons that quickly became apparent. Ethanol was added dropwise to the reaction mixture when the temperature reached 95 °C and subsequent distillation took place at 78 °C, the boiling point of ethanol. The product was expected to distil at 40-2 °C, so the presence of ethanol only serves to obscure the distillation. When the whole procedure was repeated on a small scale (7.5 g starting material) in the complete absence of ethanol, distillation of a product boiling at 40-1 °C was collected in 61 % yield. This product was confirmed to be methylene cyclobutane by ¹H NMR, and it was further characterised by its pungent ethereal aroma (which was even apparent when stored at -18 °C in the

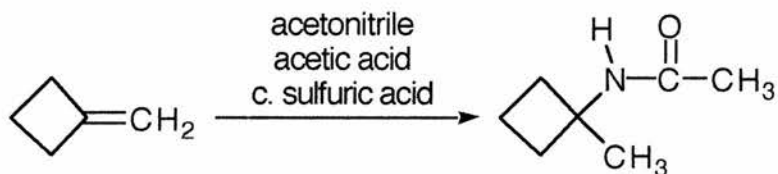
¹⁶ Roberts J. D., Sauer C. W., *J. Am. Chem. Soc.*, **71**, (1949) 3927

¹⁷ Shand Jnr W., Schomaker V., Fischer J. R., *J. Am. Chem. Soc.*, **66**, (1944) 636

¹⁸ Conia J.-M., Leriverend P., Ripoll J. L., *Bull. Soc. Chim. France*, (1961) 1803

freezer). A larger scale preparation, with 75 g pentaerythrityl tetrabromide, yielded 6.30 g of methylene cyclobutane in 48 % yield.

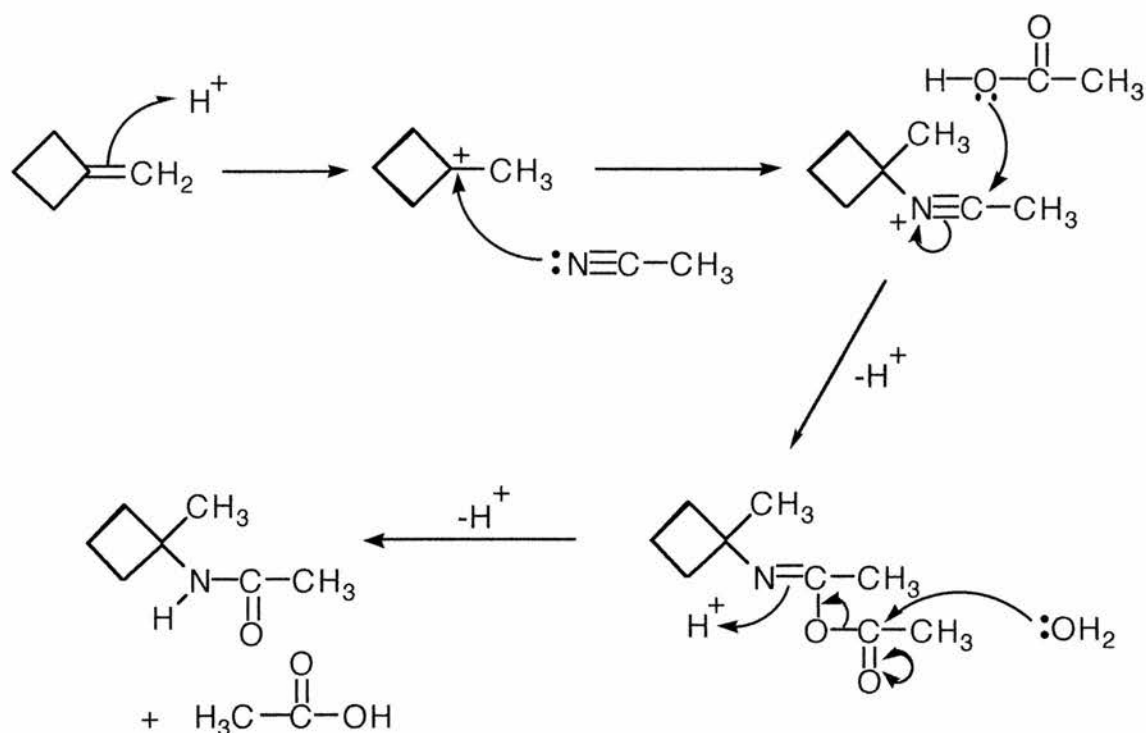
preparation of *N*-(1-methylcyclobutyl)-acetamide



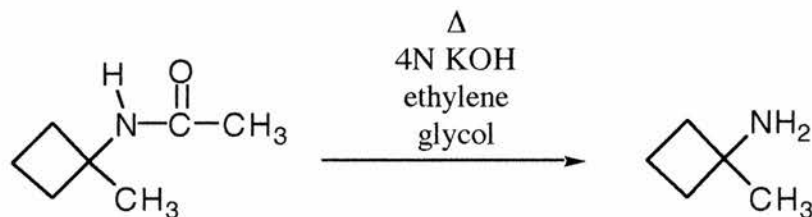
After the double bond picks up a proton (mechanism over), the lone pair on the nitrogen of the acetonitrile attacks the carbocation of the cyclobutane ring. The lone pair on the oxygen of the acetic acid attacks the positive carbon of the carbon-nitrogen double bond and hydrolysis of the acetyl moiety forms the *N*-(1-methylcyclobutyl)-acetamide and the acetic acid is regenerated.

Following method **A** of Cox *et al.*,¹⁹ methylene cyclobutane was added dropwise to a mixture of acetonitrile, glacial acetic acid and conc. sulfuric acid with ice cooling. After quenching with water and basification to pH 9, subsequent work-up yielded white crystalline *N*-(1-methylcyclobutyl)-acetamide in a yield of 33 %.

¹⁹ Cox E. F., Caserio M. C., Silver M. S., Roberts J. D., *J. Am. Chem. Soc.*, **83**, (1961) 2719

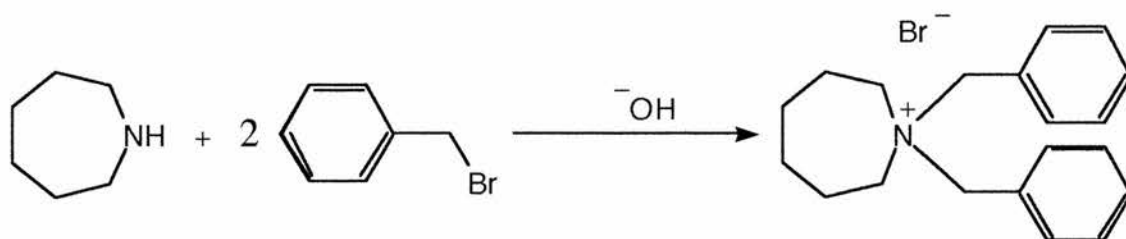


preparation of 1-methylcyclobutylamine



Deacetylation of the acetamide also followed the method in Ref. 19. The acetamide was refluxed in a 4N solution of potassium hydroxide in ethylene glycol for 48 hours (at 185-95 °C). The deacetylated amine was then to be partitioned into ether in a continuous extraction procedure. Since there was no continuous extraction apparatus available, initial attempts to extract the product merely involved carrying out 15 separate ether extractions, with no product found. Continuous extraction apparatus was fashioned from available glassware, using a modified pasteur pipette within the apparatus to funnel the condensing ether into the reaction solution. However, on evaporation of ether from the collection flask no product was found to partition into the ether; the apparatus used was obviously inefficient.

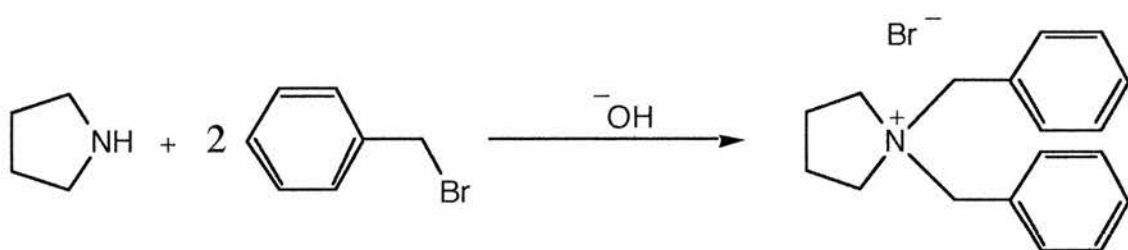
***N,N*-Dibenzylhexamethyleneiminium bromide**



Two equivalents of benzyl bromide are required to react with hexamethyleneimine (homopiperidine), with one equivalent of base required to facilitate the second benzylation. Firstly, the lone pair on the nitrogen attacks the electron deficient carbon of the benzyl group after loss of the bromide. Then, after deprotonation of the nitrogen, the lone pair initiates the second benzylation.

Benzyl bromide was added dropwise to an aqueous solution of sodium hydroxide and hexamethyleneimine, and the salt formed precipitated out. After stirring overnight the precipitate was filtered, recrystallised from water and dried under vacuum. The product was collected as large crystals in good yield (67 % recrystallised), and the ¹H NMR spectrum was clean and consistent with that expected for the product.

***N,N*-Dibenzylpyrrolidinium bromide**

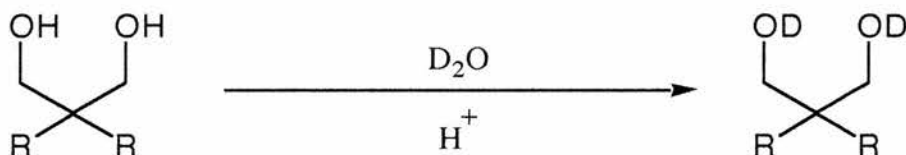


The reaction of pyrrolidine with benzyl bromide was carried out under similar methodology to the formation of *N,N*-dibenzylhexamethyleneiminium bromide above. When using water as solvent the reaction mixture separated into two layers and the reaction did not go to completion, possibly undergoing only one benzylation. When the organic layer was reduced and analysed the ¹H NMR spectrum was very complex and displayed very poor signal to noise.

When using methanol as solvent a homogeneous reaction mixture was obtained but again the ^1H NMR indicated at best incomplete reaction and, perhaps just a mixture of reactants.

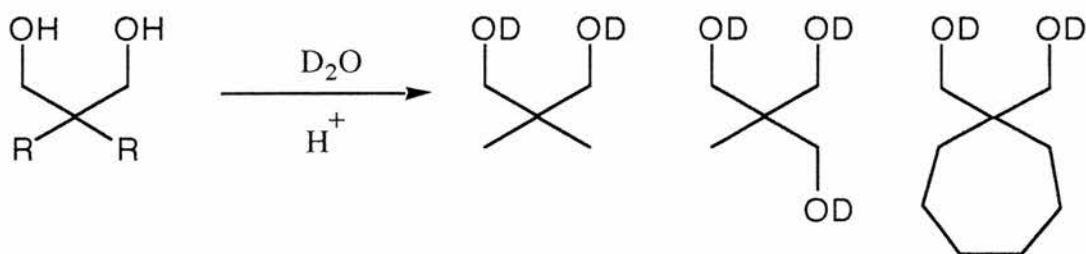
Deuteration of relevant diol type compounds

As part of the solid-state CP/MAS NMR investigation of the diol type compounds in Chapter 5, it was necessary to deuteriate the diols with deuterium oxide, D_2O . This then makes it possible to say whether the dynamic processes present may be at least partly due to hydrogen bonding effects.



The reaction has to be carried out under slightly acidic conditions to promote efficient deuterium exchange, although exchangeable deuterons should outnumber protons for the full mass action effect.

Each diol to be deuteriated was stirred in deuterium oxide (2 g in *ca.* 10 ml neat D_2O) in the presence of a drop of conc. HCl. After stirring at RT overnight the D_2O was evaporated off and the sample was dried to completion under vacuum. Diols which were deuteriated in this way included 2,2-dimethylpropane-1,3-diol, 1,1,1-tris(hydroxymethyl)ethane and 1,1-di(hydroxymethyl)cycloheptane:



^1H NMR of deuteriated 2,2-dimethylpropane-1,3-diol, for example, showed almost complete exchange had taken place due to near complete disappearance of the resonance due to the OH protons (when the same diol was stirred in D_2O in the absence of acid the exchange was very low by ^1H NMR). IR of the deuteriated diol showed the exchange was not complete, but as long as the exchange was nearing completion then the deuteriated diols were suitable for use in Chapter 5 to assess hydrogen bonding effects.

A slight depression in the melting points of the deuteriated diols was also noted (Table 1);

Melting points of protonated and deuteriated diol compounds / °C

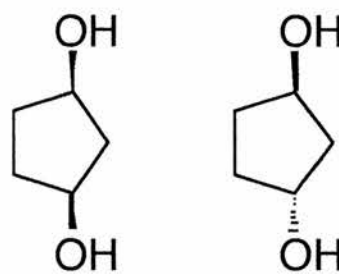
Diol compound	Protonated	Deuteriated	Lit. Value of OH compound ²⁰
2,2-Dimethylpropane-1,3-diol	126-8	124-5	123-7
2-Ethyl-2-methylpropane-1,3-diol	40-2	37-9	41-4
2,2-Diethylpropane-1,3-diol	59-61	50-2	59-61
1,1,1-Tris(hydroxymethyl)ethane	198-9	197-8	200-3

Table 1

²⁰ Aldrich Chemical Co. catalogue

Preparation of *cis*- and *trans*-Cyclopentane-1,3-diol

Two of the obvious target compounds for this project were *cis*- and *trans*-cyclopentane-1,3-diol, the preparation of which would appear to be a straightforward problem. However, the literature reveals a long-running conflict as to the correct



configuration of the isomers, despite the fact that several different methods of elucidation have been reported over the years. In order to understand the ongoing story of cyclopentane-1,3-diol, this chapter considers the literature chronologically.

Literature survey

In 1901 Thiele reported¹ the synthesis of *cis*- and *trans*-3,5-dibromocyclopentene, from the reaction of cyclopentadiene in chloroform, *en route* to the synthesis of the target compound, glutaric acid. The isomers were separated by distillation and had boiling points of 53-4 °C / 2 mm Hg and 72-5 °C / 2 mm Hg for the *cis* and *trans* isomers respectively. In addition, a melting point of 45 °C was also given for the *trans* isomer. The importance of 3,5-dibromocyclopentene in the synthetic route to cyclopentane-1,3-diol will become apparent later in the chapter.

Milas and Maloney presented a paper² in 1940 on the addition of hydroxyl groups to conjugated systems, specifically the addition of hydroxyl in 1,2-addition and 1,4-addition to cyclopentadiene. They prepared a previously unknown cyclopentane-1,3-diol from catalytic reduction of the corresponding cyclopentene-3,5-diol; the presence of a 1,3-diol was confirmed by a negative test with lead tetraacetate, which is known to oxidise 1,2-diols. They concluded that their cyclopentane-1,3-diol is *cis*, since a benzylidene derivative was obtained by condensation with benzaldehyde, a method used to determine the configuration of glycols. They also allocated melting points to the di-*p*-

¹ Thiele J., *Ann.*, **314**, (1901) 296

² Milas N. A., Maloney L. S., *J. Am. Chem. Soc.*, **62**, (1940) 1841

nitrobenzoate and diphenylurethane derivatives of their diol, although their values in the experimental section were reversed when presented in their 'Table 1' (see Table 2).

In 1945 Blomquist and Mayes reported³ on *cis-trans* isomerism in cyclopentene derivatives. They investigated more closely the bromination reactions originally studied by Thiele, and prepared both isomers of cyclopentane-1,3-diols from isomers of 3,5-dibromocyclopentene (cf. Thiele) via 3,5-diacetoxycyclopentene and cyclopentene-3,5-diol. They assigned their configurations of 3,5-dibromocyclopentene based on comparison of physical data with Thiele, and their *cis*-cyclopentane-1,3-diol was assigned based on comparison of the melting points of the ester derivatives of Milas and Maloney. Their assignments indicated overall retention of configuration from the 3,5-dibromocyclopentene through to the corresponding cyclopentane-1,3-diol.

Owen and Smith reported⁴ in 1952 anionotropic rearrangement in some reactions of 3,5-dibromocyclopentene. They admitted that comparatively little was known about cyclopentane-1,3-diol and 'available information is....of doubtful accuracy', but provided a comprehensive review of relevant literature. Based on the physical properties of their own isolated products, they agreed with the configurations of Milas and Maloney but could not give any explanation for Blomquist and Mayes' so-called *trans*-cyclopentane-1,3-diol (di-*p*-nitrobenzoate, m.p. 207 °C; diphenylurethane, m.p. 184 °C).

Young *et al.* reported⁵ the preparation of 1,2- and 1,4-dibromides from cyclopentadiene in 1956. They assigned dibromide **A**, m.p. 45 °C, to be *cis*-3,5-dibromocyclopentene, since its dipole moment of 3.40 *D* was greatly different from the calculated value of <1 *D* for *trans*-3,5-dibromocyclopentene. This is in direct disagreement with Thiele's assignment to the configuration of the isomers of 3,5-dibromocyclopentene. In addition, the new assignment was in accord with the general rule that the isomer with the higher boiling point should have the higher dipole moment. They carried out mechanistic studies, the results of which convinced them to reverse the configurations of Thiele, and of Owen and Smith.

³ Blomquist A. T., Mayes W. G., *J. Org. Chem.*, **10**, (1945) 134

⁴ Owen L. N., Smith P. N., *J. Chem. Soc.*, (1952) 4035

Saegebarth published a paper⁶ in 1960 providing a convenient preparation of *cis*-cyclopentane-1,3-diol, in response to recent interest in the synthesis of glycols by the bishydroboration-oxidation of dienes. He formed the *p*-nitrobenzylideneacetal of his diol and so labelled it *cis*, commenting that the formation of the *cis* isomer obtained from the bishydroboration was unique. His configurations were based on the assignment made by Young *et al.*, and he concluded that his *cis*-diol could be prepared from the *trans*-3,5-dibromocyclopentene of Owen and Smith with overall inversion of configuration.

Darby *et al.* reported⁷ in 1962 the formation of cyclopentane-1,3-diols from cyclopent-3-enol by its reaction with perlauric acid. Their lower boiling compound is labelled *cis* because on reduction it yields a diol, m.p. 40-2 °C, which yields a cyclic acetal on reaction with *p*-nitrobenzaldehyde, and by contrast the other isomer gave no reaction. Their diols gave ester-derivatives in good agreement with Young *et al.*, and Owen and Smith.

Brown and Zweifel commented on the 'controversy' surrounding the nature of the diol in a 1962 paper.⁸ They summarised a method of separation of the diols through treatment with *n*-butylboroxine, and observed the two isomers were isolable in the ratio 85:15. Their major product was in agreement with the properties of Saegebarth's *cis* and Darby's *trans*-diol, and on reaction with *n*-butylboroxine yielded a non-volatile boronic ester, and was assigned *trans* on this basis in agreement with Darby *et al.*

Zweifel and Brown published a paper⁹ the following year on the hydroboration of dienes with diborane, hexylborane and disiamylborane. When carrying out hydroboration of cyclopentadiene with disiamylborane they found the major diol formed after oxidation was *trans*, since disiamylborane is incapable of forming a cyclic derivative. This observation is in disagreement with Saegebarth's view that hydroboration yields the *cis*-diol.

⁵ Young W. G., Hall H. K., Winstein S., *J. Am. Chem. Soc.*, **78**, (1956) 4338

⁶ Saegebarth K. A., *J. Org. Chem.*, **25**, (1962) 2212

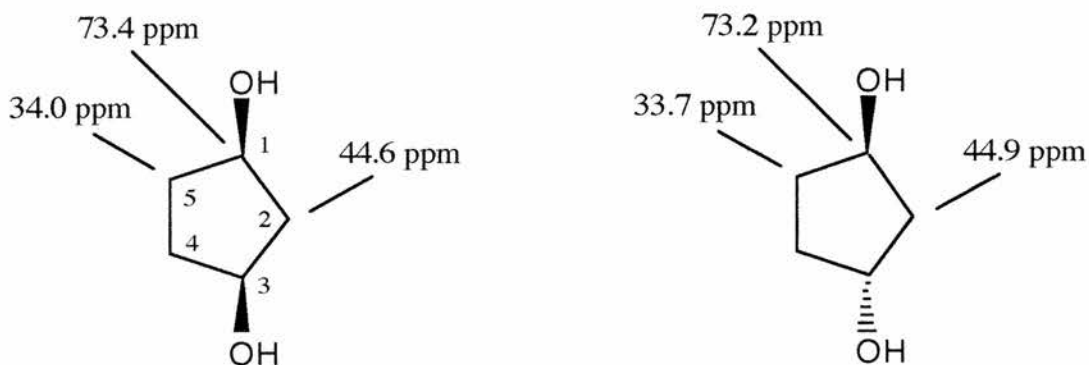
⁷ Darby A. C., Henbest H. B., McClenaghan I., *Chem. And Industry*, (1962) 462

⁸ Brown H. C., Zweifel G., *J. Org. Chem.*, **27**, (1962) 4708

⁹ Zweifel G., Brown H. C., *J. Am. Chem. Soc.*, **85**, (1963) 2066

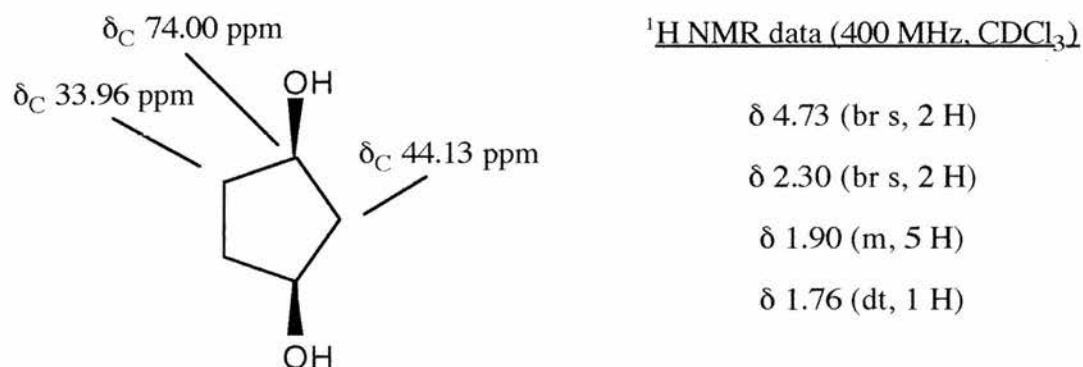
Bannard *et al.* reported¹⁰ the preparation of both isomers from de-etherification of the corresponding 3-methoxycyclopentanol in 1967. The melting points of their di-*p*-nitrobenzoate derivatives were in agreement with those of Darby *et al.*

Ritchie *et al.* reported¹¹ ¹³C NMR data, in 1975, for both isomers of cyclopentane-1,3-diol. They stated that C-4 is less shielded when O-1 and O-3 are *cis* rather than *trans*.



In 1977, Salomon and Salomon reported¹² that Pd / C catalytic hydrogenation of 2,3-dioxabicyclo[2.2.1]heptane in ethanol yielded *cis*-cyclopentane-1,3-diol with no trace of the *trans*. It was identified by ¹H NMR and GLC comparison with an authentic sample, although no data were given.

Chen and Halterman reported¹³ ¹H and ¹³C NMR data for *cis*-cyclopentane-1,3-diol in 1994. They prepared their saturated *cis*-diol based on the catalytic hydrogenation method of Sable and Posternak.¹⁴



¹⁰ Bannard R. A. B., Casselman A. A., Langstaff E. J., Moir R. Y., *Can. J. Chem.*, **45**, (1967) 2605

¹¹ Ritchie R. G. S., Cyr N., Korsch B., Koch H. J., Perlin A. S., *Can. J. Chem.*, **53**, (1975) 1424

¹² Salomon R. G., Salomon R. F., *J. Am. Chem. Soc.*, **99**, (1977) 3501

¹³ Chen Z., Halterman R. L., *Organometallics*, **13**, (1994) 3932

¹⁴ Sable H. Z., Posternak T., *Helv. Chim. Acta*, **45**, (1962) 370

Physical data (boiling points and melting points) of *cis*- and *trans*-cyclopentane-1,3-diol from the literature are summarised in Table 1. The data are quoted as given by each author, and it is clear that there is conflict in the allocated configurations of the isomers.

Melting points and boiling points of *cis*- and *trans*-cyclopentane-1,3-diol

Isomer	b.p. (°C / mm Hg)	m.p. (°C)	Authors
<i>cis</i> -	120-5 / 12		Milas, Maloney
	105 / 5	ca. 20	Blomquist, Mayes
	92 / 0.8, 90 / 1	30-2	Owen, Smith
	88-90 / 0.5		Zweifel, Brown
	86-7 / 0.5	31-2	Saegebarth
		40	Zweifel, Brown
		40-2	Darby, Henbest, McClenaghan
<i>trans</i> -	109 / 5		Blomquist, Mayes
	95 / 0.5	28-30	Zweifel, Brown
	99-100 / 0.1 torr	30	Sable, Posternak
	80-5 / 0.1	40	Owen, Smith

Table 1

Presented in Table 2 are data quoted in the literature for the di-*p*-nitrobenzoate and diphenylurethane ester derivatives, as further proof of the disagreement in the area.

trans-Cyclopentane-1,3-diol was successfully prepared by the method of Zweifel and Brown (Ref. 9), as described later in the chapter. Separation of the *cis-trans* cyclic diol mixture was afforded by esterification of the isomeric mixture with *n*-butylboronic acid; the *cis* isomer forms a volatile *cis* cyclic boronic ester which can be readily distilled from the non-volatile polymeric *trans* product which is formed. This appears to be a reliable method of allocating the *trans* isomer.

Melting points of ester derivatives of *cis*- and *trans*-cyclopentane-1,3-diol

Derivative	<i>cis</i> - m.p. (°C)	<i>trans</i> - m.p. (°C)	Authors
Di- <i>p</i> -nitrobenzoate	186-7		Saegebarth
	186	153	Owen, Smith
	178, 182	207	Blomquist, Mayes
	168-71		Milas, Maloney
	154-5	190.5-1.5	Bannard <i>et al.</i>
	153	186-7	Zweifel, Brown
	152-3	185-6	Sable, Posternak
	149-52	184-5	Darby, Henbest, McClenaghan
Diphenylurethane	179-80		Milas, Maloney
	172-3		Saegebarth
	172	162-3	Owen, Smith
	168, 171	184	Blomquist, Mayes
	162-3	173-4	Zweifel, Brown
		172-4	Brown, Zweifel
	160-1	170-1	Sable, Posternak

Table 2**Formation of *cis*-Cyclopentane-1,3-diol**

Kaneko *et al.* report¹⁵ a one step synthesis of *cis*-cyclopentene-3,5-diol from cyclopentadiene, as an alternative to surveyed literature methods which reveal that in all cases the products contain considerable proportions of cyclopentene-3,4-diols and *trans*-cyclopentene-3,5-diol. They state that an interesting and unique two-step synthesis of this compound from cyclopentadiene, *via* 1,4-epidioxi-2-cyclopentene as a key intermediate, was earlier reported by Schenck and Dunlap,¹⁶ whose epidioxide was synthesised by 1,4-addition of singlet oxygen to cyclopentadiene and then reduced, after its isolation, to the diol with thiourea in the dark. However, in order to isolate the

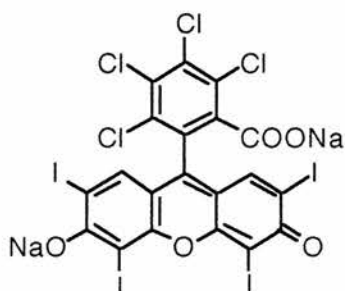
¹⁵ Kaneko C., Sugimoto A., Tanaka S., *Synthesis*, (1974) 876

¹⁶ Schenck G. O., Dunlap E. D., *Angew. Chem.*, **68**, (1956) 248

epidioxide the irradiation and the work-up had to be carried out at about $-100\text{ }^{\circ}\text{C}$ due to instability of the epidioxide (which decomposes at about $-30\text{ }^{\circ}\text{C}$).

irradiation reaction of cyclopentadiene with singlet oxygen

Keneko *et al.* found that in presence of thiourea the photosensitised oxygenation could be carried out at room temperature without isolation of the epidioxide and the desired *cis*-cyclopentane-1,3-diol could be obtained as the only product in good yield after concentration followed by distillation. Under these conditions thiourea was not observed to react with either Rose Bengal or singlet oxidation, but served to reduce the epidioxide selectively to the desired diol.



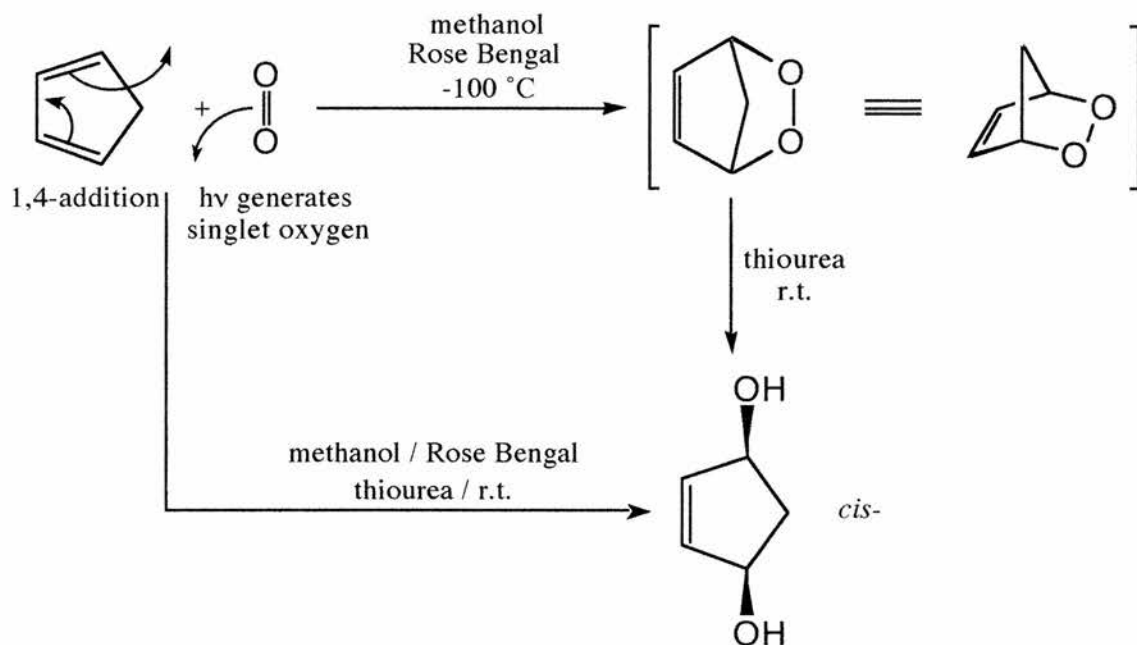
Rose Bengal

Rose Bengal is a well known photosensitiser used in this case for the production of singlet oxygen, an oxygen species which behaves as a dienophile. In many cases the absorption of the photon is not sufficiently facile and a photosensitiser is added to facilitate

electron transfer between two molecules. The use of a photosensitiser induces the transfer of excitational energy from an electronically excited molecule (the photosensitiser) to the ground state of another molecule, in this case oxygen.

Kaneko *et al.* used a 450 W mercury emission lamp as their source of $h\nu$ irradiation, but since the most powerful lamp available in the department was 400 W then the reaction time was increased accordingly, from 2.5 hours to 2 hours 50 minutes. The reaction was done in custom-made apparatus, with internal water jacket to cool the lamp. The apparatus was covered throughout the irradiation period with aluminium foil to protect observer's eyes from the $h\nu$ radiation. Oxygen was bubbled directly into the base of the reaction solution via narrow bore plastic tubing.

Firstly, cyclopentadiene for the reaction was prepared. The method of Vögel was followed¹⁷ where cyclopentadiene was generated from the dimer by distillation in paraffin at 200-40 °C. The freshly distilled cyclopentadiene, kept cold with solid carbon dioxide, was used immediately in each case to avoid reverting to the dimer.



Cyclopentadiene was distilled from the dimer and used immediately in the reaction. The Rose Bengal gives the initial reaction solution a distinct pink colour. After bubbling oxygen through for five minutes the lamp was switched on, and the outside of the apparatus was then cooled with ice to maintain a reaction temperature of 15 °C. After irradiation for 2 hours 50 minutes the lamp was switched off and stirring was continued in the dark overnight. During the irradiation reaction the solution changed in colour from pink to yellow.

After evaporation of the methanol under reduced pressure the residue was taken up in a little water and the aqueous part was washed with toluene (Ref. 15 used benzene) to remove colour. However, little or no colour was removed by this procedure, even when stirring overnight with toluene, and in addition a brown solid was seen to precipitate during this time. The precipitate was filtered off and the aqueous part was

¹⁷ Vögel A. I., Textbook of Practical Organic Chemistry, Longman Scientific and Technical, Harlow, England, 5th Ed., (1989) 1122

reduced under reduced pressure yielding a coloured viscous liquid. The liquid product was found to contain none of the desired product by ^1H NMR.

The experiment was repeated without the toluene wash and yielded a coloured viscous product. The product was found to contain the desired *cis*-cyclopentene-3,5-diol by ^1H NMR, but was also found to contain significant amounts of solvent and impurities. In view of the high dilution of the reaction and the poor yield (8 %) another route to the *cis*-cyclopentane-1,3-diol was sought, rather than attempting to purify this small quantity of product.

Formation of *trans*-Cyclopentane-1,3-diol

Zweifel and Brown report⁹ the hydroboration of cyclopentadiene to cyclopentane-1,3-diol. The nature of the borane reagent used determines the proportions of the *cis*- and *trans*-isomer which are formed, as seen in Table 3.

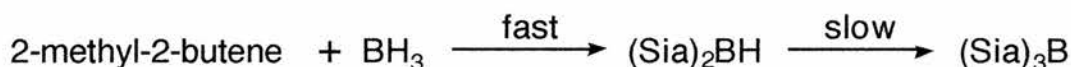
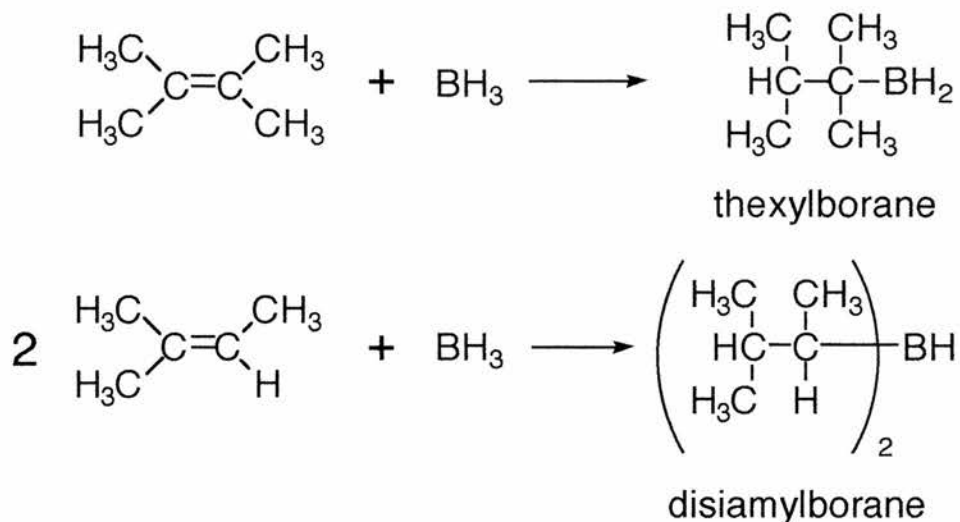
Distribution of diol isomers in hydroboration of cyclopentadiene

Hydroborating reagent	Diol distribution after distillation %		Yield of diol %
	<i>cis</i> -1,3-	<i>trans</i> -1,3-	
Borane	15	85	80
Thexylborane	13	87	71
Disiamylborane	3	97	70

Table 3

The majority of mono- and di-substituted alkenes undergo hydroboration to give trialkylboranes, which are then available for a wide variety of synthetic procedures. With some alkenes, however, alkylation of borane does not go to completion and the resulting mono- or di-alkyl boranes, such as thexylborane or disiamylborane, are useful in synthesis as modified boranes.

disiamylboronation of cyclopentadiene



Following the method of Zweifel and Brown,⁹ 2 equivalents of 2-methyl-2-butene were reacted with a THF solution of 1 equivalent of borane in dry THF under anhydrous conditions. The borane was added to the butene solution at -15 °C and the disiamylborane, assumed to be prepared in quantitative yield, was stored in the freezer overnight until use.

The prepared disiamylborane was then added dropwise to the freshly distilled cyclopentadiene in dry THF, maintained at 0 °C throughout the addition, and the reaction mixture was kept in the fridge overnight. After addition of water to destroy residual borane, oxidation with basic hydrogen peroxide and work-up, the solvent was evaporated and the residue distilled. A low melting solid was expected but cooling and scratching failed to solidify the residue. Analysis of the residue was inconclusive by ¹H NMR.

To avoid degradation of the disiamyl reagent, which was previously stored overnight, the experiment was repeated using the reagent immediately. Again, a solid was not obtained, and NMR spectra were complex and inconclusive. The method of

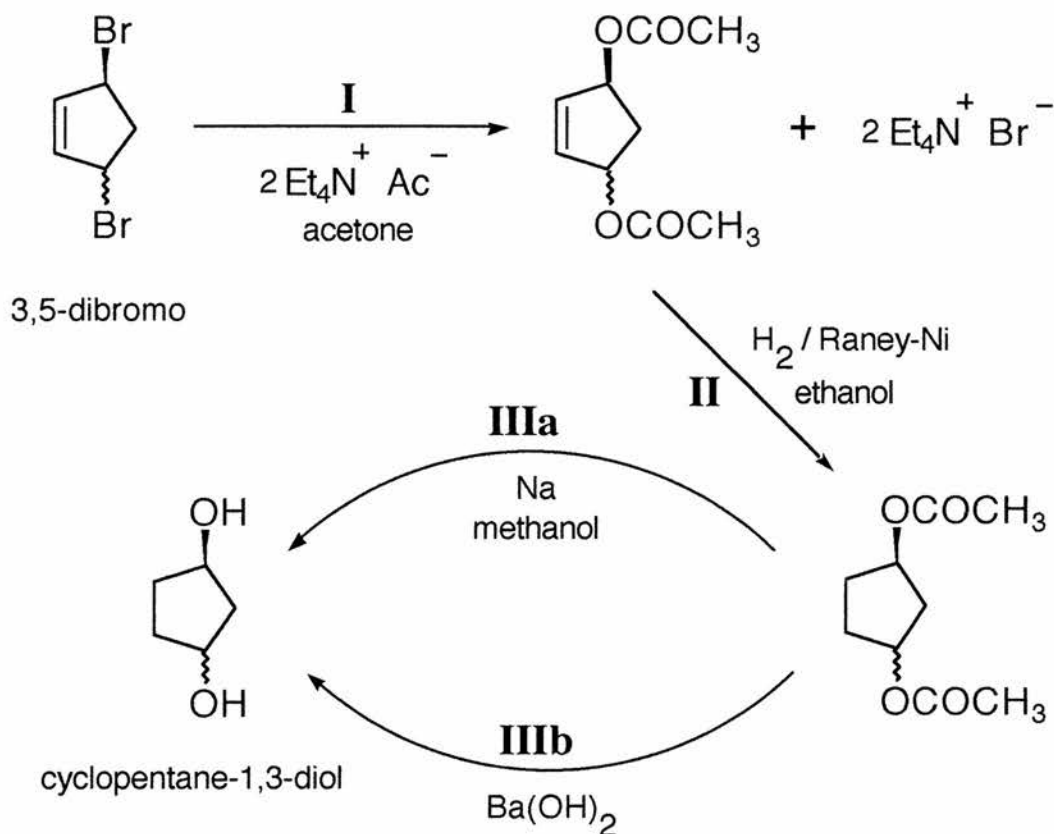
Vögel¹⁸ was then used, which employed diglyme (dimethoxydiethylether) as solvent and sodium borohydride as source of borane. Again, reagent yield was assumed to be quantitative, and the reagent was used immediately. ¹H NMR of the isolated product was again inconsistent with that expected of cyclopentane-1,3-diol. Also, removal of diglyme by washing with water proved inefficient.

Formation of *cis*- and *trans*-Cyclopentane-1,3-diol

Owen and Smith reported⁴ that early attempts to synthesise cyclopentane-1,3-diol resulted in products containing considerable proportions of cyclopentane-1,2-diol. They also reported various methods for acetylation of 3,5-dibromocyclopentene, *en route* to isolation of *cis*- and *trans*-cyclopentane-1,3-diol. They found that when they used potassium acetate or silver acetate in acetic acid that the desired 3,5-diacetoxycyclopentene was accompanied by 3,4-diacetoxycyclopentene, formed by anionotropic rearrangement. The configuration of the rearranged product is *cis* in the presence of water, but *trans* if anhydrous acetic acid is used, irrespective of the configuration of the dibromide. It is assumed that this is achieved by an anionotropic rearrangement when the first bromide is replaced, to give *trans*-3-acetoxy-4-bromocyclopentene. However, when the dibromide reacts with tetraethylammonium acetate in acetone, rearrangement does not occur, and deacetylation and hydrogenation of the product gives only cyclopentane-1,3-diol. By this method they prepared pure *cis* and *trans* isomers for the first time.

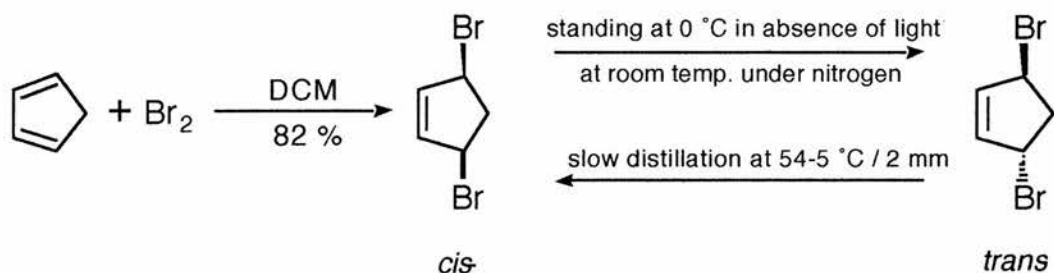
Firstly, the 3,5-dibromocyclopentene is prepared by reaction of freshly distilled cyclopentadiene with bromine in dichloromethane at -25 to -30 °C. The solvent is then immediately evaporated off under reduced pressure and the residue is distilled to yield the *cis*-dibromide as a colourless liquid. The *trans* isomer is then obtained by storage of this product in the dark at room temperature, under nitrogen for three months.

¹⁸ Vögel A. I., Textbook of Practical Organic Chemistry, Longman Scientific and Technical, Harlow, England, 5th Ed., (1989) 419; Brown H. C., Zweifel G., *J. Am. Chem. Soc.*, **83**, (1961) 1241



for *cis*-1,3-diol; **I** yield 78 %, **II** RT / 5 atm., **IIIa** RT / 24 hours; yield 54 %, **IIIb** reflux / 20 hours; yield 62 %.

for *trans*-1,3-diol; **I** yield 70 %, **II** RT / 1 atm., **IIIa** yield ~55 %, **IIIb** reflux / 5 hours; yield 55 %.



via acetylated 3,5-dibromocyclopentene

Bromine in DCM was added to freshly distilled cyclopentadiene in DCM at a rate to maintain the reaction temperature at -25 to -30 °C. As the reaction proceeded a green colour developed, consistent with observations in Ref. 4. After evaporation of the solvent the next stage, the distillation, was not started for a further two hours during

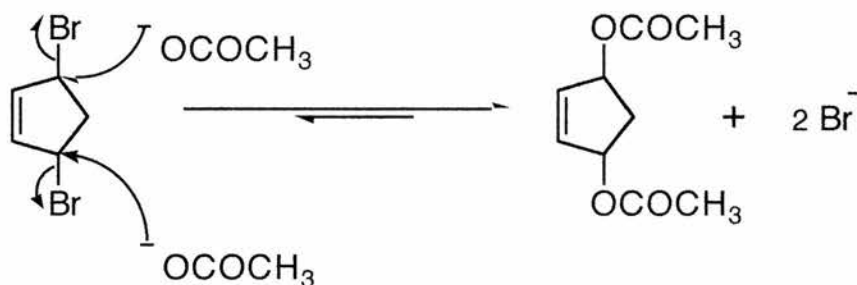
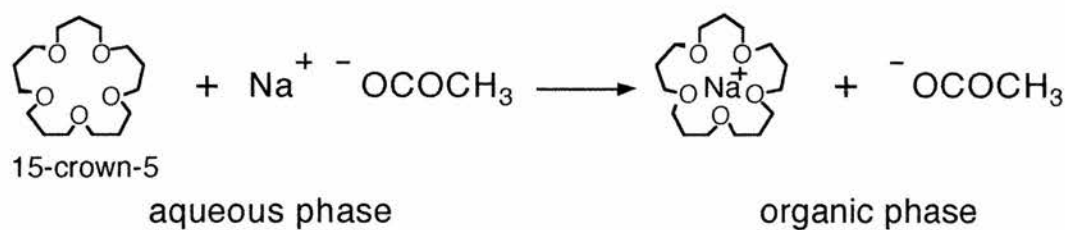
which time the reaction mixture polymerised into a 'black rubber ball'; Ref. 4 stated that '...the green residue was quickly distilled...', the reason for this was now clear.

On repeating the experiment the distillation was carried out immediately and the distilled 3,5-dibromocyclopentene (64 °C / 1.5 mm Hg) was slightly yellow in colour. After being left overnight the product had deepened in colour and was redistilled. Over time the colour went consistently deeper and small black spots appeared on the inner surface of the flask. The coloured product should therefore be distilled immediately before future use.

According to the equilibrium suggested by Owen and Smith slow distillation yields *cis*-3,5-dibromocyclopentene, so our unsaturated dibromide is assumed to be the *cis*. Standing at 0 °C under nitrogen in the dark should convert the product to the *trans* isomer, but even after 3 months only a very small shift was observed in the ratio of isomers. The product was always analysed as a mixture, although there remained a predominant isomer, but pure *cis*- or *trans*-3,5-dibromocyclopentene was never observed. When the product is subject to acetylation by means of 15-crown-5 ether, detailed next, a mixture of isomers is observed by TLC.

acetylation with 15-crown-5 ether

Various sources of acetate have been used to acetylate 3,5-dibromocyclopentene, tetraethylammonium acetate being the one used by Owen and Smith⁵ to retain configuration through to the unsaturated diacetoxy compound. As a test, an experiment was carried out using 15-crown-5 ether to aid the migration of the sufficiently nucleophilic acetate to the dibromo- substrate. 15-Crown-5 ether has a cavity perfectly suited in size to accommodate the sodium ion, as a phase-transfer catalyst. The sodium acetate in the aqueous layer was stirred vigorously with ether, which contained the substrate, 3,5-dibromocyclopentene. It was hoped that the acetate would be pulled into the organic phase along with the complexed sodium, which would then take part in an acetylation reaction, in a nucleophilic substitution for bromide.



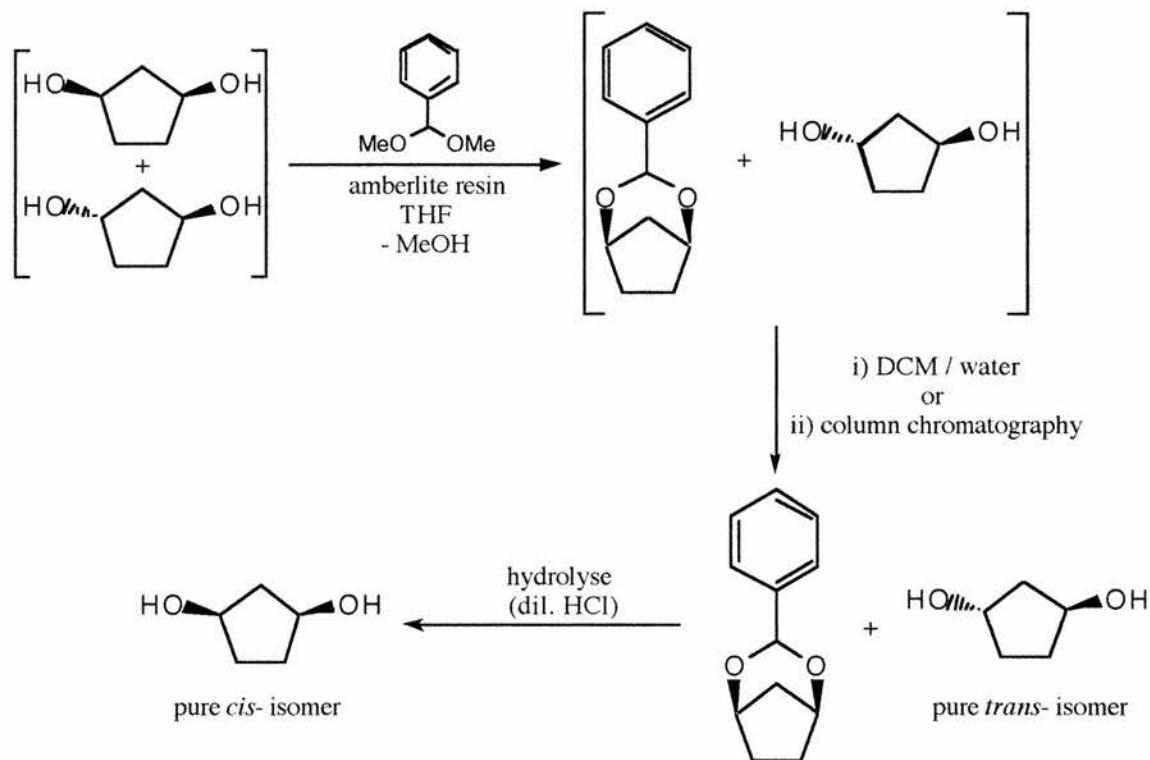
Only a catalytic amount of 15-crown-5 ether is required since the migration of sodium to the organic phase continually drives the equilibrium to the right. The reaction, at room temperature, was followed by TLC. No change was observed after several hours at room temperature, so the mixture was refluxed for two hours initially, but a total of five hours reflux was required to complete the reaction, as observed by TLC. From TLC, the dibromo- compound was seen to be a mixture of isomers, and the spots for the acetylated product reflected this.

Separation of *cis*- and *trans*-Cyclopentane-1,3-diol

separation using benzaldehyde dimethylacetal

Benzaldehyde dimethylacetal was seen as a suitable compound to complex with the *cis* isomer of cyclopentane-1,3-diol in a mixture of the two isomers (as purchased from Aldrich Chemical Co.; 95 % purity). The isomers can then be separated by column chromatography or by partitioning between DCM and water, the *trans* diol being water soluble and the *cis* complex being water insoluble.

The diol mixture in dry THF (potassium still) was treated with 1.2 equivalents of benzaldehyde dimethylacetal (w.r.t. *cis* isomer, assuming 50:50 ratio of isomers) in the presence of sufficient amberlite resin to impart slight acidity.



After reflux for one hour the solvent was evaporated under reduced pressure and the residue was distilled. Analysis of the product by ^1H NMR showed no evidence of the expected aromatic ring for the *cis* complex.

The experiment was repeated, the diol mixture being dried before reaction by refluxing with benzene, any moisture being lost as an azeotrope with benzene. Reaction was again carried out with 1.2 equivalents of benzaldehyde dimethylacetal in dry THF, but with a few crystals of tosic acid to impart slight acidity. On heating the mixture went brown, and investigation of the mixture by TLC showed that the benzaldehyde dimethylacetal had been hydrolysed to benzaldehyde, even after rigorous efforts to remove water.

separation using *n*-butylboronic acid

Brown and Zweifel reported, firstly, use of *n*-butylboroxine to separate isomeric pairs of cycloalkanediols⁸ and, more specifically, use of the boroxine to separate isomers of *cis*- and *trans*-cyclopentane-1,3-diol.⁹ The method of Zweifel and Brown (Ref. 9) was used to form a mixture of isomers using diborane as hydroboration reagent, as opposed to disiamylborane referred to previously in this chapter. Ref. 9 states that when using diborane the ratio of isomers formed is *cis* 15:85 *trans*. This was found to be the case when the isomer mixture was analysed by ¹³C NMR.

A portion of the isomer mixture (10 mmol.) was treated with 1 equivalent of *n*-butylboronic acid. The water formed was removed by azeotropic distillation with benzene and distillation at reduced pressure yielded a non-volatile residue (and a negligible amount of a volatile residue). After displacement of the boron in the non-volatile residue with ethylene glycol, a diol was collected whose ¹H NMR spectrum was consistent with that of a cyclopentane-1,3-diol. This was assumed to be the *trans* isomer from the findings of Ref. 9. Since the ratio of *cis* isomer produced is so small (15 %), none of the *cis* isomer was isolated.

Diol compounds studied by solid-state CP/MAS NMR

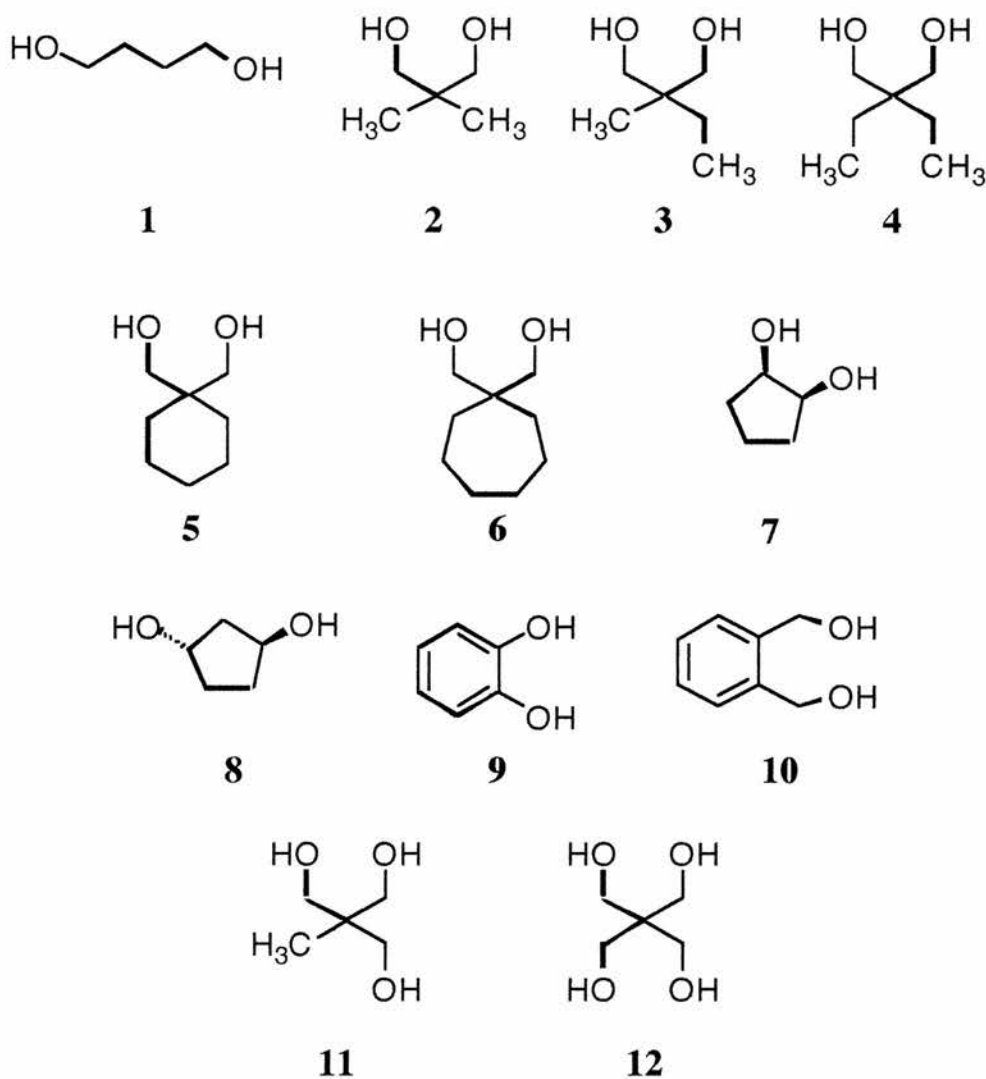
All solid-state NMR spectra were obtained on a Bruker MSL500 wide-bore spectrometer in high power mode. Solid-state ^{13}C spectra were obtained at a frequency of 125.758 MHz in the CP/MAS mode using 4 mm o.d. zirconia rotors spinning typically at 6 kHz. Compressed air was used as bearing gas and drive gas, except when operating below ambient temperature or when using a particularly moisture sensitive sample when oxygen free nitrogen was used as both bearing and drive gas. A cross polarisation contact time of 1 millisecond and a recycle time of 5 seconds was used throughout unless stated otherwise. Chemical shifts were referenced relative to the CH_2 group in adamantane at 38.56 ppm. Temperature calibration was carried out as detailed in chapter 2,¹ and all temperatures quoted are corrected.

The spin locking radio frequency fields for both carbon and hydrogen are identical when the Hartmann-Hahn condition is satisfied and were determined for each experiment (found typically to be 50-80 kHz). The same radio frequency power was used for the spin lock period in the $T_{1\rho}$ determinations which were carried out using either a standard CP pulse sequence, or a CP pulse sequence modified to incorporate a 50 μs NQS dephasing delay.

Shown over is the range of diols studied, a series of diols (**1-10**), one triol (**11**) and one tetraol (**12**). Compounds **1-4**, **7**, **11** and **12** were obtained as commercially available samples and used as received. Compounds **5** and **6** were synthesised by Volkmar Weiß as detailed in Chapter 3. Compounds **8** and **10** were synthesised by the author as detailed in Chapter 4 and Chapter 3 respectively, **8** being purified by distillation and **10** being recrystallised from ether prior to use. Compound **9** was obtained as a commercially available

¹ Actual temperature = $0.799 \times (\text{controller setting}) + 62.2$; ($r^2 = 0.999$)

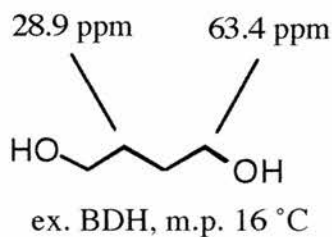
sample from BDH, and recrystallised from water prior to use. Additional purification or preparatory procedures employed, as necessary, are detailed where appropriate.



- | | |
|--|---|
| 1 Butane-1,4-diol | 7 <i>cis</i> -1,2-Cyclopentanediol |
| 2 2,2-Dimethylpropane-1,3-diol | 8 <i>trans</i> -1,3-Cyclopentanediol |
| 3 2-Ethyl-2-methylpropane-1,3-diol | 9 1,2-Dihydroxybenzene (Catechol) |
| 4 2,2-Diethylpropane-1,3-diol | 10 1,2-Di(hydroxymethyl)benzene |
| 5 1,1-Di(hydroxymethyl)cyclohexane | 11 1,1,1-Tris(hydroxymethyl)ethane |
| 6 1,1-Di(hydroxymethyl)cycloheptane | 12 Pentaerythritol |

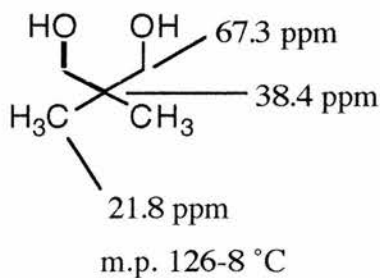
Diol compounds studied by solid-state CP/MAS NMR.

Butane-1,4-diol 1



On decreasing the temperature below RT, using nitrogen as bearing and drive gas, the first spectrum was collected at 286 K due to its low melting point (the sample was cooled in the probe, without spinning initially, and then spinning was begun once sufficiently cool). Two signals were apparent, as expected, a singlet at 63.4 ppm for the CH₂OHs and a less intense singlet at 28.9 ppm for the inner CH₂s. However, throughout the temperature range studied (200-286 K) the intensity, multiplicity and position of the peaks remained essentially unchanged, indicating no detectable dynamic effect in that range.

2,2-Dimethylpropane-1,3-diol 2



The RT spectrum of **2** showed a very broad, noisy singlet for CH₂OH, a sharp quaternary carbon signal and a broad methyl signal. On raising the temperature to 314 K another solid phase is in evidence, where the signals are all sharp and the shifts and the signal intensities are different; signals are seen at 69.7, 37.6 and 22.5 ppm, with that due to the quaternary carbon the least intense. On lowering the temperature the signal for the methyl carbons is 'frozen out' and appears as a doublet, with coalescence noted at 262 K, and the CH₂OH carbon gets appreciably sharper. Spectra 1 shows **2** over the temperature range 240 K to 314 K, and Spectra 2 shows in more detail the methyl

resonance around coalescence at 262 K. Due to the peak widths varying with temperature, indicative of a dynamic effect, $T_{1\rho}$ measurements were taken between temperature of coalescence, T_C , and the higher temperature phase (268-298 K). The $T_{1\rho}$ relaxation measurements are displayed in Table 1. (A reported phase change² at 313-6 K did not affect the collection of $T_{1\rho}$ data.)

$T_{1\rho}$ data for 2,2-dimethylpropane-1,3-diol ($\omega_1 = 65.8$ kHz)

Temperature (K)	$T_{1\rho}$ (ms)		
	CH ₂ OH	quat. C	CH ₃
266	22.0		
270	18.9		79.5
274	15.0	125	65.4
278	10.9	115	54.0
282	8.4	90	39.0
286	5.8	72	27.0
290	3.84	60	21.8
294	2.94	39	17.2
298		29.5	13.3

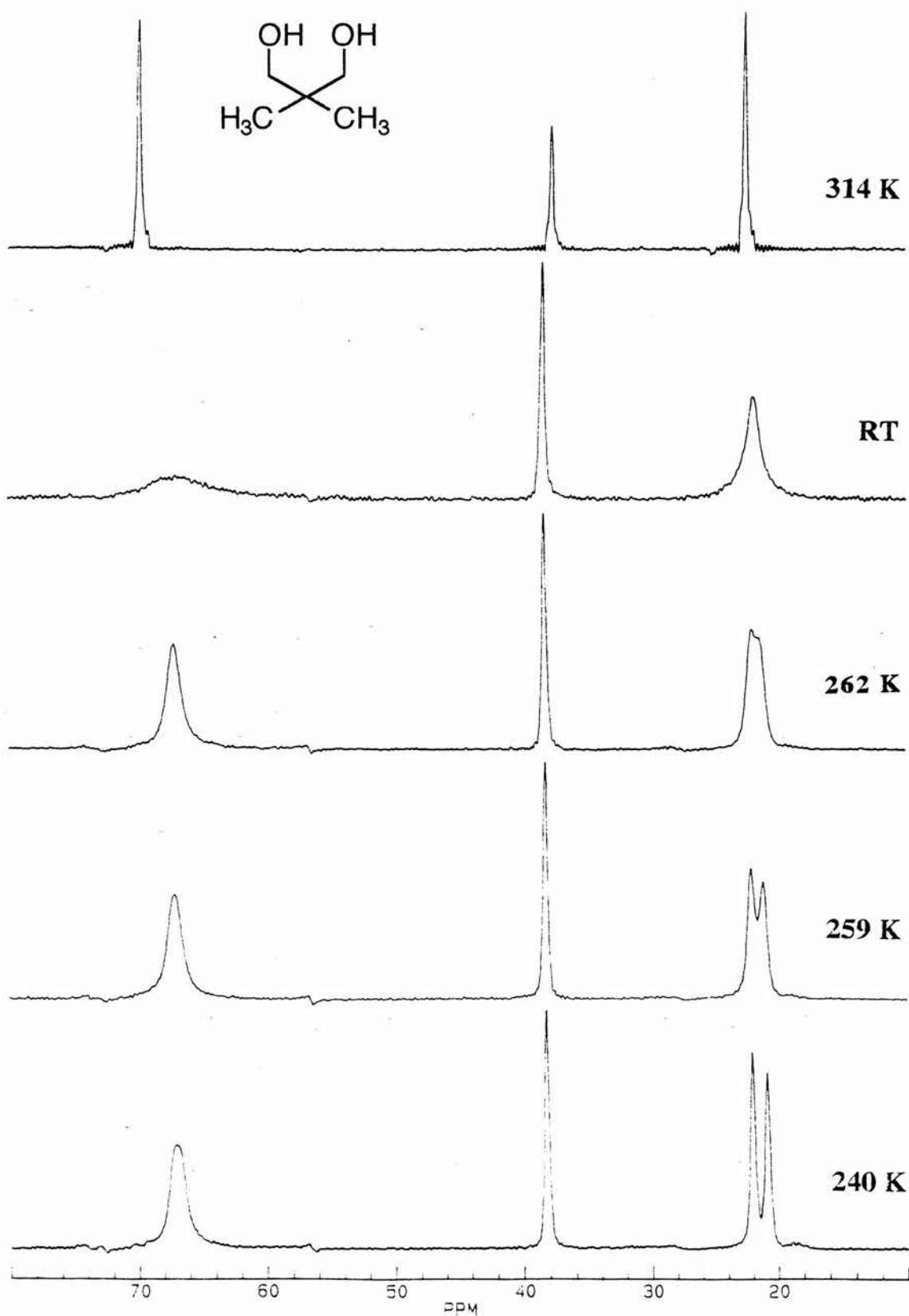
Table 1

It is clear from the data that there is no minimum of $T_{1\rho}$ observed. However, it is still possible to derive energies of activation (E_a). Since $T_{1\rho}$ is proportional to the rate, k , a plot of $\ln(T_{1\rho})$ versus $1/T$ gives E_a from the asymptotic slope, which is $-E_a/R$. Therefore $E_a = -\text{slope} \times R$.

² Murrill E., Breed L., *Thermochim. Acta.*, **1**, (1970) 239

Spectra 1

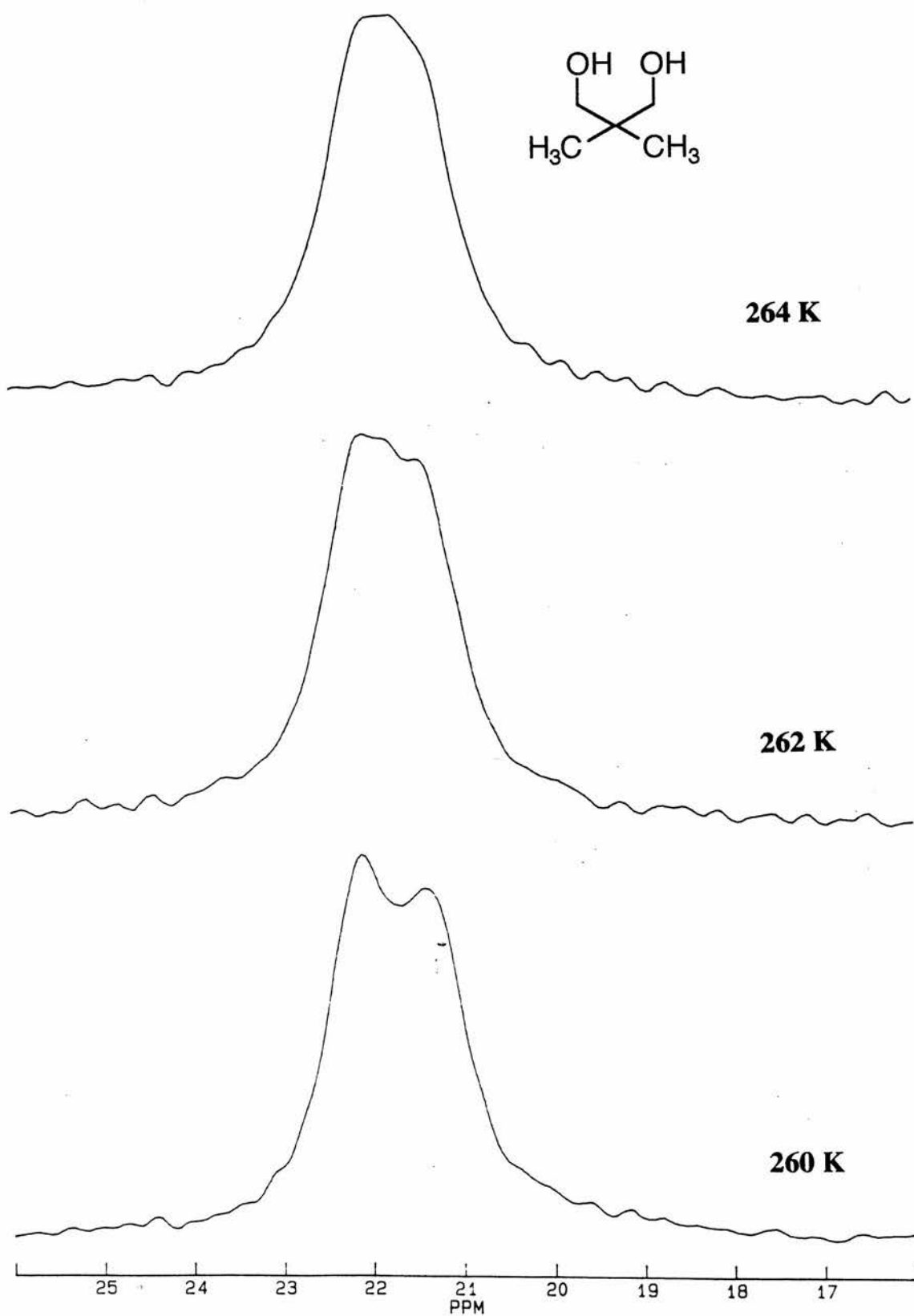
Spectra of 2,2-dimethylpropane-1,3-diol from 240 K to 314 K



Diol compounds studied by solid-state CP/MAS NMR.

Spectra 2

Spectra of methyl resonance of 2,2-dimethylpropane-1,3-diol
around coalescence at 262 K



Diol compounds studied by solid-state CP/MAS NMR.

A plot of $\ln(T_{1\rho})$ against $1/T$ for the CH_2OH and CH_3 carbons of 2,2-dimethylpropane-1,3-diol is displayed in Figure 1.

Plot of $\ln(T_{1\rho})$ against $1/T$ for 2,2-dimethylpropane-1,3-diol

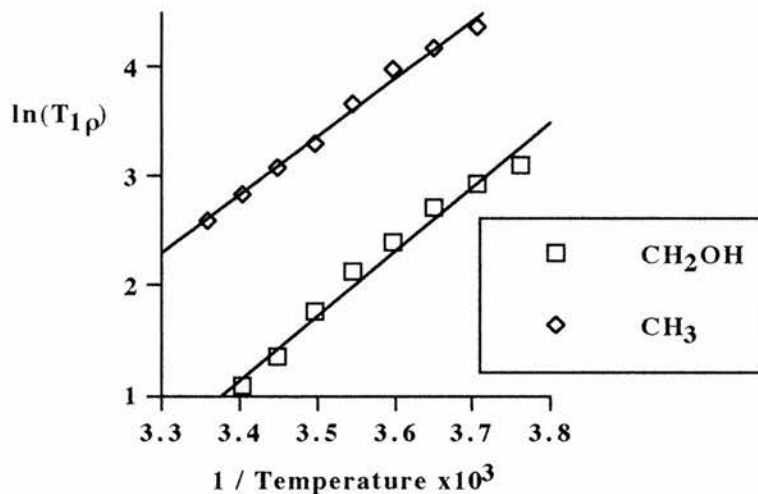


Figure 1

Energies of activation (E_a) were derived for the CH_2OH and CH_3 carbons, and the results are given in Table 2. Of these the activation energy for the CH_2OH is probably the more reliable, therefore E_a can be estimated to be $+ 48.5 \pm 3 \text{ kJ mol.}^{-1}$.

Energies of activation derived for 2,2-dimethylpropane-1,3-diol

	CH_2OH	CH_3
slope	+ 5.84	+ 5.33
r^2	0.981	0.992
E_a (kJ mol.^{-1})	+ 48.5	+ 44.3

Table 2

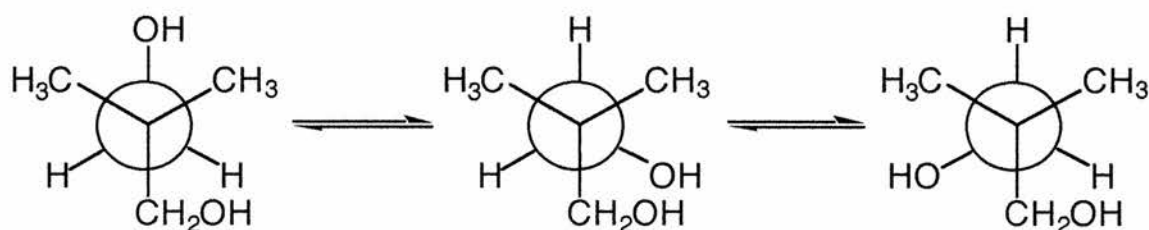
Also, the free energy of activation (ΔG^\ddagger_C) of the dynamic process, at the temperature of coalescence, (T_C), can be estimated from the difference in chemical shifts

of the 'frozen out' signals below the temperature of coalescence. This Arrhenius type relationship is shown:

$$\Delta G^\ddagger_C = 4.57T_C [9.67 + \log(T_C / \Delta\nu)]$$

where, $\Delta\nu$ is chemical shift difference in Hz

In **2** the CH_3 signal coalesces at 262 K and $\Delta\nu$ is 1.15 ppm, which gives $\Delta G^\ddagger_{262\text{ K}} = + 49.7 \text{ kJ mol.}^{-1}$, in good agreement with the E_a value. This suggests that there is a hydrogen bond exchange process with either relatively free molecular motion or with static molecules. One possible mechanism is the rotation of the CH_2OH group as a whole e.g.



investigation of deuterated 2,2-dimethylpropane-1,3-diol

One possible phenomenon taking place in these diol compounds is a hydrogen bonding or exchange process. A convenient way to check this is to compare the coalescence temperature and activation parameters of the deuterated O^{-2}H (OD) compound with the O^{-1}H (OH) compound, where the activation energies for the making and breaking of hydrogen bonds should show a kinetic isotope effect i.e. the deuterated alcohol does not take part in hydrogen exchange processes to the same extent as the hydrogenated alcohol and so this affects the physical properties.

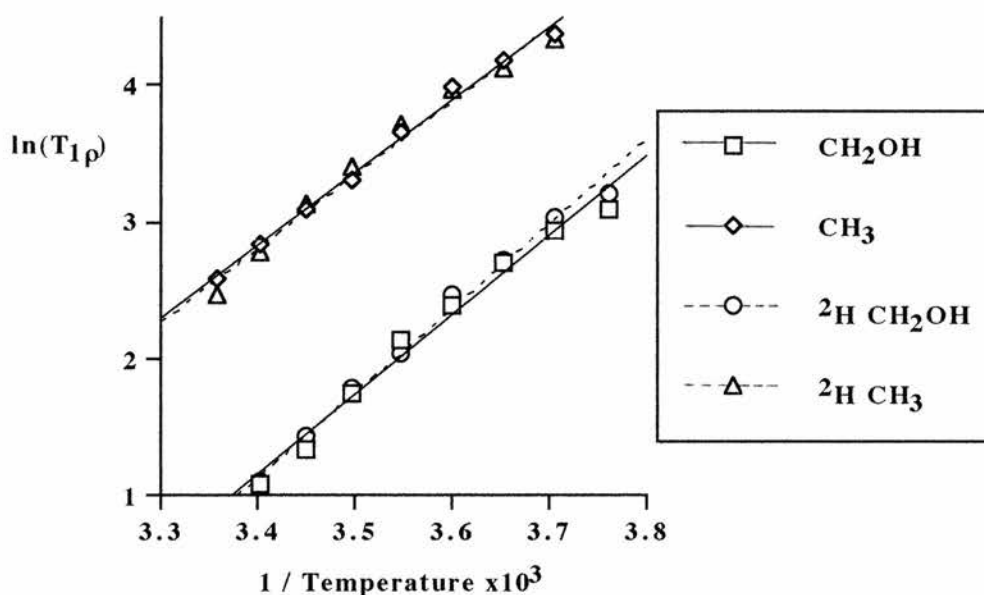
$T_{1\rho}$ data were collected from 266 to 298 K, as for **2**. The data are presented in Table 3.

$T_{1\rho}$ data for deuteriated 2,2-dimethylpropane-1,3-diol ($\omega_1 = 62.0$ kHz)

Temperature (K)	$T_{1\rho}$ (ms)		
	$\text{CH}_2\text{O}^2\text{H}$	quat. C	CH_3
266	24.9	164	
270	20.9	160	75.8
274	15.3	118	61.8
278	11.8	112	52.6
282	7.72	93.1	40.7
286	5.92	63.5	30.0
290	4.21	48.5	22.9
294	3.01	43.6	16.0
298	2.22	25.0	11.7

Table 3

The $\text{CH}_2\text{O}^2\text{H}$ data and the CH_3 data can now be directly compared with that for 2. A variation in the slopes of the plots of $\ln(T_{1\rho})$ against $1/T$ would provide evidence of a hydrogen exchange process. A direct comparison is seen in Figure 2 and the derived activation energies are shown in Table 4.

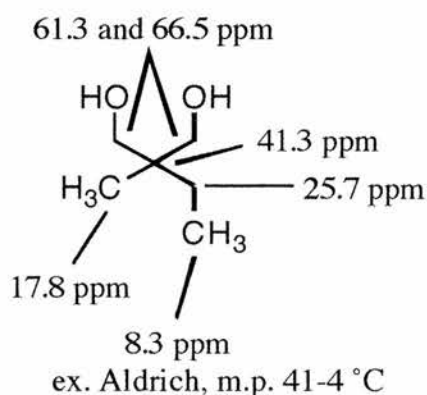
Plot of $\ln(T_{1\rho})$ against $1/T$ for O^1H and O^2H 2,2-dimethylpropane-1,3-diol**Figure 2**

Energies of activation derived for deuteriated 2,2-dimethylpropane-1,3-diol

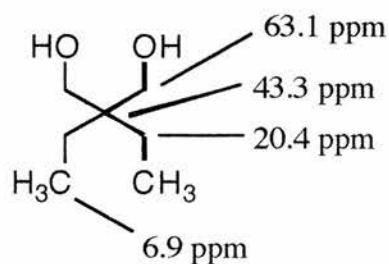
	CH ₂ O ² H	CH ₃
slope	+ 6.18	+ 5.40
r ²	0.992	0.981
E _a (kJ mol. ⁻¹)	+ 51.4	+ 44.9
2	CH ₂ OH	CH ₃
E _a (kJ mol. ⁻¹)	+ 48.5	+ 44.3

Table 4

The activation energy derived for the methyl group is essentially the same, as expected. That derived for the CH₂O²H group, however, is slightly lower. Also, the temperature of coalescence is found to be different, 266 K as opposed to 262 K for **2**. The effects are not significant, but sufficient enough to attribute at least some degree of hydrogen bond exchange. No check was done to assess the degree of OD labelling after the experiment.

2-Ethyl-2-methylpropane-1,3-diol **3**

The RT spectrum showed all signals very broad, the peaks at 66.5, 61.3 and 25.7 ppm being significantly broader but less intense. The signals did not change throughout the temperature range studied, from 232 K to 308 K. On attempting to collect $T_{1\rho}$ data from 232 K upwards ($\omega_1 = 58.1$ kHz) it was apparent there was no observable change.

2,2-Diethylpropane-1,3-diol 4

ex. Aldrich, m.p. 59-61 ppm

The RT spectrum of **4** shows two sharp signals, for the quaternary carbon and the methyls, and two broad signals, for the CH_2OH s and the CH_2CH_3 s. On decreasing the temperature below RT a split in the methyl signal was observed at 280 K, which increases in magnitude right down to 200 K where the signal begins to separate into three signals (or more correctly a low intensity signal, and a higher intensity signal with a shoulder). In addition the CH_2OH resonance is seen to split below approximately 232 K. Spectra 3 shows **4** over the temperature range 200 K to RT. The splitting of the methyl signal is curious since the signal, due to two methyl carbons, is seen to begin to separate into three separate signals when cooled to 200 K (Spectra 4). $T_{1\rho}$ measurements were collected from beyond the coalescence of the CH_3 s to just below the melting point of the solid (298 K to 318 K). The $T_{1\rho}$ data collected are presented in Table 5.

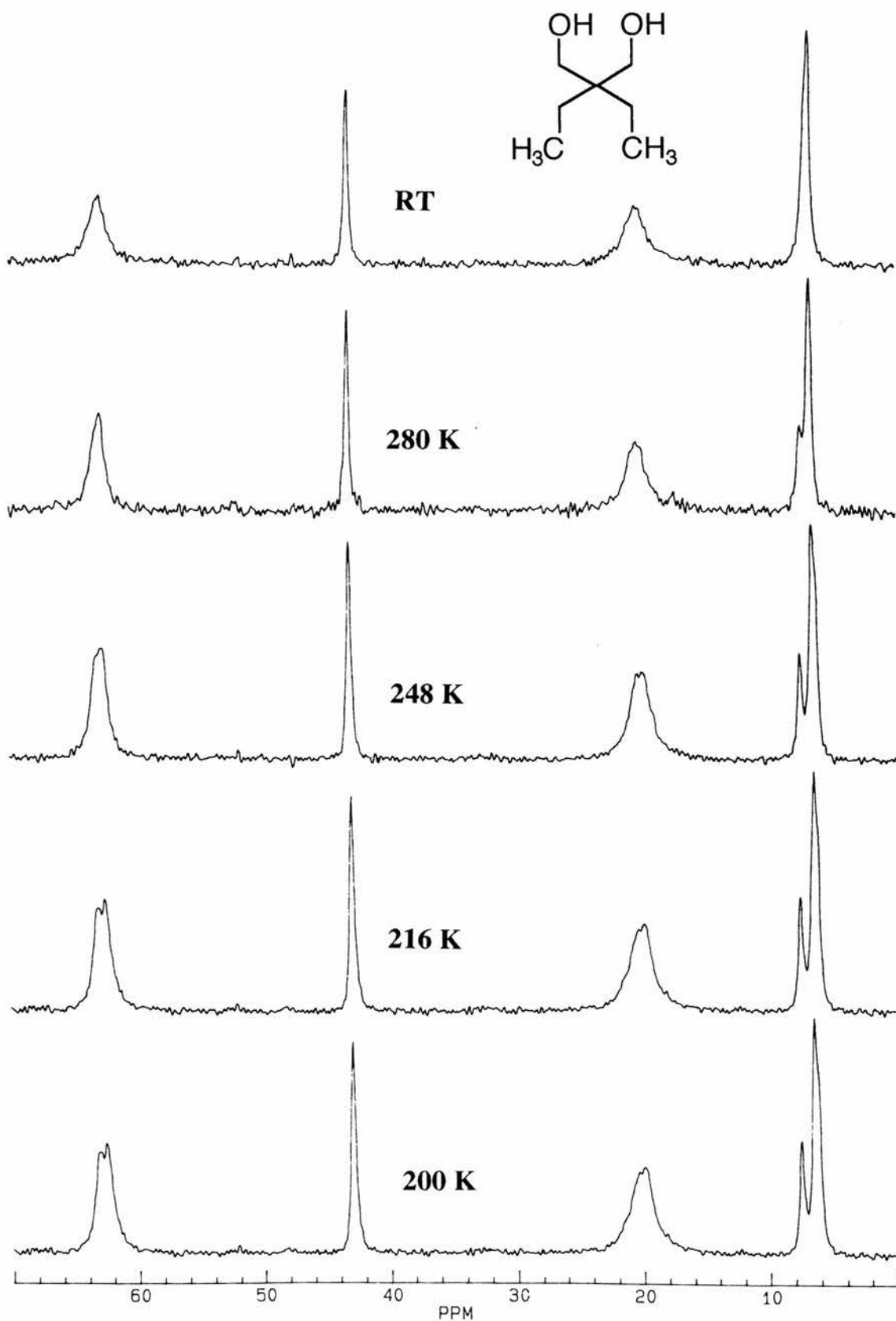
$T_{1\rho}$ data for 2,2-diethylpropane-1,3-diol ($\omega_1 = 62.5$ kHz)

Temperature (K)	$T_{1\rho}$ (ms)			
	CH_2OH	quat. C	CH_2CH_3	CH_3
298	11.4	57.4	7.48	34.6
302	8.86	36.8	4.85	22.9
306	5.95	27.0	2.81	16.0
310	4.48	15.7	2.18	10.0
318	1.84	5.27	1.21	3.84

Table 5

Spectra 3

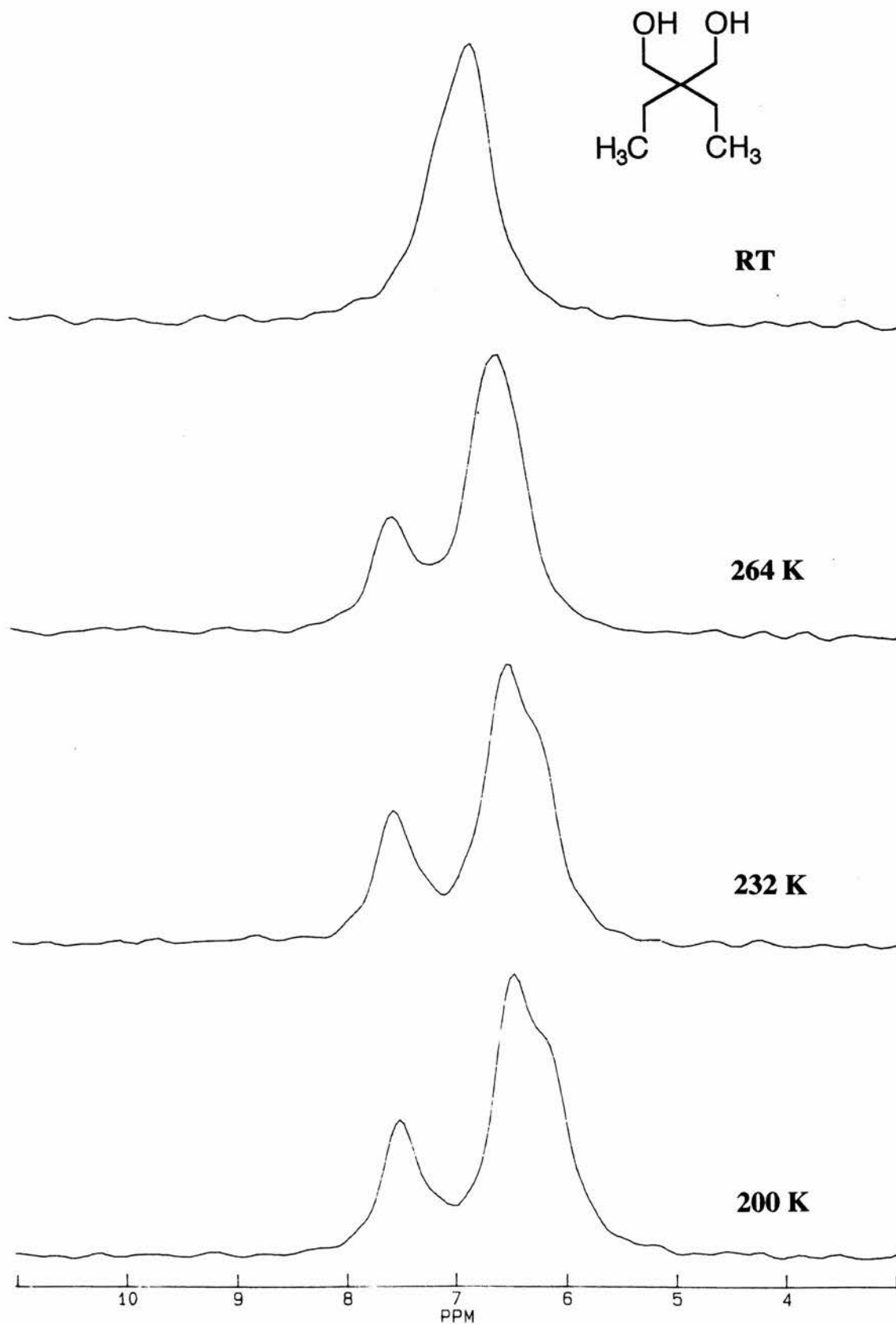
Spectra of 2,2-diethylpropane-1,3-diol from 200 K to RT



Diol compounds studied by solid-state CP/MAS NMR.

Spectra 4

Spectra of CH_3 resonance of 2,2-diethylpropane-1,3-diol
from 200 K to RT



Diol compounds studied by solid-state CP/MAS NMR.

No minimum in the $T_{1\rho}$ versus temperature curve is observed. However, energies of activation (E_a) can still be calculated from a plot of $\ln(T_{1\rho})$ against $1/T$ (Figure 3).

Plot of $\ln(T_{1\rho})$ against $1/T$ for 2,2-diethylpropane-1,3-diol

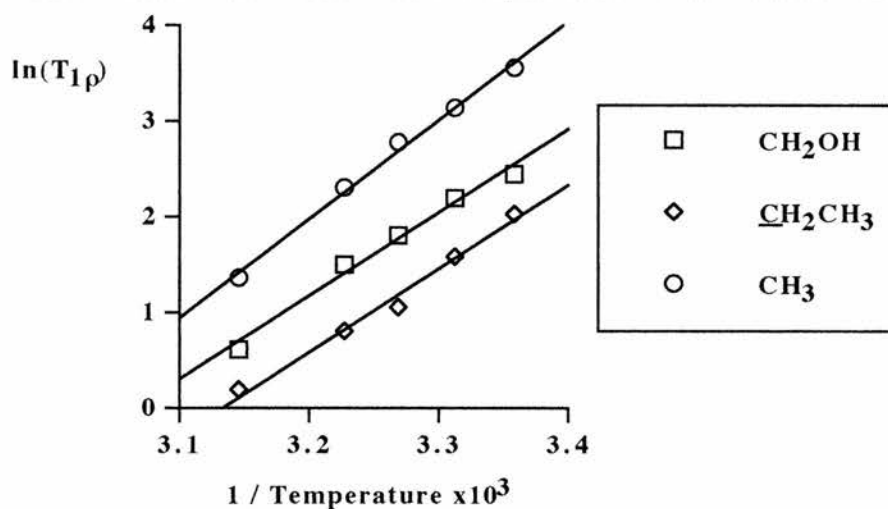


Figure 3

Energies of activation derived for **4** are presented in Table 6. These data are relatively high when compared to **2**, indicating higher barriers to rotation for the dynamic processes.

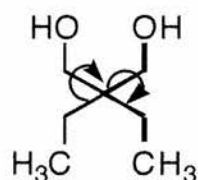
Energies of activation derived for 2,2-diethylpropane-1,3-diol

	CH ₂ OH	CH ₂ CH ₃	CH ₃
slope	+ 8.67	+ 8.62	+ 10.4
r^2	0.986	0.983	0.994
E_a (kJ mol. ⁻¹)	+ 72.1	+ 71.7	+ 86.4

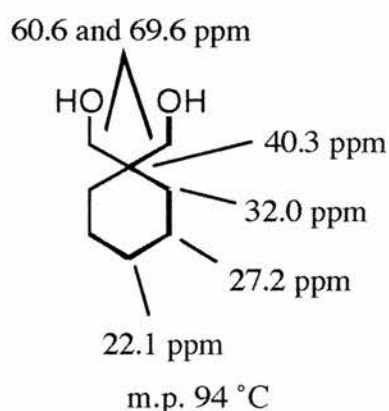
Table 6

Since the CH₃ carbons show the longest $T_{1\rho}$ relaxation (apart from the quaternary carbon) and has higher activation energy, this indicates that it is the most remote carbon

from the molecular motion giving rise to $T_{1\rho}$ effects i.e. the most likely motion is CH_2OH rotation.

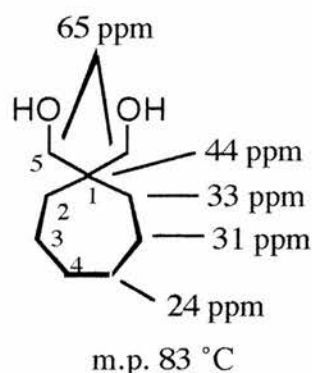


1,1-Di(hydroxymethyl)cyclohexane **5**



The RT spectrum for **5** showed broad singlets for all carbons, except the quaternary carbon which was a sharp singlet. A recycle time of 15 seconds was employed to compensate for a relatively long ^1H T_1 relaxation, and the signal to noise ratio was poor. The two CH_2OH carbons gave well separated shifts, even at elevated temperatures, since they are in different environments, one axial and one equatorial. The spectra remained the same in character over a wide temperature range, indicating no detectable dynamic behaviour.

1,1-Di(hydroxymethyl)cycloheptane **6**



The RT spectrum of **6** shows the CH₂OH signal starting to split. On raising the temperature to 307 K the signal starts to sharpen and at 315 K becomes a singlet. Closer examination indicates a temperature of coalescence, T_C , of 307 K. When raising the temperature to 323 K the CH₂OH signal was observed to reduce in intensity, due to efficient $T_{1\rho}$ relaxation. When the temperature was lowered to just below RT, 291 K, the C-3 signal as well as that due to CH₂OH was split, and when running at temperatures as low as 224 K the signal was lost altogether (no FID). Spectra 5 shows **6** over the temperature range 284 K to 323 K. $T_{1\rho}$ measurements were therefore carried out from just beyond RT to the temperature where the CH₂OH signal diminishes (306 to 322 K). The results are presented in Table 7.

$T_{1\rho}$ data for 1,1-di(hydroxymethyl)cycloheptane ($\omega_1 = 58.1$ kHz)

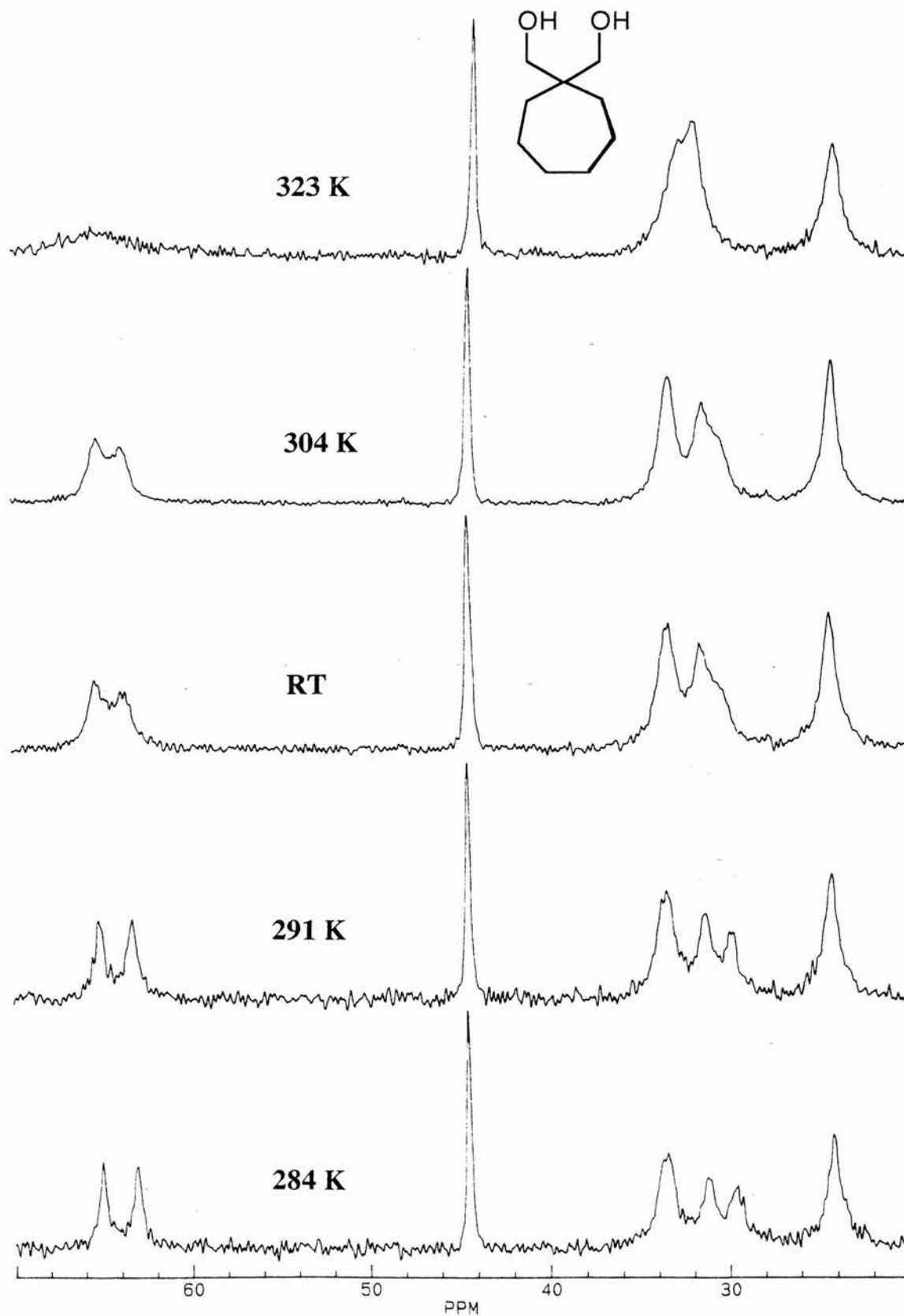
Temperature (K)	$T_{1\rho}$ (ms)			
	CH ₂ OH	C-2	C-3	C-4
306	1.65	2.80	2.60	2.80
310	1.39	2.32	2.66	2.75
314	1.22	2.06	2.45	2.72
318	0.84	1.94	2.18	2.83
322	0.71			2.24

Table 7

While the results for C-4 look unreliable, the other data can be used to derive energies of activation, E_a . A plot of $\ln(T_{1\rho})$ against $1/T$ for the CH₂OH of **6** is shown (Figure 4). If, like for C-4, $T_{1\rho}$ is short and has very little variation with temperature it suggests E_a is very low. Therefore, there may be two molecular motions modulating $T_{1\rho}$; (1) pseudorotation of 7-membered ring in which C-4 shows maximum motion and pseudorotation has low E_a , and (2) hydrogen bond exchange which is largely responsible

Spectra 5

Spectra of di(hydroxymethyl)cycloheptane from 284 K to 323 K



Diol compounds studied by solid-state CP/MAS NMR.

for C-5 relaxation. If this is the case then C-2 and C-3 should show intermediate values of E_a .

Plot of $\ln(T_{1\rho})$ against $1/T$ for 1,1-di(hydroxymethyl)cycloheptane

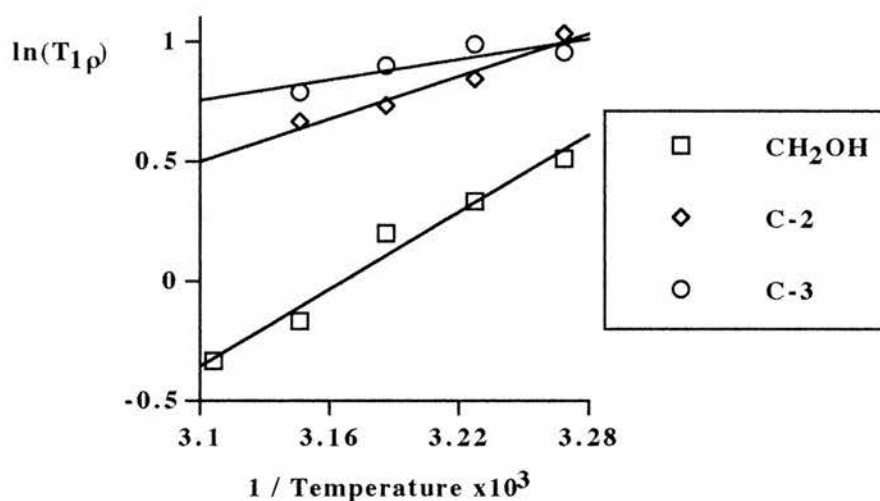


Figure 4

Energies of activation (E_a) were derived for the CH₂OH carbons and the C-2 and C-3 ring carbons, and the results are given in Table 8. As suggested, C-2 and C-3 show intermediate E_a values, which verifies the theory that there is motion at the C-4 end of the 7-membered ring which diminishes through the ring to the disubstituted part.

Energies of activation derived for 1,1-di(hydroxymethyl)cycloheptane

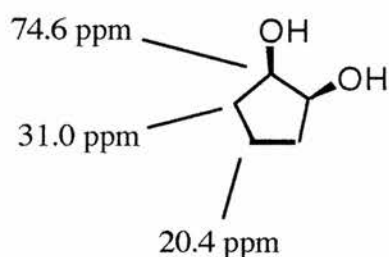
	CH ₂ OH	C-2	C-3
slope	+ 5.38	+ 2.97	+ 1.48
r_2	0.968	0.953	0.775
E_a (kJ mol. ⁻¹)	+ 44.7	+ 24.7	+ 12.3

Table 8

The free energy of activation (ΔG^\ddagger) of the dynamic process, at the temperature of coalescence, was estimated from the difference in chemical shifts of the separated signals below coalescence.

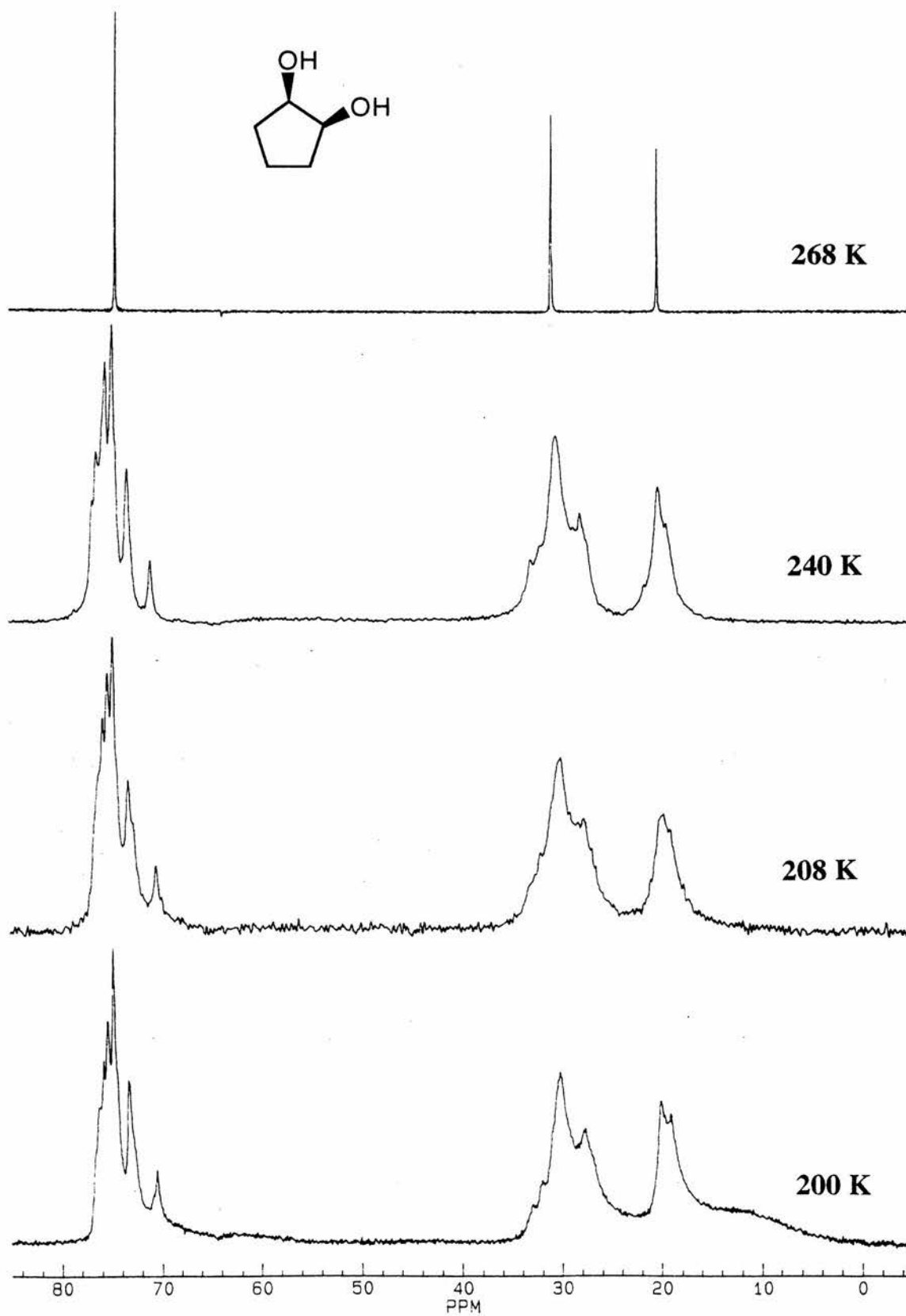
In **6** the CH_2OH group coalesces at 307 K and $\Delta\nu$ is 1.91 ppm, which gives $\Delta G^\ddagger_{307\text{ K}} = + 57.4 \text{ kJ mol}^{-1}$, which is certainly at least partly due partly to hydrogen bond exchange, as hydrogen bonds are to be expected.

cis*-1,2-Cyclopentanediol **7*

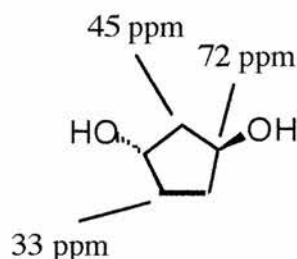


ex. Aldrich, m.p. 30-32 °C

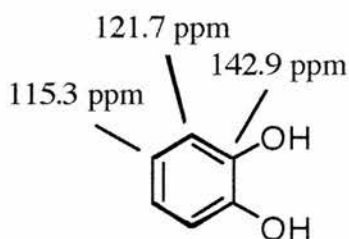
Due to the low melting point of the sample, the liquid filled rotor was cooled with nitrogen bearing gas until solidified, then drive gas applied (bearing gas alone gives typical spinning speeds of 0-200 Hz). Three sharp signals were observed at RT, at 74.6, 31.0 and 20.4 ppm, with excellent signal to noise. On decreasing the temperature, two changes were seen in the spectra; below approximately 257 K the signals appear as very broad multiplets, and when approaching 200 K a broad hump appears beneath and upfield of the multiplet signal centred at 19.5 ppm, both phenomena being clearly evident in Spectra 6. The marked change in the spectrum at *ca.* 257 K indicates a solid-solid phase transition, but on the whole the changes are too complex to interpret. The spectra above and below the temperature of the transition, however, indicate no detectable dynamic effect in that temperature range.

Spectra 6Spectra of *cis*-cyclopentane-1,2-diol from 200 K to 268 K

Diol compounds studied by solid-state CP/MAS NMR.

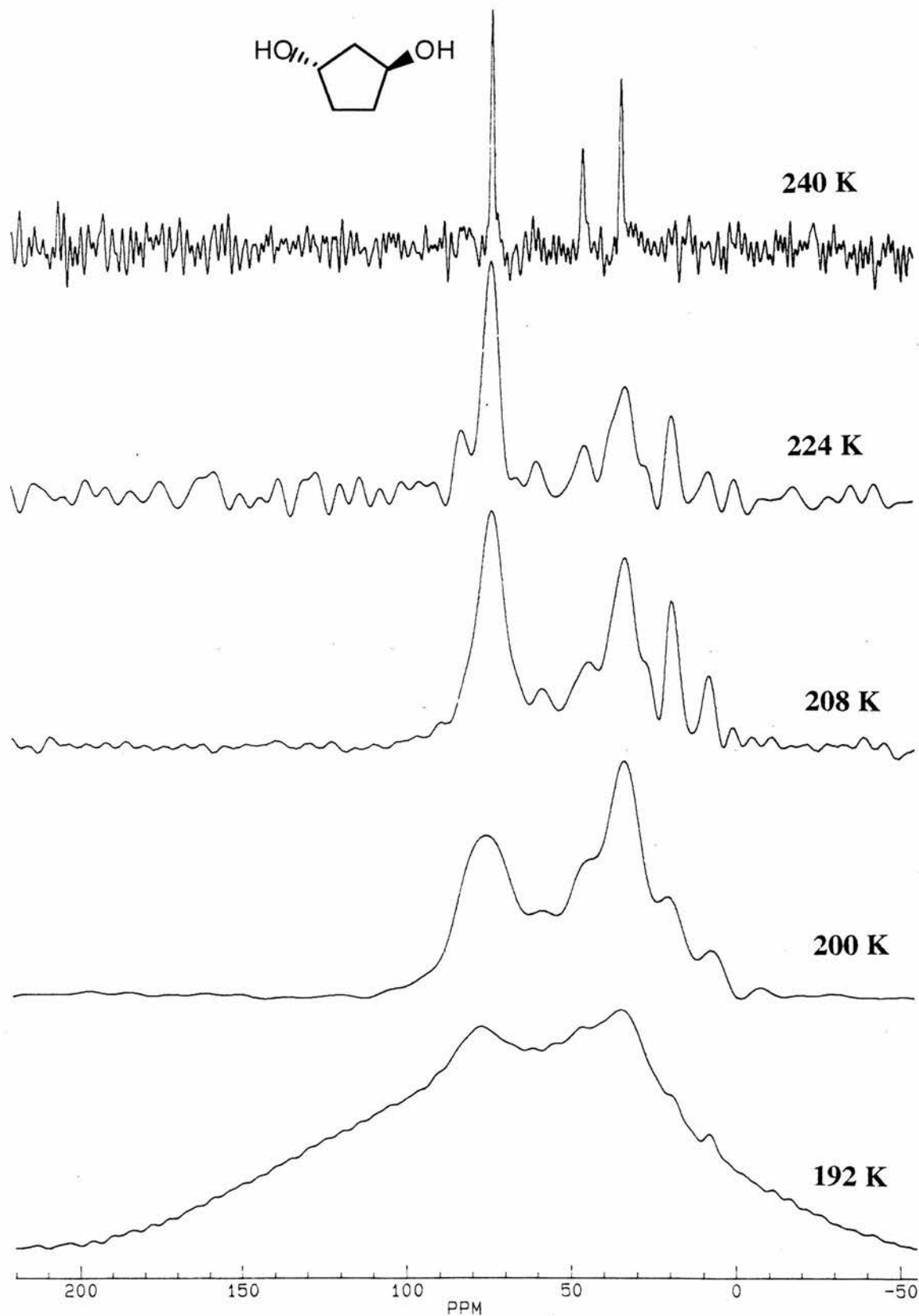
***trans*-1,3-Cyclopentane-1,3-diol 8**

The sample, like **7**, was cooled with bearing gas until solidified before applying drive gas. At temperatures down to approximately 238 K there were three sharp signals at 72, 45 and 33 ppm, although the signal to noise was poor. At 208 K there appears a greatly different spectrum; two very broad signals centred at 76 and 31 ppm and two apparently new, sharp, unexplained, peaks at 18 and 8 ppm. The shape of the broad humps represent approximately the profile of the three sharper signals seen above 238 K. At temperatures between 200 and 238 K there exists an intermediate state, with elements of both phases evident; sharp signals from the higher temperature phase are apparent, although a previously unseen peak at 57 ppm is observed. The FIDs appeared to develop better at temperatures below about 220 K. When the temperature is reduced further to 192 K the spectrum is broadened considerably, with no sharp signals apparent. Spectra **7** shows **8** from 192 K to 240 K. The phenomenon would again appear to be due to a phase transition, although it is unclear what is happening.

1,2-Dihydroxybenzene (Catechol) 9

ex. BDH and recrystallised (water), m.p. 101-4 °C

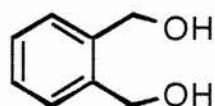
Spectra collected at RT showed singlets for each of the pairs of equivalent aromatic carbons nearest the hydroxyls, and a split in the signal due to the pair of remote carbons. RT spectra were run at 6 kHz and 7.7 kHz due to the presence of second and

Spectra 7Spectra of *trans*-cyclopentane-1,3-diol from 192 K to 240 K

Diol compounds studied by solid-state CP/MAS NMR.

third order spinning sidebands. The spectra collected at 232 K and RT showed some structure in the signal at 115.3 ppm, but spectra collected at temperatures down to 200 K showed the signal as a singlet. Since this is the opposite to an expected coalescence effect, it may indicate that there are two molecules in the asymmetric unit. Spectra collected at lower temperatures showed the singlet at 121.7 ppm to be slightly broader and less intense than at RT. A spectrum collected at above RT, 320 K, was essentially similar apart from much poorer signal to noise. Spectra 8 shows catechol over the temperature range of 200 K to 320 K. Since the spectra remained largely unchanged throughout the temperature range studied (200-320 K) it was apparent that there is no detectable dynamic effect.

1,2-Di(hydroxymethyl)benzene 10



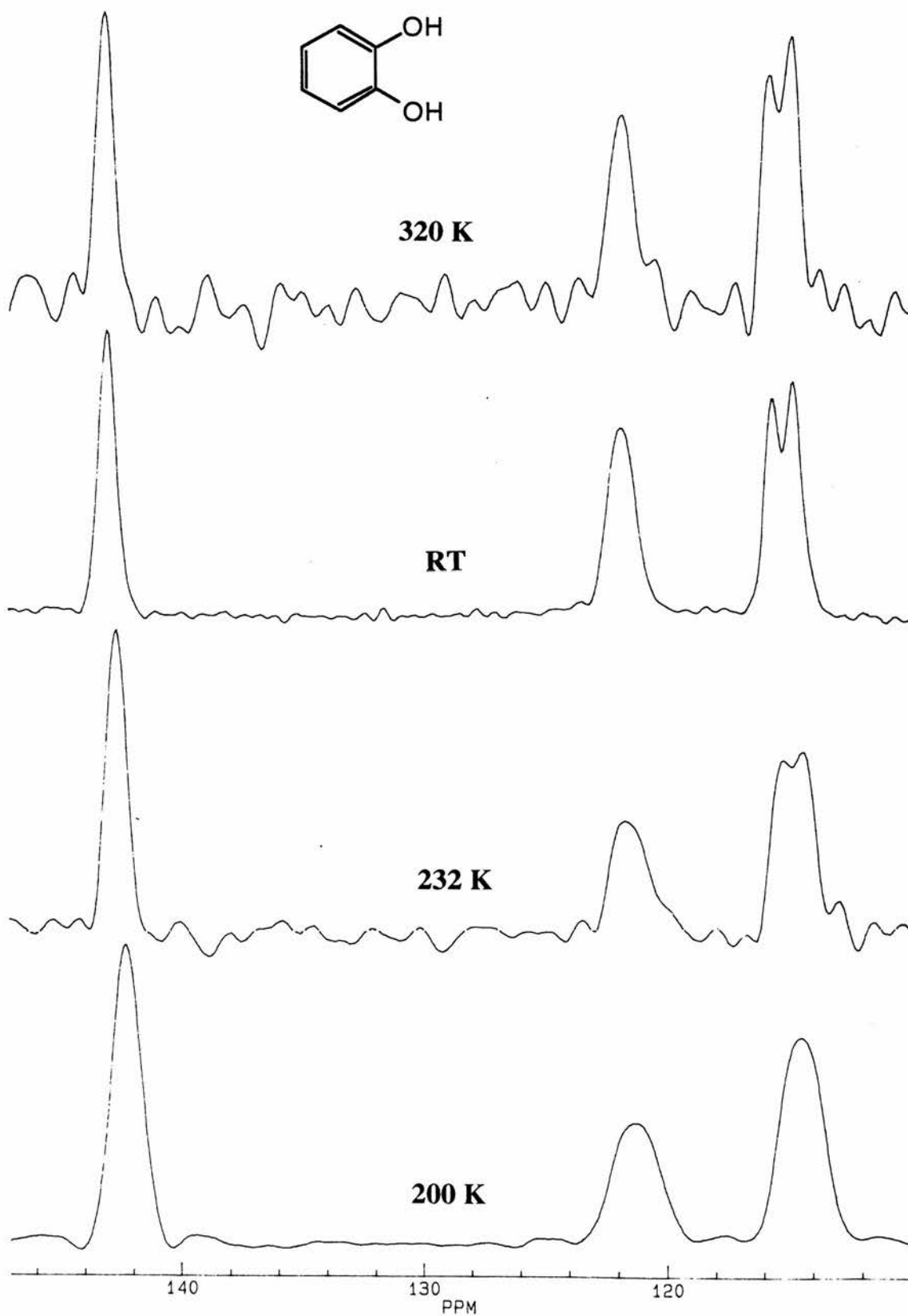
recrystallised (ether), m.p. 61-2 °C

141.1 (1 C, s, aromatic)
134.3 (1 C, s, aromatic)
131.2 (1 C, s, aromatics)
129.5 (1 C, s, aromatics)
125.1 (2 C, s with shoulder, aromatics)
64.3 (1 C, s, CH ₂ OH)
60.5 (1 C, s, CH ₂ OH)

When sample was run at RT first and second order sidebands from the aromatic region were present, so the sample was run at 6 kHz and 7.5 kHz to confirm the positions of the shifts. An optimum recycle time of 15 seconds was found appropriate for the sample. Separate resonances for the six aromatic carbons suggests the whole molecule is the asymmetric unit. Throughout the temperature range of 200 K to RT the spectra remained essentially the same. When comparing the CH₂OH signals at RT to those at 320 K, the relative intensities of the signals was found to reverse, although no large overall change in intensities occurred. There was a slight split in the CH₂OH signal at 64.3 ppm, possibly due to an impurity (for which no check was carried out). The melting point of the sample, at 334 K, curtailed an investigation beyond approximately 320 K.

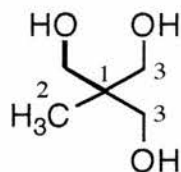
Spectra 8

Spectra of catechol from 200 K to 320 K



Diol compounds studied by solid-state CP/MAS NMR.

1,1,1-Tris(hydroxymethyl)ethane 11



ex. Aldrich, m.p. 198-9 °C

C-1	44.4 ppm
C-2	17.5 ppm
C-3	63.7 + 61.0 ppm (2:1)

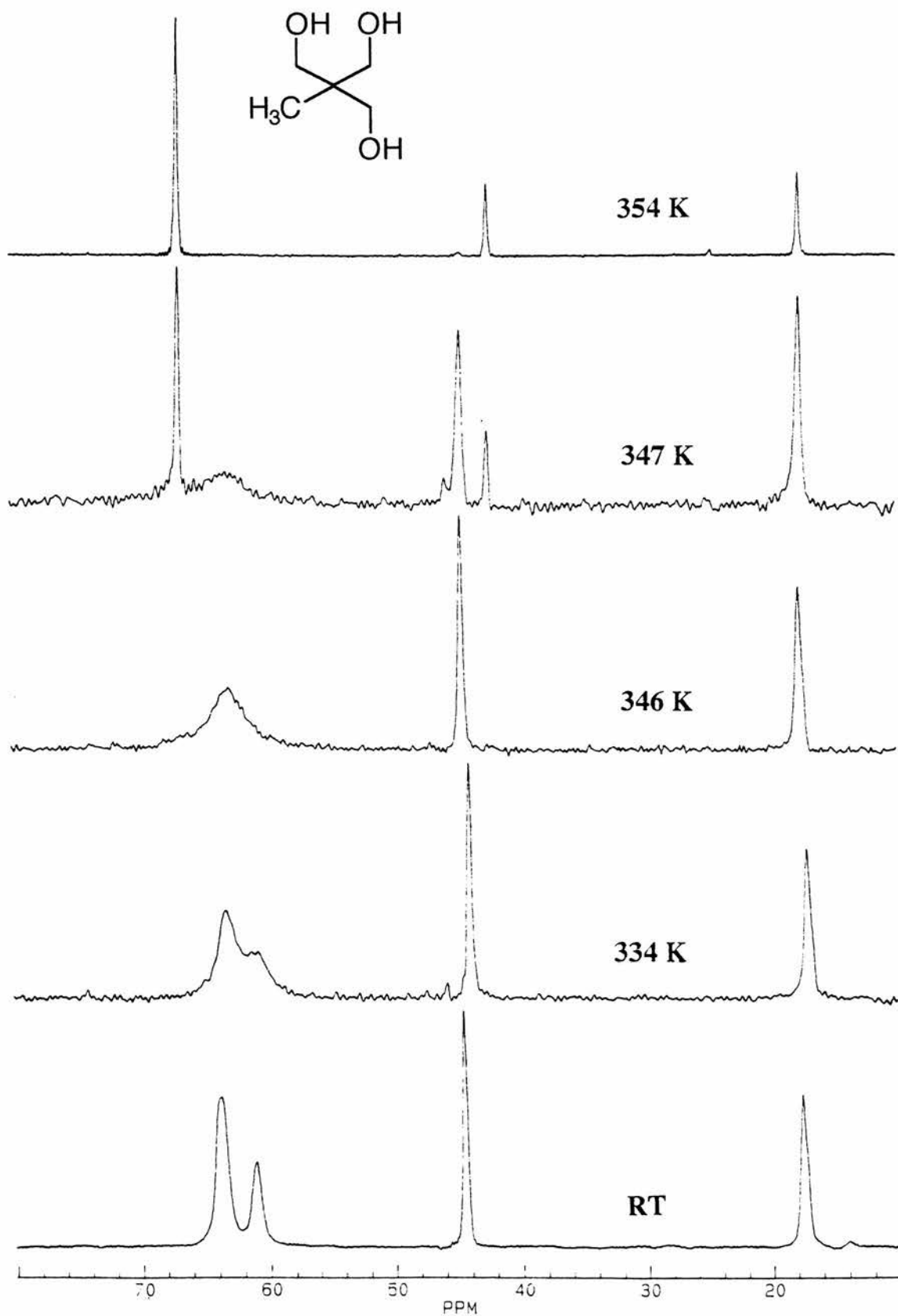
The RT spectrum shows sharp singlets for the quaternary carbon and the methyl carbon. The CH₂OH signal, interestingly, appears to be split into a doublet in the ratio 2:1; two of the three CH₂OHs may be equivalent, with the third unequivalent. When raising the temperature the CH₂OH signal merges together into a broad signal until coalescence at 334 K, and when approaching 346 K the signal is diminishing into a broad hump. When collecting a spectrum at 354 K, three sharp signals are now apparent, with very different shifts and intensities; an intense signal at 66.8 ppm and much less intense signals at 42.3 and 17.7 ppm. A spectrum at 347 K shows a mixture of the two states, including a broad hump centred at 63.1 ppm and a sharp intense signal at 66.7 ppm. Doshi *et al.* report³ the formation of a plastic crystal phase in **11** at 351.3 K. Spectra 9 shows **11** over the temperature range RT to 354 K. This phase transition curtails the region where T_{1ρ} data should be collected and so a dynamic T_{1ρ} study is not possible.

However, the free energy of activation of the dynamic process at the temperature of coalescence can still be estimated as described previously. In **11** the CH₂OH group coalesces at 334 K and Δν is 2.73 ppm, which gives ΔG[‡]_{334 K} = + 61.7 kJ mol.⁻¹.

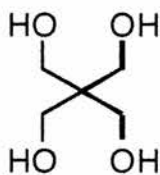
³ Doshi N., Furman M., Rudman R., *Acta Cryst.*, **B29**, (1973)143

Spectra 9

Spectra of 1,1,1-tris(hydroxymethyl)ethane from RT to 354 K



Pentaerythritol 12



ex. Aldrich, m.p. 225-9 °C

Spectra of **12** were very difficult to collect, due to long T_1 relaxation times and hence poor signal to noise and long acquisition times. Spectra which were obtained used long recycle times, of 30 and 60 seconds, and at RT showed a broad singlet at 50 ppm and a broader multiplet at 58 ppm. Spectra obtained at higher temperatures, up to 344 K, gave similarly broad signals. Pentaerythritol is therefore not suitable to study.

Summary

All the dynamic data for the diol compounds **1** to **12** are summarised in Table 9 (activation energies) and Table 10 (free energies of activation).

Activation energy (E_a) data for diol compounds

Diol compound	Activation energy (kJ mol. ⁻¹)	
	carbon	E_a
1 Butane-1,4-diol	no detectable dynamics	
2 2,2-Dimethylpropane-1,3-diol	CH ₂ OH	+ 48.5
	CH ₃	+ 44.3
3 2-Ethyl-2-methylpropane-1,3-diol	no detectable dynamics	
4 2,2-Diethylpropane-1,3-diol	CH ₂ OH	+ 72.1
	CH ₂ CH ₃	+ 71.7
	CH ₃	+ 86.4
5 1,1-Di(hydroxymethyl)cyclohexane	no detectable dynamics	
6 1,1-Di(hydroxymethyl)cycloheptane	CH ₂ OH	+ 44.7
	C-2	+24.7
	C-3	+ 12.3
7 <i>cis</i> -1,2-Cyclopentane-1,2-diol	no detectable dynamics	
8 <i>trans</i> -1,3-Cyclopentane-1,3-diol	no detectable dynamics	
9 1,2-Dihydroxybenzene (catechol)	no detectable dynamics	
10 1,2-Di(hydroxymethyl)benzene	no detectable dynamics	
11 1,1,1-Tris(hydroxymethyl)ethane	T _{1ρ} could not be measured	
12 Pentaerythritol	poor acquisition	

Table 9

Free energy of activation (ΔG^\ddagger_C) data for diol compounds

Diol compound	Group coalescing	T_C K	$\Delta\nu$ ppm	ΔG^\ddagger_C kJ mol. ⁻¹
2 2,2-Dimethylpropane-1,3-diol	CH ₃	262	1.15	+ 49.7
11 1,1,1-Tris(hydroxymethyl)ethane	CH ₂ OH	334	2.73	+ 61.7
1,1-Di(hydroxymethyl)cyclopentane ⁴	CH ₂ OH	313	0.818	+ 60.8
	ring CH ₂	315	1.17	+ 60.2
6 1,1-Di(hydroxymethyl)cycloheptane	CH ₂ OH	307	1.91	+ 57.4

Table 10**Crystallographic data**

It is useful to consider the obtained dynamic data alongside crystallographic data for the compounds, where available. In the solid state, crystal packing may obviously influence the presence and degree of any dynamic properties. There are crystallographic data available for **2** and **11**,^{5,6} although neither of these are accurate crystal structure determinations. Work was carried out in St Andrews to determine an accurate crystal structure for **11** by powder X-ray diffraction.⁷ Although the structure of **11** has not been solved completely information gained on the structure is given in Appendix A. There are a great number of crystallographic investigations reported for **12**,^{8,9,10,11,12,13,14,15,16,17} although poor acquisition made a $T_{1\rho}$ relaxation study impossible.

⁴ Ross S. R., Senior Honours Project report, University of St. Andrews, (1992)

⁵ Nakano E., Hirotsu K., Shimada A., *Bull. Chem. Soc. Japan*, **42**, (1969) 3367

⁶ Eilerman D., Lippman R., Rudman R., *Acta Cryst.*, **B39**, (1983) 263

⁷ Morris R., Riddell F. G., Tremayne M.-J., Spark R. A., to be published

⁸ Llewellyn F. G., Cox E. G., Goodwin T. H., *J. Chem. Soc.*, (1937) 883

⁹ Nitta I., Watanabé T., *Bull. Chem. Soc. Japan*, **13**, (1938) 28

¹⁰ Hvoslef J., *Acta Cryst.*, **11**, (1958) 383

¹¹ Shiono R., Cruickshank D. W. J., Cox E. G., *Acta Cryst.*, **11**, (1958) 389

¹² Ladd M. F. C., *Acta Cryst.*, **B35**, (1979) 2375

¹³ Eilerman D., Rudman R., *Acta Cryst.*, **B35**, (1979) 2458

¹⁴ Hope H., Nichols B. G., *Acta Cryst.*, **A37**, (1981) C-136

¹⁵ Chandra D., Fitzpatrick J. J., Jorgensen G., *Adv. X-ray Anal.*, **28**, (1985) 353

¹⁶ Semmingsen D., *Acta Chem. Scand.*, **A42**, (1988) 279

¹⁷ Katrusiak A., *Acta Cryst.*, **B51**, (1995) 873

Investigation of deuteriated diols

As mentioned previously in this chapter, one possible phenomenon taking place in these diol compounds may be a hydrogen bonding or exchange process. A convenient way to check this is to compare the coalescence temperature, T_C , of the deuteriated ($O\text{-}^2\text{H}$ or OD) compound with that of the $O\text{-}^1\text{H}$ (OH) compound, where the activation energies for the making and breaking of hydrogen bonds should show a kinetic isotope effect. Deuteriated samples of compounds **2**, **6** and **11** were prepared as detailed in Chapter 3. This quick preparation gave typical conversions to the deuteriated compound of at least 70% as indicated by IR.

Compounds **2**, **6** and **11** all displayed slightly higher coalescence temperatures for the deuteriated compounds, when compared to the protonated compounds, as shown in Table 9.

Coalescence data for deuteriated diol compounds

Compound	T_C (K)		\pm (K)
	OH	OD	
2 2,2-Dimethylpropane-1,3-diol	262	266	+ 4
6 1,1-Di(hydroxymethyl)cycloheptane	334	335-6	+ 1-2
11 1,1,1-Tris(hydroxymethyl)ethane	307	308	+ 1

Table 11

Although the effects appear small, they are reproducible and suggest that there is indeed some hydrogen bonding or exchange process taking place inside the crystalline samples. The effects for **6** and **11** are especially small, but + 4 K for **2** is a sufficient change, and previous data for 4,4-dimethyl-*trans*-cyclopentane-1,2-diol shows the $O\text{-}^2\text{H}$ derivative to have a coalescence temperature 6 K higher.¹⁸

¹⁸ Riddell F. G., Cameron K. S., Holmes S. A., Strange J. H., *J. Am. Chem. Soc.*, **119**, (1997) 7555

Conclusion

This simple series of diols (including one triol and one tetraol) is seen to display a number of dynamic phenomena. The making and breaking of hydrogen bonds is almost certainly being observed. The nature of the other processes is not certain, although several other modes of motion may also be involved. Firstly, because of the appreciable $T_{1\rho}$ effect for the CH_2OH carbons, there appears to be rotation around the C- CH_2OH bond, certainly observed for 2,2-dimethylpropane-1,3-diol and 2,2-diethylpropane-1,3-diol. In addition, because of the symmetrical nature of the molecules, and the very small $T_{1\rho}$ effect for the quaternary carbon, there can be assumed to be a degree of rotation around the whole C_2 , or C_n , axis of the molecule.

1,1-Di(hydroxymethyl)cycloheptane displays another phenomenon in addition to hydrogen bond exchange and C- CH_2OH bond rotation; E_a values which diminish throughout the ring suggest sizable libration at the remote end of the ring compared to the disubstituted end (pseudorotation of 7-membered ring in which C-4 shows maximum motion).

Tetraalkylammonium Halides

Kenneth Cameron previously studied a series of tetraalkylammonium halides,¹ where the alkyl was methyl, ethyl, *n*-propyl and *n*-butyl, and the halide was chloride, bromide and iodide. This study was seen as a natural progression from a previous study of 3,3-diethylpentane. A more extensive review of the literature for the tetraalkylammonium halides as a whole is given in Reference 1. It was thought necessary to reinvestigate the series of tetraethylammonium halides and tetrapropylammonium halides, due to inconclusive results in Ref. 1. The $T_{1\rho}$ relaxation measurements were incomplete

The analysis of tetraethylammonium halides by ^1H solid-state NMR has been carried out by Szafranska and Pajak² ($X = \text{F}, \text{Cl}, \text{Br}$ and I) and Cheng *et al.*³ ($X = \text{Br}$ and I). Their Differential Scanning Calorimetry (DSC) analyses identify the solid-solid phase transitions, shown in Table 1.

Differential Scanning Calorimetry data for tetraalkylammonium halides

Compound	$T_{\text{tr}} (\text{K})^{\text{a}}$	$\Delta S_{\text{tr}} (\text{JK}^{-1}\text{mol.}^{-1})^{\text{a}}$	$T_{\text{tr}} (\text{K})^{\text{b}}$	$\Delta S_{\text{tr}} (\text{JK}^{-1}\text{mol.}^{-1})^{\text{b}}$
TEACl	346, 368	7.6, 16.2		
TEABr	437, 460	40.3, 3.1	448, 463	44.6, 3.2
TEAI	467	44.0	471	44.3
TPACl	none found ⁴		none found ⁴	
TPABr			382, 396	44.4, 0.9
TPAI			225, 419	6.4, 35.8

^a = Szafranska and Pajak (Ref. 2)

^b = Cheng *et al.* (Ref. 3)

T_{tr} = temperature of transition

ΔS_{tr} = ΔS at temperature of transition

Table 1

¹ Cameron K. S., Ph.D. Thesis, University of St Andrews, (1996) 61

² Szafranska B., Pajak Z., *J. Mol. Structure*, **99**, (1983) 147

³ Cheng J., Xenopoulos A., Wunderlich B., *Mol. Cryst. Liq. Cryst.*, **220**, (1992) 105

⁴ Cameron K. S., Ph.D. Thesis, University of St Andrews, (1996) 80

The only NMR work found in the literature for the tetrapropylammonium halides was reported in Ref. 3 ($X = \text{Br}$ and I), and DSC data for these compounds is shown in Table 1. The only DSC data available for tetrapropylammonium chloride was collected in St. Andrews.⁴

NMR work from Ref. 1-3 is discussed throughout the chapter for each tetraalkylammonium halide in turn.

Drying of samples for the study

Samples for this study (Table 2) were all from the Aldrich Chemical Company. The samples are all extremely hygroscopic, the TEACl existing as a hydrate in its natural state. These samples were not purified further prior to study, other than recrystallising once from absolute alcohol.

Purity and melting point of tetraalkylammonium halides

Compound	Purity*	M.p.*
TEACl.xH ₂ O		
TEABr	98 %	285 °C (dec.)
TEAI	98 %	>300 °C
TPACl	98 %	240-2 °C
TPABr	98 %	270 °C (dec.)
TPAI	98+ %	283 °C (dec.)

* purity and m.p., as detailed in Aldrich Chemical Co. catalogue

Table 2

Throughout the study it was found that T_{1p} values for these compounds differed significantly if the samples were first dried carefully. So as to give data for the pure crystalline form of each compound, rather than a hydrated sample, measures were taken to expel any water present. All samples were treated as follows;

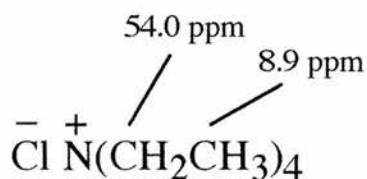
- recrystallised once from absolute ethanol,
- heated at ambient pressure in a rotating Kugelrohr apparatus; when water of hydration is lost at *ca.* 80 °C, sample appears to ‘melt’,
- on heating further, sample hardens and all moisture from the hydrate appears to be lost,
- sample dried finally by heating under vacuum at *ca.* 110 °C,
- a nitrogen filled glove bag was used to provide a moisture free environment while packing the rotor with each sample,
- all samples run under MAS conditions used nitrogen as drive and bearing gas, unless otherwise stated, to ensure no moisture enters the samples during NMR analysis.

These measures were seen as sufficient to expel any moisture from the samples, the dried samples being prepared as required and analysed immediately. Because of this no quantitative checks were carried out for moisture.

A good indication of the importance of using properly dried samples can be seen clearly in the $T_{1\rho}$ data acquired for both tetrapropylammonium chloride and bromide (TPACl and TPABr).

Tetraethylammonium chloride (TEACl)

Reference 1 states that the ^{13}C CP/MAS spectra showed signal to noise ratio decrease markedly from 349 K until just above the $T_{1\rho}$ minimum, at 320 K, and then improving at 299 K. The methyl resonance at 8.9 ppm also sharpens ($w_{1/2} = 160$ Hz to 52 Hz) as the sample is warmed from 320 K to 349 K. The methylene shows largest effects, due to $T_{1\rho}$ relaxation and maximum dipolar broadening. Rate data was obtained for the methyl groups and gave activation parameters of $\Delta H^\ddagger = + 57.8 \pm 3.4$ kJ mol. $^{-1}$, $\Delta S^\ddagger = + 45.9 \pm 10.9$ kJ mol. $^{-1}$ and $E_a = 60.5 \pm 3.4$ kJ mol. $^{-1}$ (compared to $E_a = 50.3$ kJ mol. $^{-1}$ in Ref. 2). The motion occurring is the reorientation of the ethyl groups, with cation tumbling not becoming significant until above the phase transition at 368 K.

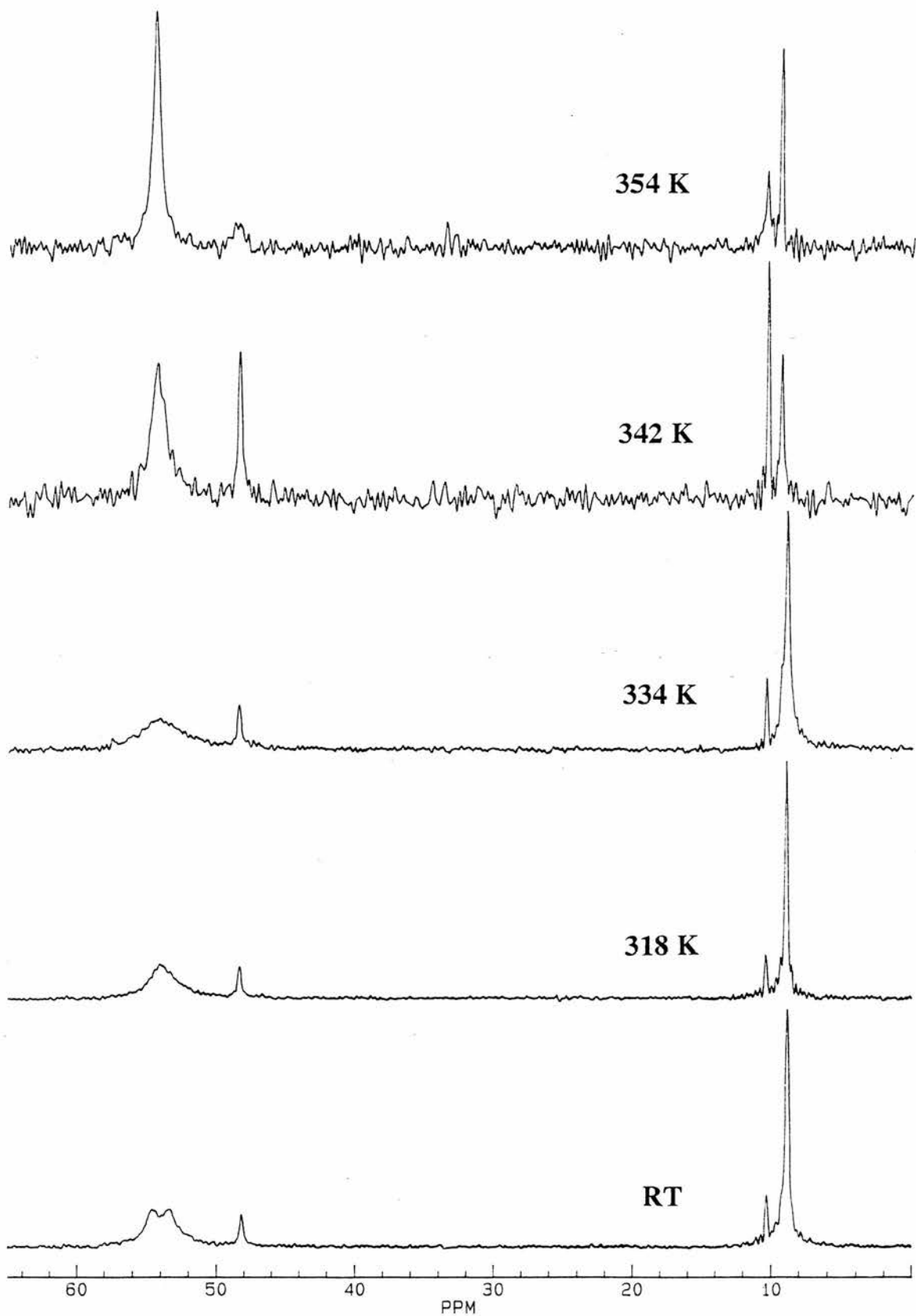


The spectrum collected at RT had a split methylene resonance, compared to that in Ref. 1 which was a broad singlet. In addition there were two small peaks at 10.4 ppm and 48.2 ppm which were initially thought to be due to a contaminant in the rotor, but on repacking the rotor the small peaks remained, and their intensities appeared to increase as the temperature was raised. The spectrum at 318 K shows that the methylene signal has coalesced into a single broader peak. Spectra of TEACl from RT to 354 K are seen in Spectra 1, and show the presence of two different solid phases.

$T_{1\rho}$ measurements were taken from RT to 342 K, just below the solid phase transition at 346 K (Table 1). Data were collected twice (nitrogen was used as bearing and drive gas for the second experiment), and a comparison with data from Ref. 1 can be seen in Table 3.

Spectra 1

Spectra of TEACl from RT to 354 K



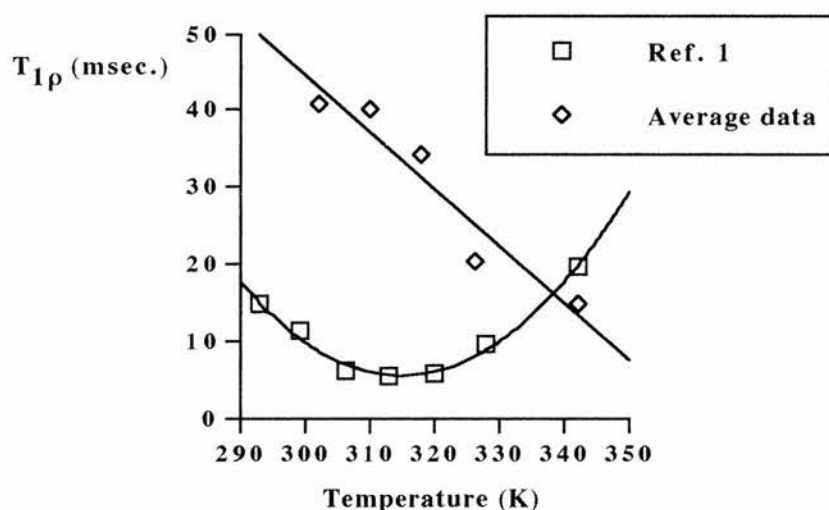
Tetraalkylammonium halides.

$T_{1\rho}$ data for TEACl, in msec.

Temperature (K)	$\underline{\text{C}}\text{H}_2\text{CH}_3$			Ref. 1	CH_3		
	Data 1	Data 2	Average ^a		Data 1	Data 2	Average ^a
293				14.6			
299				11.4			
302	27.2	37.0	32.1		39.2	42.6	40.9
306				6.24			
310	23.2	19.0	21.1		38.3	42.0	40.1
313				5.31			
318	12.2	14.4	13.3		30.3	38.0	34.1
320				5.63			
326	8.83	7.61	8.22		19.5	20.9	20.2
328				9.59			
334		4.56	4.56			12.5	12.5
342	2.94	3.04	2.99	19.47	16.6	12.6	14.6

^a of Data 1 and Data 2for Data 1, $\omega_1 = 64.9$ kHz; for Data 2, $\omega_1 = 61.7$ kHz**Table 3**

It is acceptable here to quote an average from the two datasets since the ω_1 value for both can be regarded as similar within experimental error. The data from Table 3 is presented in Figure 1.

Plot of $T_{1\rho}$ against temperature for methyl carbons of TEACl**Figure 1**

The data from Ref. 1 gave a distinctive bell shaped curve, whereas the data obtained here gives a linear plot and is clearly in disagreement with Ref. 1. The only activation parameter it is possible to derive from this data is the activation energy, E_a . Figure 2 shows a plot of $\ln(T_{1\rho})$ against $1/T$ for both the $\underline{\text{C}}\text{H}_2\text{CH}_3$ and the CH_3 carbons, where the slope gives E_a since $E_a = -\text{slope} \times R$. Activation energies derived from the plots are detailed in Table 4.

Plot of $\ln(T_{1\rho})$ against $1/T$ for TEACl

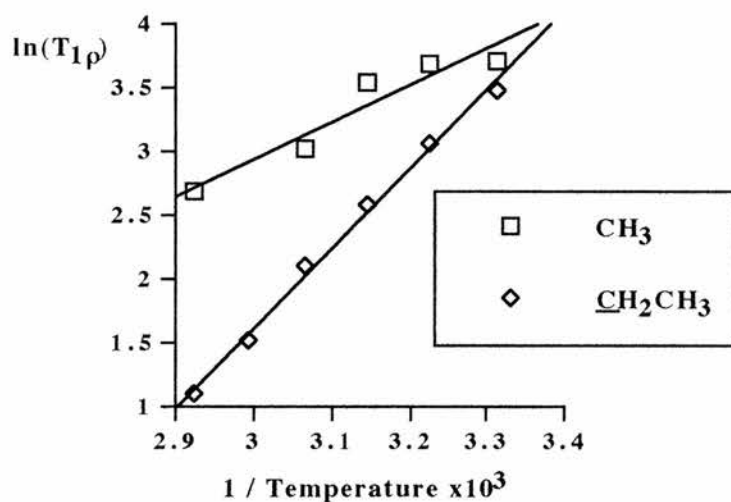


Figure 2

Energies of activation derived for TEACl

	$\underline{\text{C}}\text{H}_2\text{CH}_3$	CH_3
slope	+ 6.24	+ 3.37
r^2	0.994	0.871
E_a (kJ mol. ⁻¹)	+ 51.9	+ 28.1

Table 4

The activation energies for the methyl carbons are significantly lower than those given in both Ref. 1 (60.5 ± 3.4 kJ mol.⁻¹) and Ref. 2 (50.3 kJ mol.⁻¹). The activation energy for the methyls is much lower than for the methylenes, indicating that methyl

rotation is faster than rotation of the ethyl groups as a whole, perhaps due to their increased distance from the sterically hindered quaternary centre.

Tetraethylammonium bromide (TEABr) and iodide (TEAI)

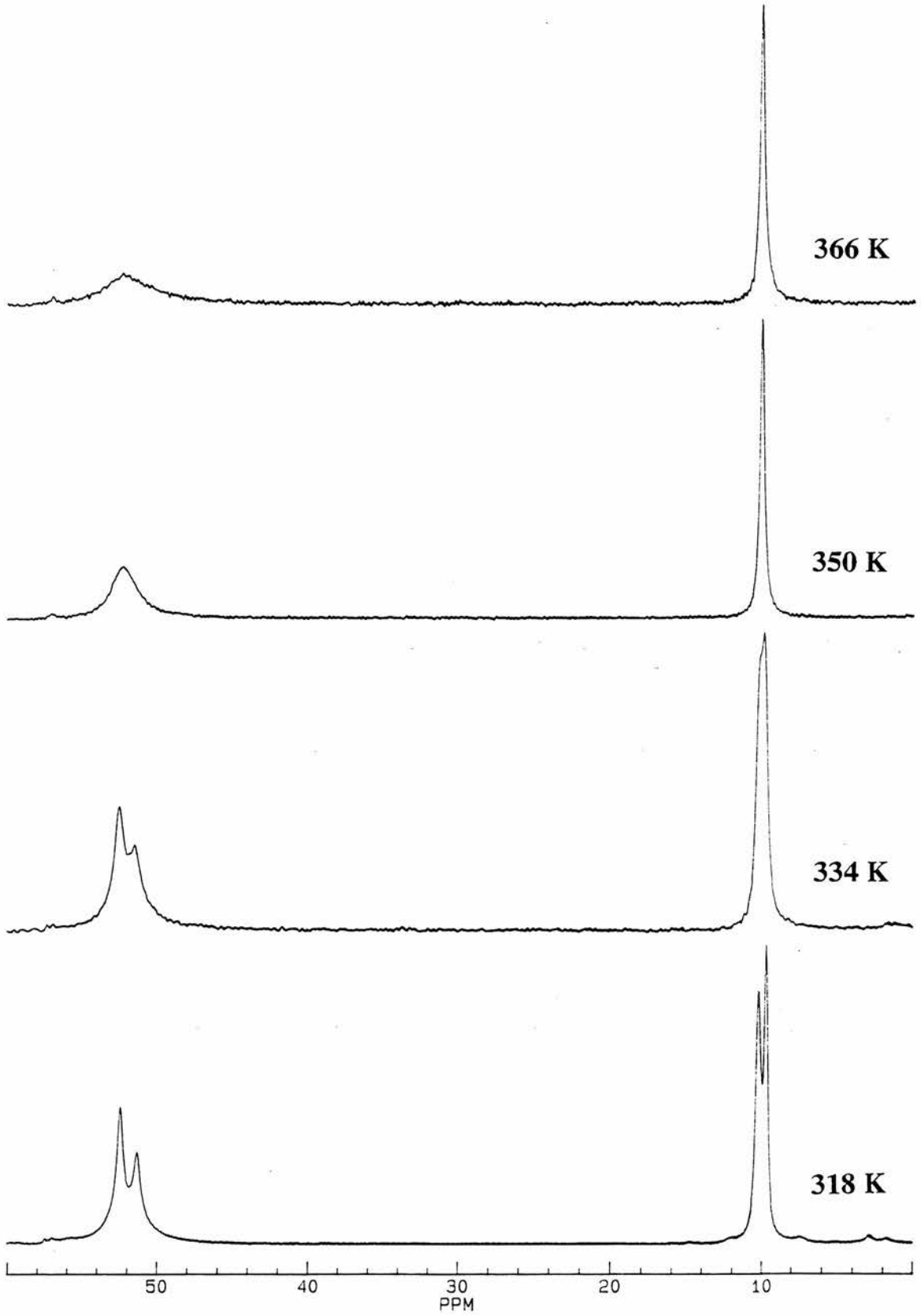
Ref. 1 states that the ^{13}C $T_{1\rho}$ values do not change with temperature. Ref. 2 indicates that reorientation of the ethyl groups does not start until 390 K and 413 K for TEABr and TEAI respectively, and cation tumbling starts just after the phase transition to the plastic phase at 437 K and 440 K respectively.



Spectra for TEABr at ambient temperature showed both the methylene and the methyl resonances were split. Coalescence took place at somewhere approaching 350 K, beyond which point the methylene signal broadened significantly (Spectra 2). $T_{1\rho}$ studies carried out from 350 K to the temperature limit of the probe at *ca.* 375 K proved difficult and uninformative, due to the small temperature range and the unreliable nature of the data. TEAI gave sharp signals throughout the operating temperature range of the MAS probe, and the intensities of the signals remained similar, indicating no significant detectable dynamic effect.

Since the reorientation of the methyl groups does not start until at least 390 K for these compounds,⁴ the maximum operating temperature of the MAS probe restricts a full study of this particular motion.

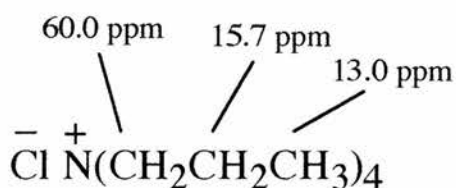
Spectra 2
Spectra of TEABr from 318 K to 366 K



Tetraalkylammonium halides.

Tetrapropylammonium chloride (TPACl)

Ref. 1 states there is a small $T_{1\rho}$ effect for the methylenes and the methyls, approaching a $T_{1\rho}$ minimum at 368 K. The $T_{1\rho}$ values for the methylenes are much lower than those for the methyls, indicating rotation about the bond between the two methylenes. However, the $T_{1\rho}$ values are very low and show only a gradual change with temperature. $T_{1\rho}$ data gave relatively low activation energies, E_a , of $11.7 \pm 8.1 \text{ kJmol}^{-1}$ and $11.1 \pm 9.1 \text{ kJmol}^{-1}$ for the methylenes and methyls respectively. Because of steric repulsions restricting rotational freedom around the bond between the methylenes, the small $T_{1\rho}$ effect was attributed to small libration in the propyl chains.



$T_{1\rho}$ data was collected for TPACl from RT to just below the maximum operating temperature of the MAS probe (376 K).

T_{1ρ} data for TPACl, in msec.

Temperature (K)	ex. Ref. 1			experimental		
	CH ₂ -N	CH ₂ CH ₃	CH ₃	CH ₂ -N	CH ₂ CH ₃	CH ₃
297	1.19	1.38	10.1	215	90.3	188
304	0.94	1.02	8.25	179	86.0	220
312	0.83	0.87	7.43	119	69.6	
320	0.72	0.77	7.32			
328	0.75	0.79	6.71	62.9		170
336	0.62	0.79	5.92			
344	0.63	0.64	6.26	49.3	48.0	168
352	0.52	0.55				
360	0.48	0.56	5.47	44.3	60.1	104
368	0.37	0.53	5.75			
376			5.31			

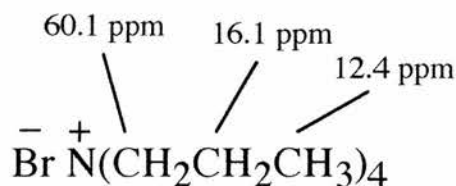
for experimental, $\omega_1 = 60.6$ kHz

Table 5

It is obvious from these plots that the use of a carefully dried sample results in much longer relaxation times; the presence of the hydrate, found readily in most laboratory samples of this kind would appear to greatly shorten the T_{1ρ} relaxation times, as would be expected. The relaxation times recorded here are orders of magnitude greater than those quoted in Ref. 1. Unfortunately, the data quoted in Table 5 cannot be used reliably to derive activation parameters since values of over about 30 milliseconds are susceptible to significant errors (within the group it is generally accepted that T_{1ρ} relaxation values over 30 ms are unreliable since it is more than twice the magnitude of the longest time delay used). However, they still serve to demonstrate the huge difference in T_{1ρ} values obtained when using an efficiently dried sample compared to a normal laboratory sample.

Tetrapropylammonium bromide (TPABr)

Reference 3 states that this compound does not cross polarise effectively above the phase transition at 382 K, since it is then a plastic crystal displaying rapid molecular motion and possibly diffusion. Due to steric reasons, Ref. 1 attributes any $T_{1\rho}$ effect to a librational type motion in the propyl chain, similar to TPACl, although this effect was not shown to vary with temperature.



To demonstrate the difference when using a dried sample, two experiments were carried out with TPABr, one with an undried sample and one with a sample carefully dried, originally from the same sample, as outlined earlier. The variation of $T_{1\rho}$ with temperature in either case is seen in Table 6.

 $T_{1\rho}$ data for TPABr, in msec.

Temperature (K)	undried sample			dried sample		
	N-CH ₂	<u>C</u> H ₂ CH ₃	CH ₃	N-CH ₂	<u>C</u> H ₂ CH ₃	CH ₃
297	8.16	10.68	54.9			
300				64	54	169
308	8.03	10.63	54.6	59	47	140
316	7.73	9.86	51.3			
324	8.06	9.81	52.9	70	60.5	134
332	7.38	9.42	41.8			
340				71	142	
348	7.02	8.90	41.3			
356				88	60	174

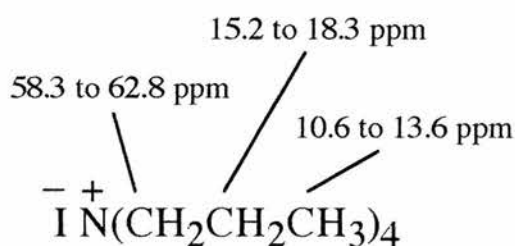
for undried sample, $\omega_1 = 47.0$ kHz; for dried sample, $\omega_1 = 66.6$ kHz

Table 6

It is again obvious from this data that there is a significant difference when using a properly dried sample. It is not worthwhile to derive activation parameters from either data, since any such results would be lacking in accuracy and credibility.

Tetrapropylammonium iodide (TPAI)

TPAI was shown to be the most interesting tetrapropylammonium halide studied. Ref. 1 states that each carbon has four distinct resonances below 224 K; the four methyl carbons are best resolved at 212 K, and the C-2 methylene carbons are best resolved at 190 K where one signal has a shoulder, due to the fourth resonance. The four C-N bond lengths are found to be different by X-ray diffraction, since each of the four C-1 carbons are in different proximity to the iodide ion. $T_{1\rho}$ measurements proved to be difficult due to dipolar broadening, a strong $T_{1\rho}$ effect at ambient temperature and above, and the coalescence of the methyl resonances at or approaching the maximum operating temperature of the MAS probe. Free energy values (ΔG^\ddagger_C) of 45.5 kJ mol^{-1} for the methyl carbons ($T_C = 241 \text{ K}$) and 46.9 kJ mol^{-1} for the methylene carbons ($T_C = 226 \text{ K}$) were derived from the coalescence of the methyl and methylene signals.



The spectra obtained at low temperatures ($< ca. 225 \text{ K}$) gave well defined structure for all resonances; all four N-CH₂ carbons gave separate shifts, the CH₂ carbons gave three shifts with the fourth carbon forming a shoulder in one peak, and the methyl region was generally made up of two single peaks and one double peak. $T_{1\rho}$ measurements were taken from 190 K to 222 K, just below the first reported solid-solid

phase transition. Any measurements at such low temperatures are always potentially troublesome, so careful attention needs to be given to relaxation measurements at such temperatures.

$T_{1\rho}$ values were collected, but again, as for TPABr, $T_{1\rho}$ changes with temperature were found to vary inconsistently with temperature, and because they were anything up to several hundred milliseconds they were considered to be unreliable.

Conclusion

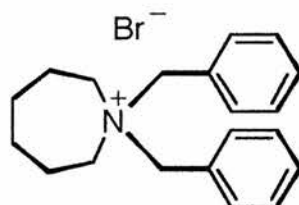
Firstly, it was found necessary to carefully dry samples before the study, due to their hygroscopic nature and their readily hydrated state. When comparing $T_{1\rho}$ data for dried and undried samples the $T_{1\rho}$ relaxation times observed for the anhydrous samples was very much longer. This meant, however, that very long relaxation times for these samples made for unreliable results.

Reliable results were obtained for the anhydrous TEACl. Energies of activation, E_a , of 51.9 and 28.1 kJ mol.⁻¹ were derived for the $\underline{\text{C}}\text{H}_2\text{CH}_3$ and CH_3 carbons respectively. This was indicative of methyl rotation being faster than rotation of the ethyl group as a whole.

Other compounds studied

A small number of other, miscellaneous, samples were studied; samples which do not fall conveniently into previous chapters, and samples provided by colleagues from other institutions where our solid-state NMR spectrometer can provide useful additional information to other more readily available techniques; due to the increased resolution that can be achieved with solids at high field using CP/MAS, and the range of probes available for 1D and 2D solid-state and high-resolution solution work. This increased resolution with solids on a high-field spectrometer simplifies the collection of complex spectra and allows for the measurement of relaxation data where it might otherwise not be possible.

***N,N*-Dibenzylhexamethyleiminium bromide**

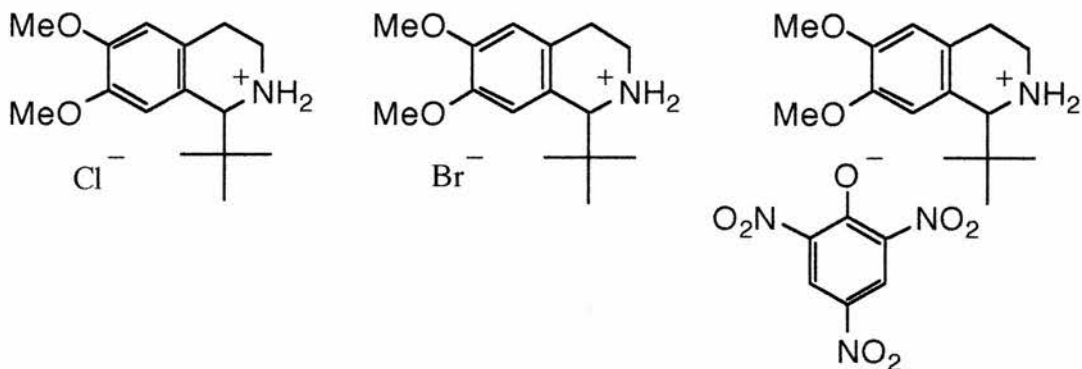


m.p. 153-7 °C

The RT spectrum contained a lot of signals in the aromatic region, perhaps indicative of more than one molecule in the asymmetric unit. This, coupled with the poor signal to noise ratio and the long acquisition times (recycle time 20 seconds) make it unsuitable for further study.

Compounds supplied by Ferenc Fülöp

Professor Ferenc Fülöp, of the Institute of Pharmaceutical Chemistry at the Albert Szent-Györgyi Medical University, Szeged, Hungary, supplied three salts of 6,7-dimethoxy-1-*tert*-butyl-1,2,3,4-tetrahydroisoquinoline (reference number FF/675); the chloride, bromide and picrate (over).



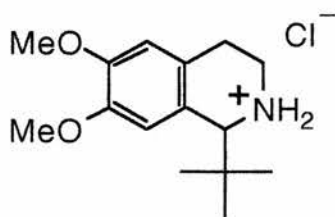
The melting points of these compounds were provided (Table 1). A $T_{1\rho}$ relaxation study was carried out on the chloride and the bromide. The samples were not dried before the experiment.

Melting points of FF/675 salts

FF/675 salt	melting point °C
Chloride	243-5
Bromide	276-8
Picrate	152-4

Table 1

FF/675 Chloride



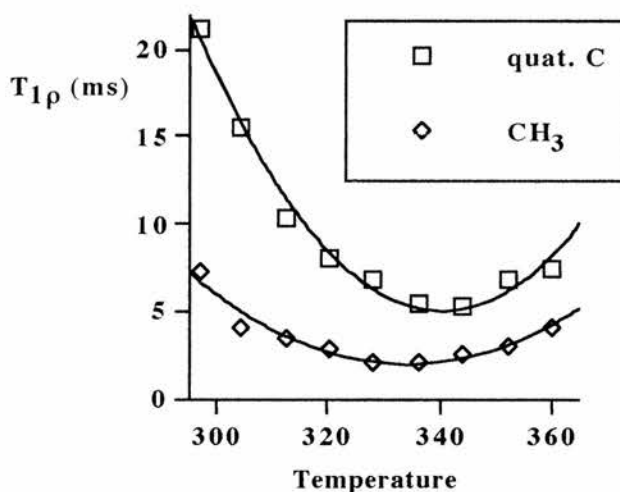
In order to measure $T_{1\rho}$ relaxation for the *tert*-butyl group of FF/675 chloride, measurements were taken from 297 K to 360 K. Calculated $T_{1\rho}$ relaxation values for the quaternary carbon and the methyl carbons are given in Table 2.

$T_{1\rho}$ data for FF/675 chloride ($\omega_1 = 62.7$ kHz)

Temperature	$T_{1\rho}$ (ms)	
	quaternary C	CH ₃
297	21.22	7.32
304	15.54	4.08
312	10.32	3.45
320	8.02	2.90
328	6.78	2.11
336	5.42	2.07
344	5.33	2.47
352	6.85	3.02
360	7.43	4.02

Table 2

When a graph is compiled of $T_{1\rho}$ against temperature the distinctive bell shaped curve is seen for both data (Figure 1), allowing B^2 to be calculated from the minimum of $T_{1\rho}$. As would be expected the $T_{1\rho}$ relaxation values for the methyl carbons are less than those for the corresponding values of the quaternary carbon, since the methyls are normally rotating faster than the *tert*-butyl group as a whole.

Plot of $T_{1\rho}$ against temperature for FF/675 chloride**Figure 1**

The minimum of $T_{1\rho}$ for the methyl carbons of FF/675 chloride is found experimentally to be 2.07 ms. This value was calculated to be 0.74 ms using a computer program developed at the University of Canterbury.¹ The experiment was repeated twice, but the lowest $T_{1\rho}$ minimum achieved was 2.07 ms.

Correlation times and rate constants derived for methyl carbons of FF/675 chloride

Temperature (K)	τ (sec.)	k (sec. ⁻¹)
256		4.0×10^4 ^a
260		5.0×10^4 ^a
264		6.0×10^4 ^a
268		8.0×10^4 ^a
272		1.2×10^5 ^a
276		1.7×10^5 ^a
297	1.79×10^{-5}	1.68×10^5
304	9.46×10^{-6}	3.17×10^5
312	7.74×10^{-6}	3.88×10^5
320	6.14×10^{-6}	4.89×10^5
328	3.14×10^{-6}	9.55×10^5
336	2.58×10^{-6}	1.16×10^6
344	1.40×10^{-6}	2.14×10^6
352	1.02×10^{-6}	2.94×10^6
360	7.15×10^{-7}	4.20×10^6

^a derived from lineshape analysis
 $B^2 = 3.75 \times 10^8 \text{ sec.}^{-2}$

Table 3

¹ developed by S. A. Holmes. Details available in Appendix B.

B^2 was calculated to be $3.75 \times 10^8 \text{ sec.}^{-2}$, which allowed correlation times (τ) and subsequently rate constants to be calculated. Lineshape analysis was carried out to complement the experimental NMR data. The experimentally derived correlation times, and the rate constants for both the NMR data and the lineshape analysis, are shown in Table 3. A plot of $\ln(k)$ against $1/T$ is shown in Figure 2.

Plot of $\ln(k)$ against $1/T$ for FF/675 chloride

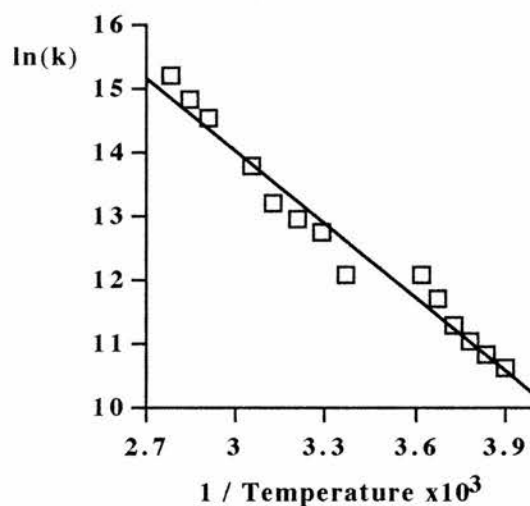


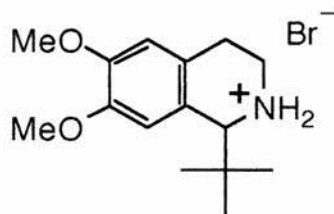
Figure 2

Since the experimentally derived part of the plot (the upper part) is not in good agreement with the lineshape derived part of the plot (although the gradients are similar), it is only possible to derive an approximate energy of activation from the slope of the plot (Table 4), calculated to be approximately 32 kJ mol.^{-1} .

Energies of activation derived for methyl of FF/675 chloride

	CH ₃
slope	+ 3.82
r^2	0.962
Ea (kJ mol.⁻¹)	+ 31.8

Table 4

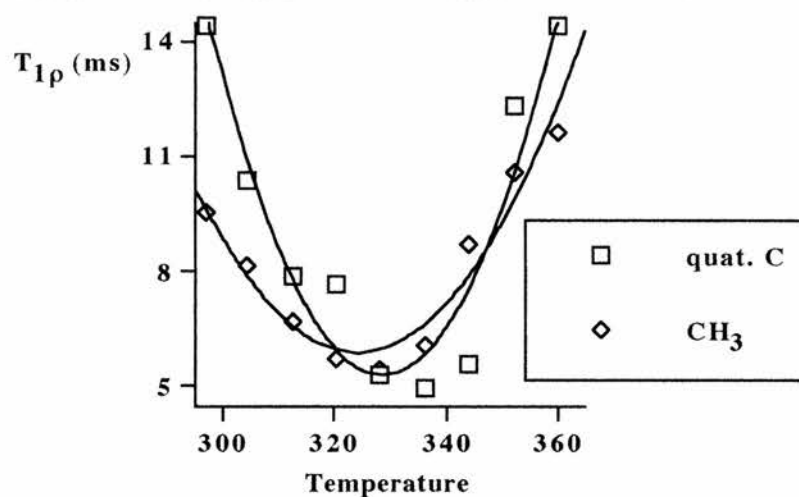
FF/675 Bromide

$T_{1\rho}$ data were collected for FF/675 bromide from RT to 360 K. Since one of the CH_2 s in the ring obscured the CH_3 resonance, the $T_{1\rho}$ pulse sequence had NQS incorporated to remove the CH_2 resonance and so make measurement of the CH_3 resonance much clearer. The data are presented in Table 5. The data do not appear reliable since the $T_{1\rho}$ relaxation minimum for the quaternary carbon (4.93 ms) appears lower than that for the methyl carbon (5.47 ms), as seen in Figure 3, which is not possible since each methyl group would be expected to rotate at a faster rate than the *tert*-butyl group as a whole.

$T_{1\rho}$ data for FF/675 bromide ($\omega_1 = 54.3$ kHz)

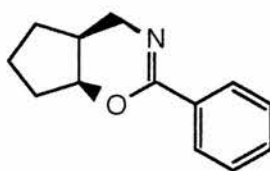
Temperature	$T_{1\rho}$ (ms)	
	quaternary C	CH_3
297	14.40	9.52
304	10.38	8.13
312	7.90	6.72
320	7.63	5.75
328	5.27	5.47
336	4.93	6.08
344	5.59	8.72
352	12.33	10.61
360	14.42	11.64

Table 5

Plot of $T_{1\rho}$ against temperature for FF/675 bromide**Figure 3**

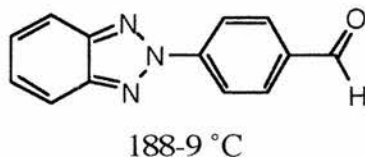
It would be interesting to repeat the experiment, but unfortunately time did not allow during this study.

Dihydrooxazine



This sample (FF/112) was claimed to have a curious melting point phenomenon; m.p. of 45 °C under normal conditions, which was lowered to 28 °C if the sample was recrystallised from ether, giving crystals on cooling below 0 °C. The melting point is then noted to return to 45 °C after a further two weeks at room temperature. Some sort of phase change may be responsible. However, these observations were found to be irreproducible in the laboratory; the sample when stored at room temperature melted at 39-41 °C, and the lowest melting point observed for the compound recrystallised from ether (several attempts) was 37-39 °C.

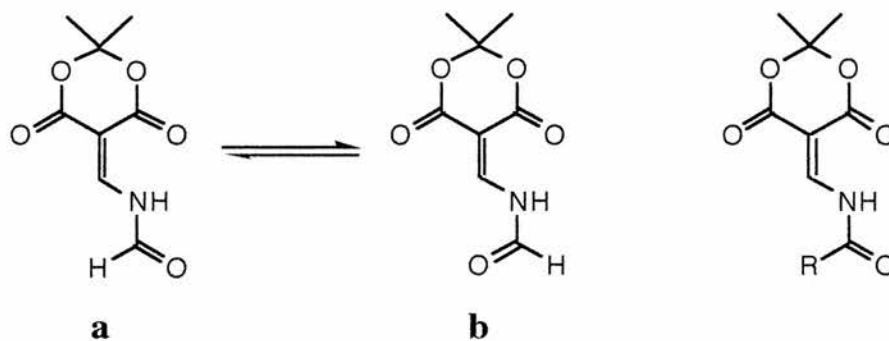
Heterocyclic aldehyde



Very long recycle times (60 seconds) were required to get any sort of signal, and the spectra which resulted had poor signal to noise ratios. Due to the difficulty of acquisition a full study was not pursued.

Meldrum's Acid derivatives

Hamish McNab, of the Department of Chemistry at the University of Edinburgh, supplied a formamido derivative of so-called Meldrum's acid for solid-state NMR investigation.



When the amido group contains an alkyl substituent, R, the compounds are well behaved and adopt only the conformation shown. However, for the formamido case there is restricted rotation around the N-CHO bond which gives rise to very broad peaks in the RT solution NMR. At low temperatures the conformers were 'frozen out' in the ratio **a** 1:2 **b**. A room temperature X-ray crystal structure indicated a ratio of **a** 38:62 **b**. Confirmation of this ratio by solid-state NMR was requested, as was possible evidence of restricted rotation in the solid at high temperature.

Initial studies with the formamido derivative, after the sample had been stored in the freezer, by solid-state NMR did indeed show a ratio of approximately 1:2, assumed to be for **a**:**b**, in agreement with the solution NMR and X-ray crystal structure. The region at around 160 ppm was useful in deciding approximate ratios since six signals, for the three carbonyls of each conformer, were in evidence. When the experiment was repeated after the sample had sat at room temperature for five days, the ratio of products was seen to increase almost exclusively towards **b**.

Under investigation by solid-state NMR the findings of the solution NMR and the X-ray crystallography were confirmed; the conformers were frozen out in the ratio **a** 1:2 **b**.

Experimental

Melting points were carried out on a Gallenkamp melting point apparatus, Infra Red spectra were recorded on a Perkin Elmer 1310 IR spectrophotometer and ^1H and ^{13}C NMR solution spectra were recorded on a Varian Gemini 200 NMR spectrometer, operating at 200 MHz and 50 MHz for ^1H and ^{13}C respectively.

1,2-Benzenedimethanol

Firstly, stock diethyl phthalate was purified¹ by washing with aqueous sodium carbonate solution, then water, and dried over CaCl_2 . The filtered product was distilled under reduced pressure and stored over phosphorus pentoxide. A solution of diethyl phthalate (5 g, 22.5 mmol.) in ether (40 ml) was added to a mixture of lithium aluminium hydride (1.70 g, 44.8 mmol.) and ether (20 ml) over one hour with ice cooling. Reflux was started and continued for 4 hours. 20 % potassium carbonate in water was added to destroy residual hydride. The mixture was filtered and the filtrate extracted with ether, the combined ether was dried (MgSO_4) and concentrated under reduced pressure. The viscous residue crystallised when pulled with an oil vacuum pump. Recrystallised with ether (colourless plates ground to off-white powder). Yield 0.90 g, 29 %. M.p. 61-2 °C (lit.² m.p. 63-5 °C). NMR (CDCl_3), δ_{H} 7.35 (4 H, m, Ar-H), 4.75 (4 H, s, CH_2OH), 2.45 (2 H, broad s, OH).

cis-Ethyl cyclopentanol-2-carboxylate³

A glass sleeve was charged with ethyl cyclopentanone-2-carboxylate (3.5 g, 22.4 mmol.), Raney-Nickel catalyst (3.2 g; 50 % aqueous slurry, 6.4 g slurry) and ethanol

¹ Perrin D. D., Armarego W. L. F., Purification of Laboratory Chemicals, 3rd Ed., Pergamon Press, Oxford, (1988) 149

² Aldrich Chemical Co. catalogue

³ Kovács Ö., Szilágyi J., Schneider G., *Magyar Kémiai Folyóirat*, **71**, (1965) 93

(20 ml) and secured in an autoclave. The autoclave was pressurised with hydrogen to 80 bar and the reaction mixture was stirred overnight at 50 °C. The pinkish solution was filtered and the filtrate was concentrated under reduced pressure. Kugelrohr distillation (lit.³ b.p. 54-5 °C / 0.1 mm Hg) yielded a colourless liquid. Yield 3.13 g, 88 %. NMR (CDCl₃), δ_{H} 4.3 (1 H, small quart., CHOH), 4.2 (2 H, quart. ($J = 7,7$ Hz), CH_2CH_3), 3.1 (1 H, broad s, OH), 2.7 (1 H, CHCOOR), 2.0 (3 H, m, ring CHs), 1.8 (2 H, m, ring CHs), 1.65 (1 H, m, ring CH), 1.3 (3 H, t ($J = 7$ Hz), CH_3).

cis-2-(Hydroxymethyl)cyclopentanol³

cis-Ethyl hydroxycyclopentane-2-carboxylate (1.0 g, 6.32 mmol.) in ether (10 ml) was added to lithium aluminium hydride (0.5 g, 13.2 mmol.) in ether (20 ml) over 1 hour, and the mixture was refluxed for 4 hours. Excess of hydride was destroyed with 20 % acetic acid in water (5 ml) and the mixture was filtered and washed with ether. The combined ether was dried (MgSO₄), concentrated under reduced pressure and Kugelrohr distillation (lit.³ b.p. 98-100 °C / 0.4 mm Hg) yielded a colourless viscous liquid. Attempts to recrystallise yielded only an oil. ¹H NMR indicated incomplete reaction; presence of ethyl group from ester, δ_{H} (CDCl₃) 4.2 (quart., CH₂), 1.3 (t, CH₃). 1.23 and 2.1 equivalents of lithium aluminium hydride gave ratios of starting material to product of 1:2 and 2:5 respectively by ¹H NMR.

trans-2-(Hydroxymethyl)cyclopentanol³

Sodium ethoxide (sodium (0.4 g, 17.4 mmol.) in abs. ethanol (25 ml)) was added to a mixture of ethyl cyclopentanone-2-carboxylate (2.6 g, 16.6 mmol.), Raney-Nickel catalyst (2.5 g; 50 % aqueous slurry, 5.0 g slurry) and ethanol (20 ml) in a glass sleeve and secured in an autoclave. The autoclave was pressurised with hydrogen to 50 bar and the reaction mixture was stirred overnight at RT. Acetic acid (1.5 ml) was added to the pinkish mixture, the catalyst was filtered off and the filtrate was concentrated under

reduced pressure. The residue was dissolved in water (10 ml) and extracted with ether (4 x 10 ml). The combined ether, now a scarlet colour, was washed with water then 5 % sodium bicarbonate solution, and the ether was evaporated under reduced pressure. Kugelrohr distillation yielded a colourless liquid product, leaving a deep coloured residue. Yield 1.46 g. ^1H NMR indicated incomplete reaction.

Diethyl 1,1-cyclobutanedicarboxylate⁴

Sodium ethoxide (sodium (9.2 g, 0.4 mol.) in abs. ethanol (170 ml)) was added dropwise to a solution of anhydrous diethyl malonate (32.05 g, 0.4 mol.) and anhydrous 1-bromo-1-chloropropane (31.5 g, 0.2 mol.) by means of nitrogen pressure at such a rate so as to maintain reflux. As more ethoxide was added so the reaction became more vigorous, the addition took 30 minutes and reflux was continued for a further 75 minutes. Ethanol was removed by atmospheric distillation where 90-95 % of the ethanol was recovered. The reaction mixture was cooled to below 50 °C before adding water (60 ml) to dissolve all inorganic salts. The layers were separated and the aqueous part was extracted with ether (3 x 50 ml). The combined ether was washed with saturated brine, dried (Na_2SO_4) and concentrated under reduced pressure. Vigreux distillation (b.p. 80-6 °C / 2 mbar) of the residue yielded the diester as a colourless liquid. Yield 18.46 g, 46 %. NMR (CDCl_3), δ_{H} 4.2 (4 H, quart. ($J = 7,7$ Hz), CH_2CH_3), 2.53 (4 H, t ($J = 8$ Hz), $\text{CH}_2\text{CH}_2\text{CH}_2$), 1.96 (2 H, quint., $\text{CH}_2\text{CH}_2\text{CH}_2$), 1.24 (6 H, t ($J = 7$ Hz), CH_2CH_3); evidence of impurities at δ_{H} 3.35 and 1.72, which are identical with those observed for an authentic sample of diethyl 1,1-cyclobutanedicarboxylate (ex. Lancaster).

⁴ Mariella R. P., Raube R., *Org. Synth.*, **33**, (1953) 23

1,1-Di(hydroxymethyl)cyclobutane

A solution of diethyl 1,1-cyclobutanedicarboxylate (5 g, 25 mmol.) in ether (60 ml) was added dropwise to lithium aluminium hydride (1.90 g, 50 mmol.) in ether (25 ml) at such a rate so as to maintain reflux, over 30 minutes, and reflux was then continued for 5 hours. Excess hydride was destroyed with 20 % potassium carbonate solution and the resultant filtrate was extracted with ether. The combined ether was dried (MgSO_4), concentrated under reduced pressure and purified by Kugelrohr distillation. ^1H NMR indicated incomplete reaction; 2.0 equivalents of lithium aluminium hydride gave a ratio of starting material to product of 3.8:100, which improved to 2.1:100 after the crude product was twice distilled.

Pentaerythrityl bromide⁵

Pentaerythritol (34.04 g, 0.25 mol.) was heated on a boiling water bath with stirring in a flask connected to a trap, containing dilute caustic solution, to absorb evolved HBr. Freshly distilled phosphorus tribromide (135.5 g, d 2.85, 47.5 ml; 0.5 mol.) was added dropwise, then the mixture was stirred at 170-180 °C for 20 hours. A deep orange-red colour developed during the reaction. When exposing the mixture to air in readiness for the next step, the solid ignited spontaneously (due to the formation of spontaneously inflammable hydrides of phosphorus as warned in Ref. 5) and so the flaming solid was extinguished immediately with carbon dioxide.

Pentaerythrityl bromide⁶

Pentaerythritol (12.12 g, 89 mmol.) and pyridine (60 ml) were stirred together, and benzenesulfonyl chloride (69.2 g, d 1.384, 50 ml; 0.39 mol.) was added dropwise at such a rate that the temperature did not exceed 35 °C. The slurry was stirred for 1 hour at 40 °C before adding to a solution of conc. hydrochloric acid (75 ml), water (100 ml) and

⁵ Schurink H. B., *Org. Synth.*, **17**, (1937) 73 (*Org. Synth.*, Coll. Vol. **2**, (1943) 476)

methanol (200 ml) (firstly, a small portion of the slurry was mixed with a little of the solution and scratched until a crystalline precipitate was formed. This was added to seed the main batch, before adding the bulk of the slurry). A white granular suspension of pentaerythrityl benzene sulfonate was formed. The slightly wet benzene sulfonate was mixed with diethylene glycol (100 ml) and sodium bromide (56 g, 0.54 mol.; 6.1 equiv.), before stirring slowly (60-120 rpm) overnight at 140-150 °C. The orange coloured mixture was cooled to 90 °C before adding ice-water (200 ml) and cooling further to 10 °C by direct addition of ice. The precipitate was filtered, washed with water (200 ml) and pressed dry. The tan crystalline solid was recrystallised from acetone. Repeated concentration and cooling of the filtrate recovered further product. Combined yield 18.84 g, 55 %. M.p. 153-59 °C (lit. m.p. 159-60 °C,⁶ 158-60 °C⁵ for first crop in each case). NMR (CDCl₃); δ_H 3.55 (8 H, s, CH₂), δ_C 34.1 (CH₂), 43.1 (quat. C).

Methylene cyclobutane⁷

To a stirred solution of zinc bromide (0.15 g), ethanol (0.5 ml) and water (15 ml) was added zinc dust (7 g, 0.11 mol.). The mixture was heated to 90 °C and pentaerythrityl bromide (10 g, 26 mmol.) was added portionwise to avoid frothing. The flask was fitted with, in series, splash head, water condenser and receiver flask cooled with dry-ice. Steam distillation yielded no hydrocarbon layer, and no evidence of the product was found by ¹H NMR.

Methylene cyclobutane⁸

To a mixture of pentaerythrityl tetrabromide (7.5 g, 19.3 mmol.) was added water (10 ml) with stirring. To the flask was fitted, in series, splash head, water condenser, dry-ice condenser and receiver flask cooled with ice. The mixture was heated to 95 °C where distillation took place at 40-1 °C (lit.⁸ b.p. 41.39 °C / 750 mm Hg). The collected

⁶ Herzog H. L., *Org. Synth.*, **31**, (1951) 82

⁷ Roberts J. D., Sauer C. W., *J. Am. Chem. Soc.*, **71**, (1949) 3927

⁸ based on method of Shand Jnr W., Schomaker V., Fischer J. R., *J. Am. Chem. Soc.*, **66**, (1944) 636

product had the distinctive ethereal aroma of methylene cyclobutane. Yield 0.81 g, 61 %. NMR (CDCl₃), δ_{H} 4.7 (2 H, m, =CH₂), 2.7 (4 H, m, C-3 H₂), 1.9 (2 H, m, C-4 H₂).

N-(1-methylcyclobutyl)acetamide⁹

A mixture of acetonitrile (0.2 ml), glacial acetic acid (2 ml) and conc. sulfuric acid (0.2 ml) was stirred with ice cooling. Methylene cyclobutane (0.22 g, 3.2 mmol.) was added and the mixture was stirred for 1 hour at RT. The solution was diluted with water (10 ml), basified with sodium carbonate and extracted with ether (5 x 15 ml). The combined ether was dried (MgSO₄), filtered and evaporated to yield white crystalline *N*-(1-methylcyclobutyl)acetamide. Yield 0.15 g, 37 %. M.p. 62-5 °C (no lit. m.p. available). NMR (CDCl₃), δ_{H} 5.8 (1 H, broad s, NH), 1.9 (3 H, s, NHCOCH₃), 1.9 (6 H, m, ring CH₂s), 1.3 (3 H, s, RCH₃).

1-Methylcyclobutylamine⁸

The acetamide (0.15 g) and 4M potassium hydroxide in ethylene glycol (10 ml) was heated at reflux for 48 hours. After adding a little water, the mixture was extracted 15 times with ether (instead of continuous extraction). The combined ether extracts were dried (KOH), filtered and evaporated leaving a very small residue which did not resemble the desired product by ¹H NMR.

N,N-Dibenzylhexamethyleneiminium bromide

Hexamethyleneimine (1.98 g, 0.02 mol.) was added to a stirred solution of sodium hydroxide (0.8 g, 0.02 mol.) in water (20 ml). Benzyl bromide (6.84 g, 0.04 mol.) was added dropwise, to form the salt which soon precipitated. The precipitate was filtered

⁹ Cox E. F., Caserio M. C., Silver M. S., Roberts J. D., *J. Am. Chem. Soc.*, **83**, (1961) 2719

off, recrystallised from water and dried under vacuum. Yield 6.55 g (91 %). M.p. 153-7 °C (no lit. m.p. available). NMR (CDCl₃), δ_H 7.5 (10 H, m, Ph), 5.1 (4 H, s, NCH₂Ph), 3.75 (4 H, m, NCH₂CH₂), 1.5 (8 H, m, other CH₂).

N,N-Dibenzylpyrrolidinium bromide

Pyrrolidine (1.42 g, 0.02 mol.) was added to a stirred solution of sodium hydroxide (0.8 g, 0.02 mol.) in methanol (25 ml). Benzyl bromide (6.84 g, 0.04 mol.) was added dropwise and the reaction mixture was stirred overnight. The solution was concentrated to dryness under reduced pressure and the solid was collected and dried. Crude m.p. 89-92 °C (no lit. m.p. available). ¹H NMR indicated a crude mixture of products, which was not purified.

cis-Cyclopentene-3,5-diol¹⁰

Cyclopentadiene (3.2 g, 24 mmol.; distilled from dicyclopentadiene¹¹), Rose Bengal (100 mg), thiourea (2.5 g, 16.4 mmol.) and distilled methanol (1 l) were added to custom irradiation apparatus. After bubbling through O₂ for 5 minutes, the pinkish solution was irradiated with a 400 W mercury emission lamp. The stirred solution was irradiated for a total of 2 hours 50 minutes with water cooling and continued O₂ bubbling through. Irradiation was stopped and the mixture was stirred, in the dark, overnight. After evaporation of the methanol under reduced pressure, the residue was dissolved in a little water. After washing with benzene to remove colour (with little effect) the aqueous part was separated and evaporated under reduced pressure leaving a coloured residue. Kugelrohr distillation yielded a colourless liquid. Yield 1.35 g. No evidence of desired product by ¹H NMR.

¹⁰ Kaneko C., Sugimoto A., Tanaka S., *Synthesis*, (1974) 876

¹¹ Vögel A. I., *Textbook of Practical Organic Chemistry*, Longman Scientific and Technical, Harlow, England, 5th Ed., (1989) 1122

Disiamylborane¹²

Borane in THF (22.5 ml, 1.0 M, 22.5 mmol.) was added dropwise to 2-methyl-2-butene in THF (45 ml, 2.0 M, 0.09 mol.) at -15 °C. The disiamyl borane reagent was used immediately. Yield assumed to be quantitative, 22.5 mmoles.

***trans*-Cyclopentane-1,3-diol¹²**

Prepared disiamylborane (22.5 mmol.) was added dropwise to cyclopentadiene (1.2 g, 18.2 mmol.; distilled from dicyclopentadiene¹¹) at 0 °C and reacted overnight at 0 °C, before oxidation with 3N NaOH (13 ml) and 35 % hydrogen peroxide (11 ml). The aqueous part was extracted with THF (3 x) and the combined organic part was dried (MgSO₄) and concentrated under reduced pressure. The oily residue was distilled on Kugelrohr apparatus to yield a colourless liquid. Yield 1.26 g. No evidence of desired product by ¹H NMR.

Disiamylborane¹³

To 2-methyl -2-butene (27.23 g, 0.33 mol.) in diglyme (20 ml), diglyme (80 ml) and sodium borohydride (4.7 g, 0.125 mol.) in ice was added boron-trifluoride etherate (23.5 g, 0.165 mol.) over 30 minutes. The semi-solid mixture was stored in the freezer prior to use. Yield assumed to be quantitative, 0.165 moles.

***trans*-Cyclopentane-1,3-diol^{12,14}**

Cyclopentadiene (5.45 g, 82.4 mmol.; distilled from dicyclopentadiene¹¹) was added dropwise to prepared disiamylborane (0.165 mol.) with cooling and stirred for 3 hours at RT, before oxidation with 3N NaOH (46 ml) and 35 % hydrogen peroxide (40 ml). The

¹² Zweifel G., Brown H. C., *J. Am. Chem. Soc.*, **85**, (1963) 2066

¹³ Vögel A. I., Textbook of Practical Organic Chemistry, Longman Scientific and Technical, Harlow, England, 5th Ed., (1989) 419; Brown H. C., Zweifel G., *J. Am. Chem. Soc.*, **83**, (1961) 1241

¹⁴ Zweifel G., Brown H. C., *J. Am. Chem. Soc.*, **83**, (1961) 1241

aqueous part was extracted with ether, and the combined ether was washed with water (4 x) to remove diglyme before drying (MgSO_4) and Kugelrohr distillation. Product collected contained significant amounts of diglyme which further washing with water and subsequent distillation failed to reduce.

cis-3,5-Dibromocyclopentene¹⁵

Bromine (49.37 g, d 3.119, 15.8 ml; 0.31 mol.) in DCM (30 ml) was added to cyclopentadiene (3.2 g, 24 mmol.; distilled from dicyclopentadiene¹¹) in DCM (30 ml), maintaining the temperature at -25 to -30 °C. The green residue was distilled quickly (b.p. 64 °C / 1.5 mm Hg (lit.¹⁵ b.p. 60-3 °C / 0.5 mm Hg)) to yield a slightly yellowed liquid. Yield 50.76 g, 73 %. Colour deepened in the product overnight and was distilled (b.p. 64 °C / 1.5 mm Hg) through a column packed with glass beads. Yield 37.66 g, 54 % overall. Over time colour deepened and small black spots formed, due to polymerisation, so it was always redistilled before use.

cis-3,5-Diacetoxycyclopentene

A mixture of 3,5-dibromocyclopentene (1 g, 4.4 mmol.), sodium acetate (1 g, 12.2 mmol.), 15-crown-5 ether (5 drops, catalytic amount), water (20 ml) and ether (20 ml) was stirred at RT and followed by TLC (ether 1:4 petrol 40 / 60). After a few hours there was no change so the mixture was stirred at reflux for 5 hours until TLC indicated complete reaction. The aqueous layer was separated and extracted with ether (3 x). The combined ether was dried (MgSO_4) and concentrated under reduced pressure. Crude yield 0.34 g, 48 %. Kugelrohr distillation under reduced pressure yielded a colourless liquid. TLC indicated a mixture of isomers (for both the dibromo- and the unsaturated diacetoxy compounds).

¹⁵ Owen L. N., Smith P. N., *J. Chem. Soc.*, (1952) 4035

Separation of *cis*- and *trans*-cyclopentane-1,3-diol

Mixture of *cis*- and *trans*-cyclopentane-1,3-diol refluxed in benzene (5 ml) to expel moisture, before distilling off the benzene. Diol mixture (100 mg, 97.9 μmol .) reacted with benzaldehyde dimethylacetal (90 mg, 591 μmol ., 1.2 equiv. w.r.t. *cis*-diol assuming *cis* 50:50 *trans*) in presence of tosic acid (few crystals) at 80 °C. The mixture went brown within a few minutes and was found to contain benzaldehyde by TLC (ether 1:4 petrol 40 / 60), indicative of hydrolysis even after measures taken to expel moisture.

Separation of *cis*- and *trans*-cyclopentane-1,3-diol¹²

Borane in THF (100 ml, 1.0 M, 0.1 mol.) was added dropwise to cyclopentadiene (13.2 g, 0.2 mol.; distilled from dicyclopentadiene¹¹) at 0 °C, during which time the reaction mixture turned into a gel; reaction was continued at RT for 12 hours. Excess hydride was decomposed by adding water. The organoborane was oxidised at 50-60 °C with 3N NaOH (44 ml) and 35 % hydrogen peroxide (38 ml). The aqueous phase was saturated with potassium carbonate. The THF extract was dried (MgSO_4), concentrated under reduced pressure and the residue was distilled (95 °C / 0.5 mm Hg) under reduced pressure. Yield 14.3 g, 70 %. ¹³C NMR indicated 85:15 isomer mixture, allocated *trans* 85:15 *cis* in agreement with Ref. 12. A portion of the diol (1.03 g, 10 mmol.) was treated with *n*-butylboronic acid (1.02 g, 10 mmol.) and the water formed was removed by azeotropic distillation with benzene. Distillation at reduced pressure yielded a negligible amount of a volatile distillate and 1.35 g of a non-volatile residue. The non-volatile residue (1.35 g) yielded, after displacement of the boron with ethylene glycol (1 ml), *trans*-cyclopentane-1,3-diol. Yield 0.54 g, 52 % from diol mixture (lit.¹² b.p. 95 °C / 0.5 mm Hg, lit.¹² m.p. 28-30 °C). NMR (solid-state), δ_{C} 72 (2 C, CHR_2OH), 45 (1 C, C-2), 33 (2 C, C-4,5).

Appendix A

Crystal structure of 1,1,1-tris(hydroxymethyl)ethane

The best attempt at the solution of the structure of 1,1,1-tris(hydroxymethyl)ethane from "single crystal" X-ray diffraction came from Eilerman *et al.*¹ who noted that crystals from sublimation or grown from solution exhibit four-fold twinning, thereby forming a pseudo-body-centred-tetragonal unit cell. They concluded that the systematic absences were consistent with a tetragonal space group and refined their space group in the assumed space group I-4. The structure they arrived at is an averaged, disordered structure derived from the intense *h* reflections alone. It transpires from this work that the space group is not I-4 but is most likely to be A_{bm2} .

Other attempts at single crystal analysis have resulted in a preliminary communication with no follow up² or in references to unpublished work suggesting 32 molecules in the asymmetric unit,³ which, in the light of the solid-state NMR data, is unlikely; when studying 1,1,1-tris(hydroxymethyl)ethane by ¹³C CP/MAS NMR, the spectrum consists of four lines at just below RT in the approximate ratio 2:1:1:1 with the CH₂OH carbons appearing as a 2:1 doublet. As the temperature is increased the 2:1 doublet undergoes a coalescence ($T_C = 334$ K) and appears a singlet at higher temperatures. The ¹³C CP/MAS spectra are consistent with only one molecule in the asymmetric unit (2:1 ratio of independent CH₂OH units) and with the molecules containing a plane of symmetry rendering two of the CH₂OH groups equivalent.

¹ Eilerman D., Lippman R., Rudman R., *Acta Cryst.*, **B39**, (1983) 263

² Nakano E., Hirotsu K., Shimada A., *Bull. Chem. Soc. Japan*, **42**, (1969) 3367

³ Carter R. L., Kahr B., McBride J. M., unpublished work cited in Kahr B., McBride J. M., *Angew. Chem. Int. Eng. Ed.*, **31**, (1992) 1

Powder X-ray diffraction⁴

X-ray powder diffraction data were collected on two polycrystalline samples of 1,1,1-tris(hydroxymethyl)ethane, one directly supplied from Aldrich and the other obtained after sublimation. The powder diffraction data from both samples proved to be very similar although the data obtained from the sublimed sample was better quality.

Powder diffraction data were initially collected on the high-resolution Stoe STADI/P diffractometer at the University of St. Andrews. This data clearly showed the presence of extra peaks not present in the powder pattern simulated from the single crystal structure but the reliable structural information could not be obtained from these data and so synchrotron data were recorded.

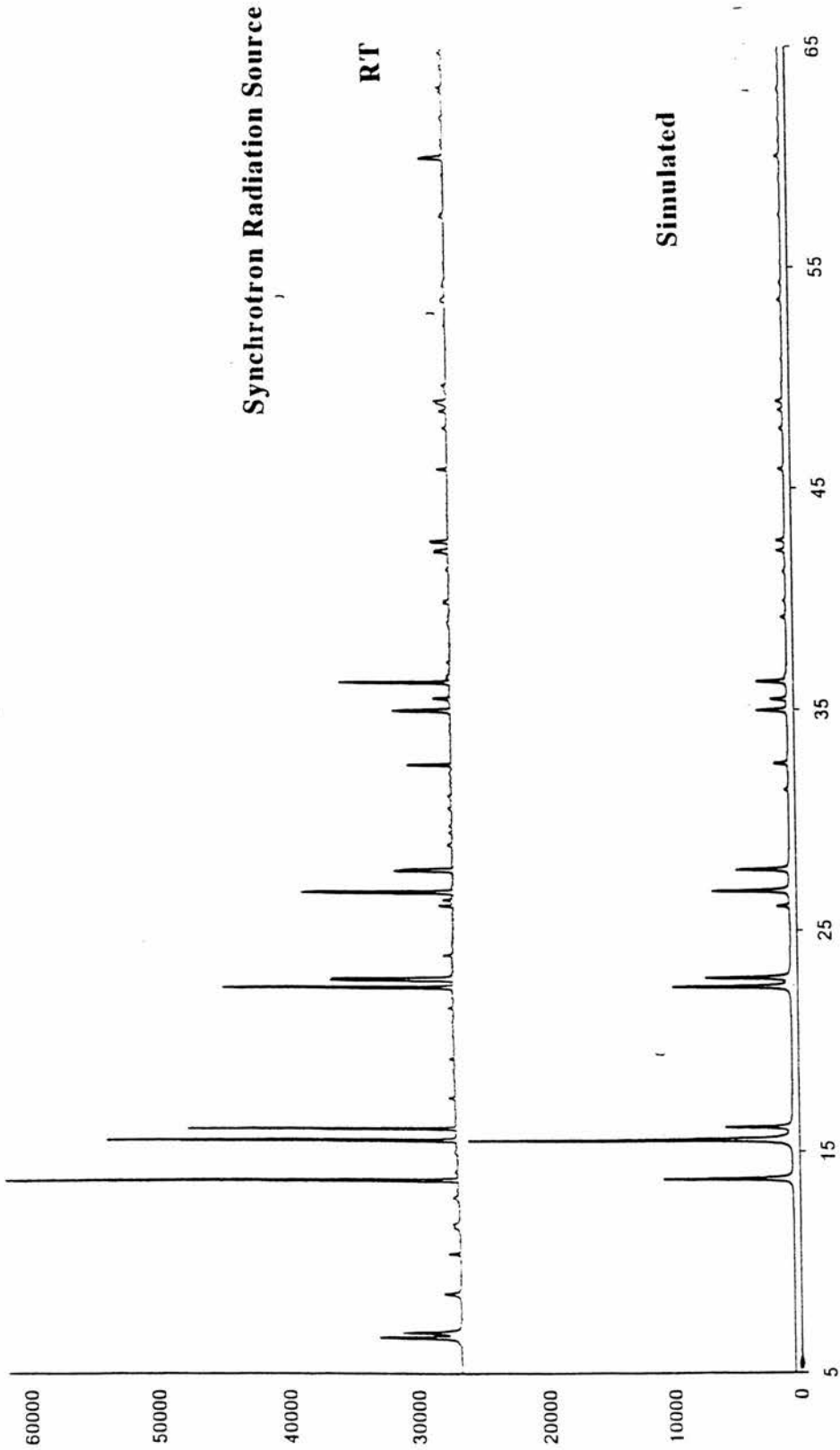
X-ray powder diffraction data were collected on station 9.1 at the SRS Daresbury (synchrotron radiation source), UK. The samples were loaded into 0.7 mm quartz capillaries to a depth of approximately 3 cm. The wavelength of the X-rays used was 1.2000 Å and the beam size was 1.0 x 10 mm². In the first instance a number of data sets were collected at room temperature and combined to give the diffraction data. Additional data sets were then collected at low temperature, 120 K, with the sample cooled using an Oxford Cryosystems cryostream.

Comparison of SRS data from the sublimed sample at RT with powder data simulated from the single crystal structure solution¹ is shown on page 131.

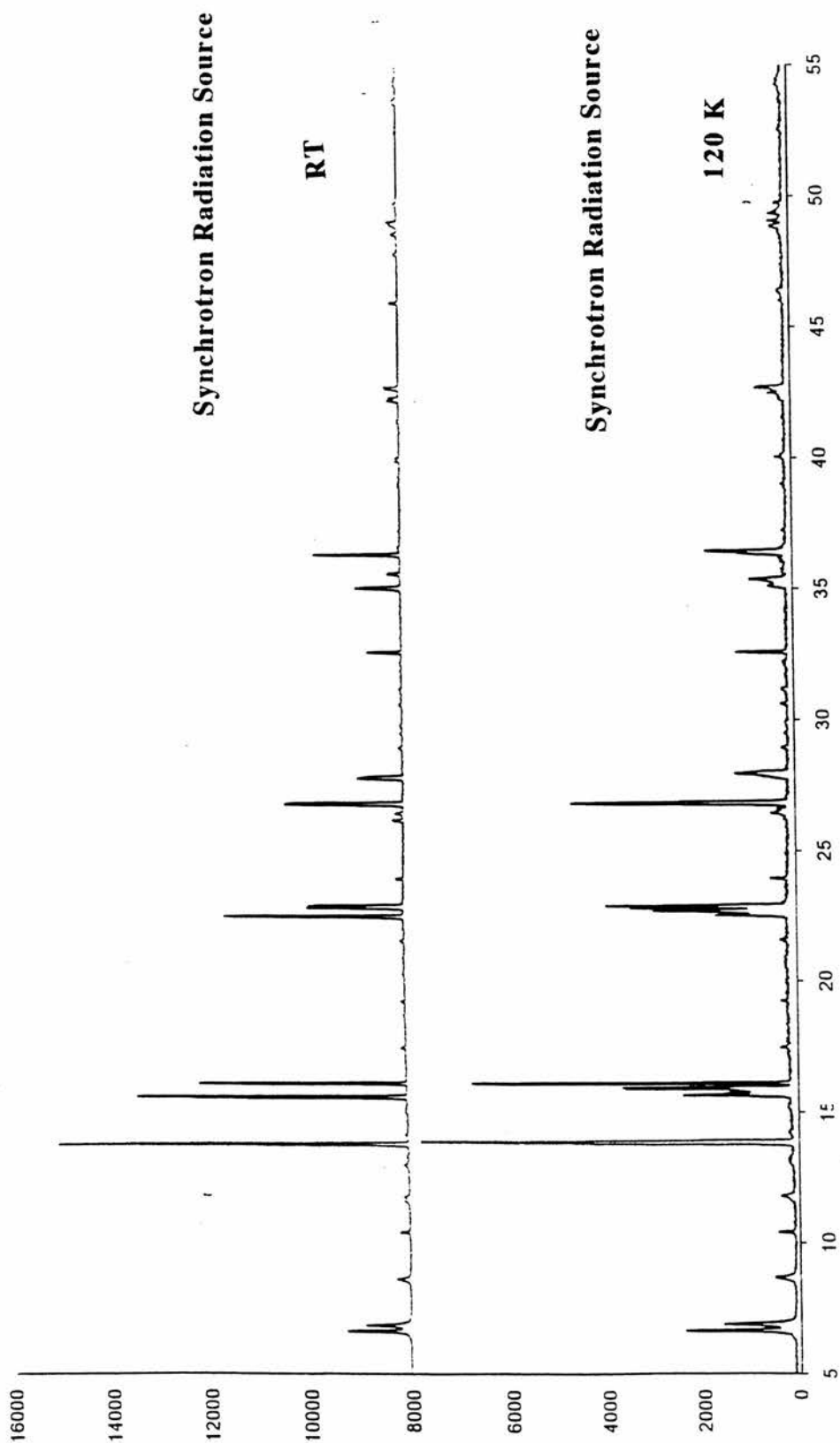
Comparison of SRS data from the sublimed sample at RT and low temperature (120 K) can be seen on page 132.

⁴ crystallography carried out by M.-J. Tremayne, School of Chemistry, University of St Andrews, Fife, KY16 9ST

**SRS data at RT compared with powder data simulated
from single crystal structure solution**



**SRS data at RT compared with SRS data at
low temperature (120 K)**



Results

The original single-crystal structure for $\text{CH}_3\text{C}(\text{CH}_2\text{OH})_3$ is tetragonal with cell parameters (Ref. 1):

$$a = b = 6.05 \text{ \AA}, c = 8.87 \text{ \AA}, \text{ volume} = 324.7 \text{ \AA}^3, Z = 2, \text{ space group} = I-4$$

However, the molecule does not have the required site symmetry -4 and hence the structure requires the presence of a statically disordered molecule. The powder diffraction pattern obtained from the SRS at room temperature was indexed using the program TREOR⁵ on the basis of the first 28 observable lines. The following triclinic unit cell was obtained with a figure of merit $M_{20} = 39$:⁶

$$a = 10.5306 \text{ \AA}, b = 10.5505 \text{ \AA}, c = 6.1601 \text{ \AA},$$

$$\alpha = 105.356^\circ, \beta = 91.166^\circ, \gamma = 99.997^\circ, \text{ and volume} = 648 \text{ \AA}^3.$$

This cell was obtained independently from the powder diffraction pattern i.e. there was no reference to the single-crystal structure at this stage. The powder cell is approximately twice the size of the tetragonal cell implying $Z = 4$. The clear relationship between these two cells was confirmed after interconversion between these cells was achieved.

From a comparison of the experimental powder data and that calculated from the single-crystal structure it is obvious that the positions and orientations of the molecules defined by the tetragonal cell are very close to those in the larger triclinic cell. For complete structure determination, positions for the four symmetry independent molecules in the new triclinic cell will need to be calculated by applying the conversion used between the two unit cells. A subsequent Rietveld refinement will also be required. Note that the presence of four symmetry inequivalent molecules in the lowest symmetry implies a different conformation within the molecule although this may only be slight.

⁵ Werner P.-E., Eriksson L., Westdahl M., *J. Appl. Cryst.*, **18**, (1985) 367

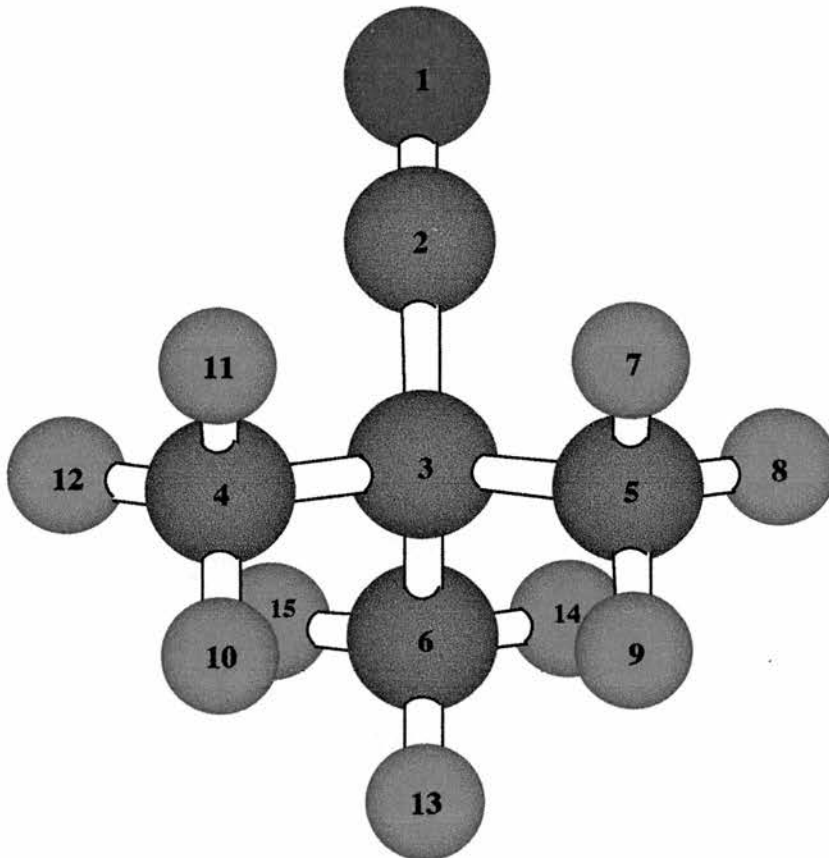
⁶ de Wolff P. M., *J. Appl. Cryst.*, **1**, (1968) 108

Appendix B

Computer program to calculate relaxation times¹

Given crystallographic details of a molecular crystal and types of rotations occurring within it, this program will calculate the relaxation times T_1 , $T_{1\rho}$ and T_2 as a function of temperature.

Throughout, *tert*-butyl cyanide (below), which has a uniaxial rotation and also methyl rotation, will be used as an example to illustrate how the program works. The program calculates relaxation times only for molecules where the motion leaves the molecule looking the same, e.g. methyl rotation, *tert*-butyl motions.



¹ program developed by S. A. Holmes, School of Physical Sciences, University of Kent, Canterbury, Kent, CT2 7NS

Input information

1. Enter values of the B_0 and B_1 field in Teslas.
2. Enter number of A groups.
3. Enter number of B groups within each A group.
4. Running through all groups ($A_1 B_1$, $A_1 B_2$, ..., $A_2 B_1$, $A_2 B_2$, ...) enter the number of atoms that it contains, their Cartesian coordinates in Angstroms (\AA) and what element they are, using standard abbreviations (using 'a' for an atom which is included for convenience but contributes nothing), and whether each atom may be considered to be one of the resonant atoms. If it is, it is then necessary to enter how many atoms it represents.
5. If groups with an A group rotate exchanging positions as whole groups, enter how many sets of such groups, then which groups constitute each set. Give the number of jumps to return to the original configuration and the activation energy (kJ mol^{-1}) and coefficient constant (seconds).
6. If atoms within B groups rotate, enter the number of jumps to return to original position, activation energy and coefficient constant.
7. Enter the total number of atoms which are considered to be resonant.
8. Enter temperature range (K) of interest, whether equal spacing of temperature or inverse temperature is required and how fine the scale should be.
9. Enter filename to output should be written.

Defining A and B groups

The atoms are assigned to A and B groups. An A group is a collection of atoms which has the same type of motion and is independent of the atoms in a different A group. Each A group is then divided up into B groups that have the common motion of the A group but also have a further movement independent of each other. In this way it is possible to motion up to four relative motions.

For *tert*-butyl cyanide the A and B groups would be as follows:

A group	B group	atom
A1	B1	1
A1	B1	2
A1	B1	3
A2	B1	4
A2	B2	5
A2	B3	6
A2	B4	7
A2	B4	8
A2	B4	9
A2	B5	10
A2	B5	11
A2	B5	12
A2	B6	13
A2	B6	14
A2	B6	15

There will be two sets of groups rotating within A2. B1, B2 and B3 form the first set, B4, B5 and B6 the second. Each of the second set having a further rotation.

Results from given command file

The results will appear in the chosen file in the form:

$10^3/\text{Temperature}$	T_1	$T_{1\rho}$	T_2
.	.	.	.
.	.	.	.
.	.	.	.

Program parameters

These should be kept as small as possible in order to minimise running time.

- nag** maximum number of a groups
- nbg** maximum number of B groups within an A group
- naig** maximum number of atoms within a B group
- natoms** maximum number of atoms to be considered
this needs to be entered in subroutines relsame and reldiff
- njumps** maximum number of jumps for a rotation
this needs to be entered in subroutines relsame and reldiff
- ntypes** maximum number of probability models used
this needs to be entered in subroutines relsame and reldiff

For example:

- **nag** = 2
- **nbg** = 6
- **naig** = 3
- **natoms** = 15
- **njumps** = 3
- **ntypes** = 20

The program

```

□
□ integer nag,nbg,naig,natoms,njumps
□ parameter (nag=10,nbg=10,naig=50,natoms=100,
□ + njumps=3,ntypes=20)
□ integer i,j,k,l,m,n,o,p,i1,na,nb(0:nag),nc(nag,nbg),
□ + numA(0:nag),num(0:nag,0:nbg),num2,number,
□ + sum,add,c1(nag),d1(natoms),add9,
□ + xi(natoms,3),noA(natoms),
□ + noB(natoms),ntot,mt(natoms),nt(natoms),setno(nag),
□ + set(nag,nag,njumps),add1,add2,
□ + Bnj(natoms,njumps),ico,icount,
□ + resno(nag,nbg,naig),resi(natoms),
□ + tune,low,high,first,last,med,grad

```



```

□ la(3,3)=1.5d+0
□ la(4,2)=2.0d+0
□ la(4,3)=1.0d+0
□ la(4,4)=1.0d+0
□ la(5,2)=1.25d+0-dsqrt(5.0d+0)/4.0d+0
□ la(5,3)=la(5,2)
□ la(5,4)=1.25d+0+dsqrt(5.0d+0)/4.0d+0
□ la(5,5)=la(5,4)
□ la(6,2)=2.0d+0
□ la(6,3)=1.5d+0
□ la(6,4)=1.5d+0
□ la(6,5)=0.5d+0
□ la(6,6)=0.5d+0
□ con(1,1,1)=1.0d+0
□ con(2,1,1)=0.5d+0
□ con(2,1,2)=0.5d+0
□ con(2,1,1)=0.5d+0
□ con(2,2,1)=-0.5d+0
□ con(3,1,1)=1.0d+0/3.0d+0
□ con(3,1,2)=con(3,1,1)
□ con(3,1,3)=con(3,1,1)
□ con(3,2,1)=con(3,1,1)
□ con(3,2,2)=-con(3,1,1)
□ con(3,3,1)=con(3,1,1)
□ con(3,3,3)=-con(3,1,1)
□ do i=1,4
□   con(4,1,i)=0.25d+0
□ enddo
□ con(4,2,1)=0.25d+0
□ con(4,2,2)=-0.25d+0
□ con(4,2,3)=0.25d+0
□ con(4,2,4)=-0.25d+0
□ con(4,3,1)=0.5d+0
□ con(4,3,3)=-0.5d+0
□ do i=1,5
□   con(5,1,i)=0.2d+0
□ enddo
□ con(5,2,1)=0.3d+0-dsqrt(5.0d+0)/10.0d+0
□ con(5,2,2)=-con(5,2,1)
□ con(5,2,3)=0.1d+0-dsqrt(5.0d+0)/10.0d+0
□ con(5,2,5)=-con(5,2,3)
□ con(5,3,1)=0.1d+0+dsqrt(5.0d+0)/10.0d+0
□ con(5,3,2)=0.2d+0
□ con(5,3,3)=-0.2d+0
□ con(5,3,4)=-con(5,3,1)
□ con(5,4,1)=0.3d+0+dsqrt(5.0d+0)/10.0d+0
□ con(5,4,2)=-con(5,4,1)
□ con(5,4,3)=con(5,3,1)
□ con(5,4,5)= con(5,3,1)
□ con(5,5,1)=con(5,2,3)
□ con(5,5,2)=0.2d+0
□ con(5,5,3)=-0.2d+0
□ con(5,5,4)=-con(5,2,3)
□ do i=1,6
□   con(6,1,i)=1.0d+0/6.0d+0
□ enddo
□ con(6,2,1)=con(6,1,1)
□ con(6,2,2)=-con(6,1,1)
□ con(6,2,3)=con(6,1,1)
□ con(6,2,4)=-con(6,1,1)
□ con(6,2,5)=con(6,1,1)
□ con(6,2,6)=-con(6,1,1)
□ con(6,3,1)=con(6,1,1)
□ con(6,3,2)=-con(6,1,1)

```

```

 con(6,3,4)=con(6,1,1)
 con(6,3,5)=-con(6,1,1)
 con(6,4,1)=con(6,1,1)
 con(6,4,3)=-con(6,1,1)
 con(6,4,4)=con(6,1,1)
 con(6,4,6)=-con(6,1,1)
 con(6,5,1)=con(6,1,1)
 con(6,5,2)=con(6,1,1)
 con(6,5,4)=-con(6,1,1)
 con(6,5,5)=-con(6,1,1)
 con(6,6,1)=con(6,1,1)
 con(6,6,3)=-con(6,1,1)
 con(6,6,4)=-con(6,1,1)
 con(6,6,6)=con(6,1,1)
 c initialise variables and arrays
 do i=1,natoms
   T0A1(i)=1.0d+0
   T0A2(i)=1.0d+0
   ExpA1(i)=1.0d+0
   ExpA2(i)=1.0d+0
   T0B1(i)=1.0d+0
   T0B2(i)=1.0d+0
   ExpB1(i)=1.0d+0
   ExpB2(i)=1.0d+0
 enddo
 c set values for constants

   pi=4.0d+0*datan(1.0d0)
   Boltz=1.380626d-23
   hbar=1.05d-34
   mu=1.0d-7

   write(*,*)'Enter values for B0 field and B1 field (T)'
   read(*,*,err=999)B0,B1


 c read in number of A and B groups, the coordinates and
 c element of the atoms within each group

   write(*,*)'How many A groups?'
   read(*,*,err=999) na
   write(*,*)'How many B groups within each A group?'
   read(*,*,err=999)(nb(i),i=1,na)
   do i=1,na
     do j=1,nb(i)
       write(*,10)'How many points in A',i,' B',j,' group'
       format(A,I3,A,I3,a)
       read(*,*,err=999) nc(i,j)
       write(*,*)'Give cartesian coordinates of points, type
       + of atom and whether it is one of resonant atoms'
       do k=1,nc(i,j)
         read(*,*,err=999) (xyz(i,j,k,l),l=1,3),atom(i,j,k),
         + resq
         if(resq.eq.'y')then
           write(*,*)'How many atoms does it represent?'
           read(*,*,err=999)resno(i,j,k)
         endif
       enddo
     enddo
   enddo
 enddo


 c read in which A groups have groups within them which exchange
 c positions due to jumping and the activation energy and

```

```

□c coefficient constant
□c read in which B groups have atoms which exchange positions
□c due to rotational jumping and their activation energy and
□c coefficient constant
□
□   l=0
□   do i=1,na
□     write(*,*)'Do groups within A',i,' rotate with each other?:
□     +   y or n'
□     read(*,*,err=999) qra
□     if (qra.eq.'y')then
□       write(*,*)'How many sets of groups?'
□       read(*,*,err=999) setno(i)
□       write(*,*)'How many groups?'
□       write(*,*)'i.e. number of jumps to return to original
□       +   position'
□       read(*,*,err=999)c1(i)
□       do j=1,setno(i)
□         write(*,*)'Which groups in set ',j
□         read(*,*,err=999)(set(i,j,k),k=1,c1(i))
□       enddo
□       write(*,*)'Give estimate of activation energy and coeff const'
□       read(*,*,err=999) EA(i),TA(i)
□     else
□       setno(i)=0
□       c1(i)=1
□       EA(i)=0.0d+0
□       TA(i)=1.0d+0
□     endif
□     do j=1,nb(i)
□       l=l+1
□       write(*,40)'Does A',i,' B',j,' group rotate within itself?:
□       +   y or n'
□40   format(A,I3,A,I3,A)
□       read(*,*,err=999) qrb
□       if (qrb.eq.'y')then
□         write(*,*)'Give number of jumps to return to original
□         +   position'
□         read(*,*,err=999) d1(l)
□         write(*,*)'Give estimate of activation energy and coeff
□         +   constant'
□         read(*,*,err=999) EB(i,j),TB(i,j)
□       else
□         d1(l)=1
□         EB(i,j)=0.0d+0
□         TB(i,j)=1.0d+0
□       endif
□     enddo
□   enddo
□
□
□c calculate number of atoms in each group A
□   do i=1,na
□     numA(i)=0
□     do j=1,nb(i)
□       numA(i)=numA(i)+nc(i,j)
□c Calculate where each B group ends
□   num2=num2+nc(i,j)
□   num(i,j)=num2
□   enddo
□   ntot=ntot+numA(i)
□   enddo
□c Calculate flags for A group, B group, number within B group,
□   number=0

```

```

□ do i=1,na
□ sum=0
□ do j=1,i-1
□ sum=sum+numA(j)
□ enddo
□ do j=sum+1,sum+numA(i)
□ xi(j,1)=i
□ noA(j)=c1(i)
□ enddo
□ if(setno(i).ne.0)then
□ add1=0
□ add2=0
□ do j=1,setno(i)
□ add1=add1+add2
□ add2=0
□ do k=1,c1(i)
□ do l=1,nc(i,(j-1)*c1(i)+k)
□ add2=add2+1
□ do m=1,c1(i)
□ Bnj(sum+add1+add2,m)=set(i,j,m)
□ enddo
□ enddo
□ enddo
□ endif
□ do j=1,nb(i)
□ number=number+1
□ if(j.eq.1)then
□ add=0
□ do k=num(i-1,nb(i-1))+1,num(i,j)
□ xi(k,2)=j
□ add=add+1
□ xi(k,3)=add
□ do l=1,3
□ xd(k,l)=xyz(i,j,add,l)
□ enddo
□ shxc(k)=atom(i,j,add)
□ resn(k)=resno(i,j,add)
□ noB(k)=d1(number)
□ enddo
□ else
□ add=0
□ do k=num(i,j-1)+1,num(i,j)
□ xi(k,2)=j
□ add=add+1
□ xi(k,3)=add
□ do l=1,3
□ xd(k,l)=xyz(i,j,add,l)
□ enddo
□ shxc(k)=atom(i,j,add)
□ resn(k)=resno(i,j,add)
□ noB(k)=d1(number)
□ enddo
□ endif
□ enddo
□ enddo
□ add9=0
□ do i=1,ntot
□ if(resn(i).ne.0)then
□ add9=add9+1
□ resn(add9)=resn(i)
□ resi(add9)=i
□ endif
□ enddo

```



```

□
□ write(*,*)'Enter total contributing atoms'
□ read(*,*)totat
□
□c assign spin and gyromagnetic ratio for each atom
□ do i=1,ntot
□ if(shxc(i).eq.'c')then
□ gmr(i)=6.7283d+7
□ spin(i)=0.5d+0
□ elseif(shxc(i).eq.'h')then
□ gmr(i)=26.7519d+7
□ spin(i)=0.5d+0
□ elseif(shxc(i).eq.'p')then
□ gmr(i)=10.83d+7
□ spin(i)=0.5d+0
□ elseif(shxc(i).eq.'br')then
□c gmr(i)=7.2245d+7
□ gmr(i)=6.991d+7
□ spin(i)=1.5d+0
□ elseif(shxc(i).eq.'cl')then
□ spin(i)=1.5d+0
□ gmr(i)=2.621d+7
□ elseif(shxc(i).eq.'i')then
□ spin(i)=3.5d+0
□ gmr(i)=5.3525d+7
□ elseif(shxc(i).eq.'n')then
□ spin(i)=1.0d+0
□ gmr(i)=1.934d+7
□ elseif(shxc(i).eq.'nn')then
□ spin(i)=0.5d+0
□ gmr(i)=2.713d+7
□ elseif(shxc(i).eq.'a')then
□ spin(i)=0.0d+0
□ gmr(i)=1.0d+0
□ endif
□ enddo
□ do i=1,nag
□ EA(i)=EA(i)/6.022045d+20
□ do j=1,nbg
□ EB(i,j)=EB(i,j)/6.022045d+20
□ enddo
□ enddo
□
□c calculate array ccc(i,j,k,l) where i is number of atom, j is how far B
□c group has rotated within A group, k is how far atom has rotated
□c within B group, l is x,y,z, coordinate
□
□ do i=1,ntot
□ if(noB(i).eq.1)then
□ do j=1,3
□ cc(i,1,j)=xd(i,j)
□ enddo
□ else
□ j=0
□ do k=i,ntot
□ if(xi(i,1).eq.xi(k,1).and.xi(i,2).eq.xi(k,2))then
□ j=j+1
□ do l=1,3
□ cc(i,j,l)=xd(k,l)
□ enddo
□ endif
□ enddo
□ do k=1,i-1
□ if(xi(i,1).eq.xi(k,1).and.xi(i,2).eq.xi(k,2))then

```

```

      j=j+1
      do l=1,3
      cc(i,j,l)=xd(k,l)
      enddo
      endif
      enddo
      endif
      enddo
      do i=1,ntot
      do j=1,noB(i)
      do l=1,3
      ccc(i,1,j,l)=cc(i,j,l)
      enddo
      enddo
      k=1
      if(noA(i).ne.1)then
      do j=i+1,ntot
      do m=1,njumps
      if(Bnj(i,m).ne.0.and.Bnj(i,m).ne.xi(i,2))then
      if(xi(j,1).eq.xi(i,1).and.xi(j,2).eq.Bnj(i,m).
 +      and.xi(j,3).eq.xi(i,3))then
      k=k+1
      do l=1,noB(i)
      do n=1,3
      ccc(i,k,l,n)=cc(j,l,n)
      enddo
      enddo
      endif
      endif
      enddo
      enddo
      do j=1,i-1
      do m=1,njumps
      if(Bnj(i,m).ne.0.and.Bnj(i,m).ne.xi(i,2))then
      if(xi(j,1).eq.xi(i,1).and.xi(j,2).eq.Bnj(i,m).
 +      and.xi(j,3).eq.xi(i,3))then
      k=k+1
      do l=1,noB(i)
      do n=1,3
      ccc(i,k,l,n)=cc(j,l,n)
      enddo
      enddo
      endif
      endif
      enddo
      enddo
      endif
      enddo
      c read in the temperature range of interest and the format in which
      c results are required

      write(*,*)'Enter temperature range: lower temp, upper temp
      +      in integers'
      read(*,*,err=999)low,high
      write(*,*)'Equal spacing of temp: type "t"'
      write(*,*)'Equal spacing of 1000/temp: type "i"'
      read(*,*,err=999)type
      write(*,*)'Enter gradation'
      write(*,*)'If less than 1: enter "l" and'
      write(*,*)'"a" where gradation = 1/a'
      write(*,*)'If greater than 1: enter "g" and'
      write(*,*)'"a" where gradation = a'
      read(*,*,err=999)gradt
      read(*,*,err=999)grad

```

```

 if(gradt.ne.'l'.and.gradt.ne.'g')then
   goto 999
 endif
 if(type.eq.'t')then
   if(gradt.eq.'g')then
     first=low
     last=high
     med=grad
   else
     first=low*grad
     last=high*grad
     med=1
   endif
 elseif(type.eq.'i')then
   if(gradt.eq.'g')then
     first=int(1000.0/high)
     last=int(1000.0/low)+1
     med=grad
   else
     first=int(1000.0/high)*grad
     last=(int(1000.0/low)+1)*grad
     med=1
   endif
 else
   goto 999
 endif

 c read in filename to which output will be stored
   write(*,*)'Enter filename'
   read(*,*,err=999) filename
   write(*,*)
   write(*,*)'Writing to ',filename,'...'

 c calculate Y0,Y1,Y2 for relevant nuclei
 c run over range of temperatures
   do i1=first,last,med
     if(type.eq.'t')then
       if(gradt.eq.'g')then
         therm=dreal(i1)
       else
         therm=dreal(i1)/grad
       endif
     else
       if(gradt.eq.'g')then
         therm=1000.0d+0/i 1
       else
         therm=1000.0d+0*grad/i1
       endif
     endif

 c calculate relaxation times for each dipole-dipole interaction
 c and sum over the lattice
   Sumrel1=0.0d+0
   Sumrel1p=0.0d+0
   Sumrel2=0.0d+0
   do i3=1,add9
     tune=resi(i3)
     i=resi(i3)
     add4=0
     add5=0
     add6=0
     do j=1,ntot
       if(i.ne.j)then
         if(shxc(j).ne.'a')then
 c select whether in same/different A/B groups

```

```

□ if(xi(i,1).eq.xi(j,1).and.xi(i,2).eq.xi(j,2))then
□   mt(j)=1
□   nt(j)=1
□   do k=1,noA(i)
□     do l=1,noB(i)
□       do o=1,3
□         temp(k,l,1,1,o)=ccc(j,k,l,o)-ccc(i,k,l,o)
□       enddo
□     enddo
□   enddo
□   add4=add4+1
□   p1(add4)=j
□ elseif(xi(i,1).eq.xi(j,1).and.xi(i,2).ne.xi(j,2))then
□   mt(j)=1
□   nt(j)=noB(j)
□   do k=1,noA(i)
□     do l=1,noB(i)
□       do n=1,nt(j)
□         do o=1,3
□           temp(k,l,1,n,o)=ccc(j,k,n,o)-ccc(i,k,l,o)
□         enddo
□       enddo
□     enddo
□   enddo
□   add5=add5+1
□   p2(add5,1)=j
□   p2(add5,2)=nt(j)
□ elseif(xi(i,1).ne.xi(j,1))then
□   mt(j)=noA(j)
□   nt(j)=noB(j)
□   do k=1,noA(i)
□     do l=1,noB(i)
□       do m=1,mt(j)
□         do n=1,nt(j)
□           do o=1,3
□             temp(k,l,m,n,o)=ccc(j,m,n,o)-ccc(i,k,l,o)
□           enddo
□         enddo
□       enddo
□     enddo
□   enddo
□   add6=add6+1
□   p3(add6,1)=j
□   p3(add6,2)=mt(j)
□   p3(add6,3)=nt(j)
□ endif
□ c calculate correltaion functions for powder average
□   do k=1,noA(i)
□     do l=1,noB(i)
□       do m=1,mt(j)
□         do n=1,nt(j)
□           dot=temp(1,1,1,1,1)*temp(k,l,m,n,1)+
□ + temp(1,1,1,1,2)*temp(k,l,m,n,2)+
□ + temp(1,1,1,1,3)*temp(k,l,m,n,3)
□           r1=(temp(1,1,1,1,1)**2.0d+0+temp(1,1,1,1,2)**2.0d+0+
□ + temp(1,1,1,1,3)**2.0d+0)**0.5d+0
□           r2=(temp(k,l,m,n,1)**2.0d+0+temp(k,l,m,n,2)**2.0d+0+
□ + temp(k,l,m,n,3)**2.0d+0)**0.5d+0
□           theta=dot/(r1*r2)
□           Y0(j,k,l,m,n)=2.0*(3.0*theta**2.0-1.0)/
□ + (5.0*r1**3.0*r2**3.0)
□           Y1(j,k,l,m,n)=Y0(j,k,l,m,n)/6.0d+0
□           Y2(j,k,l,m,n)=2.0d+0*Y0(j,k,l,m,n)/3.0d+0
□         enddo
□       enddo
□     enddo
□   enddo

```

```

□      enddo
□      enddo
□      enddo
□c calculate correlation times for different rotational jumps
□      T0A1(j)=TA(xi(i,1))
□      ExpA1(j)=dexp(EA(xi(i,1))/(Boltz*1000.0))
□      T0A2(j)=TA(xi(j,1))
□      ExpA2(j)=dexp(EA(xi(j,1))/(Boltz*1000.0))
□      T0B1(j)=TB(xi(i,1),xi(i,2))
□      ExpB1(j)=dexp(EB(xi(i,1),xi(i,2))/(Boltz*1000.0))
□      T0B2(j)=TB(xi(j,1),xi(j,2))
□      ExpB2(j)=dexp(EB(xi(j,1),xi(j,2))/(Boltz*1000.0))
□      endif
□      endif
□      enddo
□      add7=0
□      do i2=1,6
□          mm(i2)=0
□      enddo
□      do i2=1,add5
□          call mem(p2(i2,2),p2t(i2))
□      enddo
□      np2t=add7
□      add7=0
□      do i2=1,6
□          mm(i2)=0
□      enddo
□      do i2=1,add6
□          call mem(p3(i2,2),p3t(i2,1))
□      enddo
□      np3t=add7
□      do i2=1,np3t
□          np3ta(i2)=0
□      enddo
□      do i2=1,np3t
□          add7=0
□          do j=1,6
□              mm(j)=0
□          enddo
□          do j=1,add6
□              if(p3t(j,1).eq.i2)then
□                  call mem(p3(j,3),p3t(j,2))
□              endif
□          enddo
□          np3ta(i2)=add7
□      enddo
□      add7=0
□      if(add4.ne.0)then
□          add7=add7+1
□          do i2=1,noB(tune)
□              ptl(add7,2,i2)=la(noB(tune),i2)
□          enddo
□          do i2=1,noA(tune)
□              ptl(add7,1,i2)=la(noA(tune),i2)
□          do j=1,noB(tune)
□              do k=1,noA(tune)
□                  do l=1,noB(tune)
□                      ptcon(add7,i2,j,1,1,k,1,1,1)
□                  + =con(noA(tune),i2,k)*con(noB(tune),j,l)
□              enddo
□          enddo
□          enddo
□          enddo
□      do i2=1,add4

```

```

□      probtype(p1(i2))=add7
□      enddo
□      endif
□      do i2=1,ntypes
□        add7old(i2)=0
□      enddo
□      do i2=1,np2t
□        add7old(i2)=add7
□        add7=add7+1
□      do j=1,add5
□        if(p2t(j).eq.i2)then
□          probtype(p2(j,1))=add7
□          do k=1,j
□            if(add7.eq.add7old(p2t(k)))goto 3000
□          enddo
□          do l=1,noB(tune)
□            ptl(add7,2,l)=la(noB(tune),l)
□          enddo
□          do l=1,nt(p2(j,1))
□            ptl(add7,4,l)=la(nt(p2(j,1)),l)
□          enddo
□          do l=1,noA(tune)
□            ptl(add7,1,l)=la(noA(tune),l)
□          do m=1,noB(tune)
□            do n=1,nt(p2(j,1))
□              do l1=1,noA(tune)
□                do m1=1,noB(tune)
□                  do n1=1,nt(p2(j,1))
□                    ptcon(add7,l,m,1,n,l1,m1,1,n1)=
□                    +   con(noA(tune),l,l1)*con(noB(tune),m,m1)*
□                    +   con(nt(p2(j,1)),n,n1)
□                  enddo
□                enddo
□              enddo
□            enddo
□          enddo
□          enddo
□          enddo
□          endif
□3000 enddo
□      enddo
□      do i2=1,ntypes
□        do j=1,ntypes
□          add8old(i2,j)=0
□        enddo
□      enddo
□      do i2=1,np3t
□        do j=1,np3ta(i2)
□          add8old(i2,j)=add7
□          add7=add7+1
□        do k=1,add6
□          if(p3t(k,1).eq.i2.and.p3t(k,2).eq.j)then
□            probtype(p3(k,1))=add7
□            do l=1,k
□              if(add7.eq.add8old(p3t(l,1),p3t(l,2)))goto 4000
□            enddo
□            do m=1,noB(tune)
□              ptl(add7,2,m)=la(noB(tune),m)
□            enddo
□            do m=1,mt(p3(k,1))
□              ptl(add7,3,m)=la(mt(p3(k,1)),m)
□            enddo
□            do m=1,nt(p3(k,1))
□              ptl(add7,4,m)=la(nt(p3(k,1)),m)
□            enddo
□          enddo
□        enddo
□      enddo

```

```

□ do m=1,noA(tune)
□   ptl(add7,1,m)=la(noA(tune),m)
□   do n=1,noB(tune)
□     do o=1,mt(p3(k,1))
□     do p=1,nt(p3(k,1))
□     do m1=1,noA(tune)
□     do n1=1,noB(tune)
□     do o1=1,mt(p3(k,1))
□     do p11=1,nt(p3(k,1))
□     ptcon(add7,m,n,o,p,m1,n1,o1,p11)=
+       con(noA(tune),m,m1)*con(noB(tune),n,n1)*
+       con(mt(p3(k,1)),o,o1)*con(nt(p3(k,1)),p,p11)
□     enddo
□     enddo
□     enddo
□     enddo
□     enddo
□     enddo
□     enddo
□   endif
□4000 enddo
□ enddo
□ enddo
□ do j=1,ntot
□   if(i.ne.j)then
□     if(shxc(j).ne.'a')then
□c determine whether like or unlike atoms and call appropriate
□c subrouitne
□     Rel1=0.0d+0
□     Rel1p=0.0d+0
□     Rel2=0.0d+0
□     Rel1s=0.0d+0
□     Rel1ps=0.0d+0
□     Rel2s=0.0d+0
□     TauA1=1.0d+0
□     TauA2=1.0d+0
□     TauB1=1.0d+0
□     TauB2=1.0d+0
□     TauA1=T0A1(j)*ExpA1(j)**(1000.0d+0/therm)
□     TauA2=T0A2(j)*ExpA2(j)**(1000.0d+0/therm)
□     TauB1=T0B1(j)*ExpB1(j)**(1000.0d+0/therm)
□     TauB2=T0B2(j)*ExpB2(j)**(1000.0d+0/therm)
□     if(shxc(i).eq.shxc(j))then
□       call relsame(probtype(j),noA(i),
+         noB(i),mt(j),nt(j),gmr(i),spin(i),B0,B1,Y0,Y1,Y2,
+         TauA1,TauA2,TauB1,TauB2,Rel1s,Rel1ps,Rel2s,j)
□     elseif(shxc(i).ne.shxc(j))then
□       call reldiff(probtype(j),noA(i),
+         noB(i),mt(j),nt(j),gmr(i),gmr(j),spin(j),B0,B1,Y0,Y1,Y2,
+         TauA1,TauA2,TauB1,TauB2,Rel1,Rel1p,Rel2,j)
□     endif
□     Sumrel1=Sumrel1+(Rel1+Rel1s)*resn(tune)
□     Sumrel1p=Sumrel1p+(Rel1p+Rel1ps)*resn(tune)
□     Sumrel2=Sumrel2+Rel2+Rel2s
□     endif
□   endif
□   Relax1=(hbar**2.0d+0)*(mu**2.0d+0)*Sumrel1*1.0d+60
□   Relax1p=(hbar**2.0d+0)*(mu**2.0d+0)*Sumrel1p*1.0d+60
□   Relax2=(hbar**2.0d+0)*(mu**2.0d+0)*Sumrel2*1.0d+60
□ enddo
□c write temperature, inverse temperture, T1,T1p,T2 times to file
□   open(21,file=filename)

```

```

 do ico=1,icount
   read(21,*)ig
   enddo
   icount=icount+1
   write(21,12)1000.0d+0/therm,totat/relax1,totat/relax1p,
     +   1.0d+0/relax2
12  format(4(x,e12.6))
   close(21)
   enddo
   goto 1000
999 write(*,*)'Wrong type of data has been entered'
1000 stop
   end



c subroutine to calculate dipole-dipole interactions where atoms
c are of same type
c it determines which A and B groups the two atoms are in and calls
c the appropriate subroutine to calculate an array whose
c elements are the Fourier transform of the probability of finding
c the internuclear vector at a particular place given the original
c position
c these are then multiplied by the correlation functions and linear
c combinations formed to find r1,r1p,r2

   subroutine relsame(probt,nAi,nBi,mt,nt,gmr,spin,B0,B1,
     +   Y0,Y1,Y2,TA1,TA2,TB1,TB2,Rel1,Rel1p,Rel2,atno)

   integer njumps,natoms
   parameter (njumps=3,natoms=100,ntypes=20)
   integer i,j,k,l,nAi,nBi,mt,nt,atno
   double precision gmr,spin,B0,B1,TA1,TA2,wi,C,
     +   Y0(natoms,njumps,njumps,njumps,njumps),TB1,
     +   TB2,pwT(njumps,njumps,njumps,njumps),
     +   p2wT(njumps,njumps,njumps,njumps),J11,J22,
     +   p0(njumps,njumps,njumps,njumps),g00,g02,
     +   p2w1T(njumps,njumps,njumps,njumps),J00,J02
   double precision Y1(natoms,njumps,njumps,njumps,njumps),
     +   Y2(natoms,njumps,njumps,njumps,njumps),Rel1,Rel1p,Rel2,
     +   g11,g22,F
   integer probt
   double precision Flambda1(njumps,njumps,njumps,njumps),
     +   lambda,Flambda2(njumps,njumps,njumps,njumps),
     +   Flambda3(njumps,njumps,njumps,njumps),
     +   Flambda4(njumps,njumps,njumps,njumps),ptl,ptcon
   common /b2/ptl(ntypes,4,njumps),ptcon(ntypes,njumps,
     +   njumps,njumps,njumps,njumps,njumps,njumps)
   wi=gmr*B0
   C=3.0d+0/8.0d+0*gmr4*4.0d+0*spin*(spin+1.0d+0)
c initialise arrays
   do i=1,njumps
     do j=1,njumps
       do k=1,njumps
         do l=1,njumps
           pwT(i,j,k,l)=0.0d+0
           p2wT(i,j,k,l)=0.0d+0
           p0(i,j,k,l)=0.0d+0
           p2w1T(i,j,k,l)=0.0d+0
           Flambda1(i,j,k,l)=0.0d+0
           Flambda2(i,j,k,l)=0.0d+0
           Flambda3(i,j,k,l)=0.0d+0
           Flambda4(i,j,k,l)=0.0d+0
         enddo
       enddo
     enddo
   enddo

```



```

□      enddo
□      enddo
□
□c linear combinations formed
□      Rel1=4.0d+0*C*(J11+J22)
□      Rel1p=C*(J02+10*J11+J22)
□      Rel2=C*(J00+10*J11+J22)
□
□      return
□      end
□
□
□c subroutine to calculate dipole-dipole interactions where atoms
□c are of different type
□c it determines which A and B groups the two atoms are in and calls
□c the appropriate subroutine to calculate an array whose
□c elements are the Fourier transform of the probability of finding
□c the internuclear vector at a particular place given the original
□c position
□c these are then multiplied by the correlation functions and linear
□c combinations formed to find r1,r1p,r2
□
□
□      subroutine reldiff(probt,nAi,nBi,mt,nt,gmri,gmrj,spin,
□      +      B0,B1,Y0,Y1,Y2,TA1,TA2,TB1,TB2,Rel1,Rel1p,Rel2,atno)
□
□      integer njumps,natoms
□      parameter (njumps=3,natoms=100,ntypes=20)
□      integer i,j,k,l,nAi,nBi,mt,nt,atno
□      double precision gmri,gmrj,spin,B0,B1,TA1,TA2,
□      +      Y0(natoms,njumps,njumps,njumps,njumps),TB1,
□      +      TB2,pwT(njumps,njumps,njumps,njumps),
□      +      p1mwT(njumps,njumps,njumps,njumps),wi,ws,As,
□      +      p0(njumps,njumps,njumps,njumps),g01m,g0B1,
□      +      pw1T(njumps,njumps,njumps,njumps),g00,J01m,
□      +      pqwT(njumps,njumps,njumps,njumps),
□      +      p1pwT(njumps,njumps,njumps,njumps),JOB1,J00
□      double precision Y1(natoms,njumps,njumps,njumps,njumps),
□      +      Y2(natoms,njumps,njumps,njumps,njumps),
□      +      Rel1,Rel1p,Rel2,g1l,g1q,g2lp,J1l,J1q,J2lp
□      integer probt
□      double precision ptl,ptcon,F
□      double precision Flambda1(njumps,njumps,njumps,njumps),
□      +      lambda,Flambda2(njumps,njumps,njumps,njumps),
□      +      Flambda3(njumps,njumps,njumps,njumps),
□      +      Flambda4(njumps,njumps,njumps,njumps),
□      +      Flambda5(njumps,njumps,njumps,njumps),
□      +      Flambda6(njumps,njumps,njumps,njumps),ptl,ptcon
□      common /b2/ptl(ntypes,4,njumps),ptcon(ntypes,njumps,
□      +      njumps,njumps,njumps,njumps,njumps,njumps)
□      wi=gmri*B0
□      ws=gmrj*B0
□      As=gmri**2.0d+0*gmrj**2.0d+0*spin*(spin+1.0d+0)
□c initialise arrays
□      do i=1,njumps
□      do j=1,njumps
□      do k=1,njumps
□      do l=1,njumps
□      pwT(i,j,k,l)=0.0d+0
□      p1mwT(i,j,k,l)=0.0d+0
□      p0(i,j,k,l)=0.0d+0
□      pw1T(i,j,k,l)=0.0d+0
□      pqwT(i,j,k,l)=0.0d+0
□      p1pwT(i,j,k,l)=0.0d+0

```

```

□ Flambda1(i,j,k,l)=0.0d+0
□ Flambda2(i,j,k,l)=0.0d+0
□ Flambda3(i,j,k,l)=0.0d+0
□ Flambda4(i,j,k,l)=0.0d+0
□ Flambda5(i,j,k,l)=0.0d+0
□ Flambda6(i,j,k,l)=0.0d+0
□ enddo
□ enddo
□ enddo
□ enddo
□ do i=1,nAi
□ do j=1,nBi
□ do k=1,mt
□ do l=1,nt
□ lambda=ptl(probt,1,i)/TA1+ptl(probt,2,j)/TB1+
□ + ptl(probt,3,k)/TA2+ptl(probt,4,l)/TB2
□ Flambda1(i,j,k,l)=F(lambda,wi)
□ Flambda2(i,j,k,l)=F(lambda,wi-ws)
□ if(lambda.eq.0.0d+0)then
□ Flambda3(i,j,k,l)=0.0d+0
□ else
□ Flambda3(i,j,k,l)=2.0d+0/lambda
□ endif
□ Flambda4(i,j,k,l)=F(lambda,B1*wi/B0)
□ Flambda5(i,j,k,l)=F(lambda,ws)
□ Flambda6(i,j,k,l)=F(lambda,wi+ws)
□ enddo
□ enddo
□ enddo
□ enddo
□ do i=1,nAi
□ do j=1,nBi
□ do k=1,mt
□ do l=1,nt
□ do i1=1,nAi
□ do j1=1,nBi
□ do k1=1,mt
□ do l1=1,nt
□ pwT(i,j,k,l)=pwT(i,j,k,l)+Flambda1(i1,j1,k1,l1)*
□ + ptcon(probt,i,j,k,l,i1,j1,k1,l1)
□ p1mwT(i,j,k,l)=p1mwT(i,j,k,l)+Flambda2(i1,j1,k1,l1)*
□ + ptcon(probt,i,j,k,l,i1,j1,k1,l1)
□ p0(i,j,k,l)=p0(i,j,k,l)+Flambda3(i1,j1,k1,l1)*
□ + ptcon(probt,i,j,k,l,i1,j1,k1,l1)
□ pw1T(i,j,k,l)=pw1T(i,j,k,l)+Flambda4(i1,j1,k1,l1)*
□ + ptcon(probt,i,j,k,l,i1,j1,k1,l1)
□ pqwT(i,j,k,l)=pqwT(i,j,k,l)+Flambda5(i1,j1,k1,l1)*
□ + ptcon(probt,i,j,k,l,i1,j1,k1,l1)
□ p1pwT(i,j,k,l)=p1pwT(i,j,k,l)+Flambda6(i1,j1,k1,l1)*
□ + ptcon(probt,i,j,k,l,i1,j1,k1,l1)
□ enddo
□ enddo
□ enddo
□ enddo
□ enddo
□ enddo
□ enddo
□ enddo
□ c multiply by correlation functions
□ J01m=0.0d+0
□ J0B1=0.0d+0
□ J00=0.0d+0
□ J11=0.0d+0

```

```

□ J1q=0.0d+0
□ J21p=0.0d+0
□ do i=1,nAi
□ do j=1,nBi
□ do k=1,mt
□ do l=1,nt
□ g01m=Y0(atno,i,j,k,l)*p1mwT(i,j,k,l)
□ g0B1=Y0(atno,i,j,k,l)*pw1T(i,j,k,l)
□ g00=Y0(atno,i,j,k,l)*p0(i,j,k,l)
□ g11=Y1(atno,i,j,k,l)*pwT(i,j,k,l)
□ g1q=Y1(atno,i,j,k,l)*pqwT(i,j,k,l)
□ g21p=Y2(atno,i,j,k,l)*p1pwT(i,j,k,l)
□ J01m=J01m+g01m
□ J0B1=J0B1+g0B1
□ J00=J00+g00
□ J11=J11+g11
□ J1q=J1q+g1q
□ J21p=J21p+g21p
□ enddo
□ enddo
□ enddo
□ enddo
□ c form linear combinations
□ Rel1=As*(J01m/12.0d+0+3.0d+0*J11/2.0d+0
□ + +3.0d+0*J21p/4.0d+0)
□ Rel1p=As*(J0B1/6.0d+0+J01m/24.0d+0+3.0d+0*J11/4.0d+0
□ + +3.0d+0*J1q/2.0d+0+3.0d+0*J21p/8.0d+0)
□ Rel2=As*(J00/6.0d+0+J01m/24.0d+0+3.0d+0*J11/4.0d+0
□ + +3.0d+0*J1q/2.0d+0+3.0d+0*J21p/8.0d+0)
□
□ return
□ end
□
□ c calculates 1/tau of the Fourier transform of exp(-at/tau)
□ double precision function F(a,w)
□ double precision a,w
□
□ F=2.0*a/(a**2.0+w**2.0)
□
□ return
□ end
□
□ subroutine mem(x,k)
□
□ integer m,x,add
□ common /b1/m(6),add
□
□ if(x.ne.m(1).and.x.ne.m(2).and.x.ne.m(3).and.
□ + x.ne.m(4).and.x.ne.m(5).and.x.ne.m(6))then
□ add=add+1
□ m(add)=x
□ k=add
□ endif
□ do i=1,6
□ if(x.eq.m(i))then
□ k=i
□ endif
□ enddo
□

```

- return
- end
-

